Aus der

Medizinischen Universitätsklinik und Poliklinik Tübingen

Abteilung Innere Medizin I

(Schwerpunkt: Gastroenterologie, Gastrointestinale Onkologie, Hepatologie, Infektiologie und Geriatrie)

Examining the role of *let-7* microRNA transfer in the metastatic niche

Inaugural-Dissertation
zur Erlangung des Doktorgrades
der Medizin

der Medizinischen Fakultät
der Eberhard Karls Universität
zu Tübingen

vorgelegt von

Shi, Ying

2023

Dekan: Professor Dr. B. Pichler

1. Berichterstatter: Professor Dr. N. P. Malek
2. Berichterstatter: Professorin Dr. J. Skokowa, Ph.D

Tag der Disputation: 19.12.2022

Contents

CONTENTS I
List of Figures V
List of Tables VI
List of abbreviations VII
1. INTRODUCTION 1
1.1 Cancer metastasis 1
1.2 Post-transcriptional gene regulation 3
1.3 RNA-binding protein 5
1.4 Biogenesis and homeostasis of miRNA 6
1.5 MiRNA in cancer 8
1.6 *Let-7* miRNA 10
1.7 LIN28 and LIN28-mediated regulation 11
1.8 Cell-to-cell communication 14
1.9 Exosomes and exosomal miRNAs 14
1.10 Aim of the work 16
2. MATERIALS AND METHODS 17
2.1 Materials 17
2.1.1 Cells 17
2.1.2 Cell culture reagents 18
2.1.3 Materials for mRNA and miRNA assays 19
2.1.4 Materials for protein assays 20
2.1.5 Antibodies for protein assays 21
2.1.6 Materials for exosome isolation 21
2.1.7 Materials for molecular assays 22
2.1.8 Experimental equipments 23
2.2 Methods 23
2.2.1 Cell culture 23

2.2.2 Viral packaging and production....24
2.2.3 Generation of stable cell line with constitutive gene expression....25
2.2.4 Cell co-culture....26
2.2.4.1 The generation of a dual-luciferase reporter-based co-culture system....26
2.2.4.2 The generation of a microporous insert-based co-culture system....26
2.2.4.3 The generation of a cell culture conditioned medium system....27
2.2.4.4 The generation of an exosome-rich conditioned medium system....27
2.2.4.5 The generation of a fluorescence-based co-culture system....27
2.2.5 Cell-free exosome isolation....28
2.2.5.1 Exosome isolation with ultracentrifugation....28
2.2.5.2 Exosome isolation with OptiPrep-UC....28
2.2.5.3 Exosome isolation with ExoQuick....29
2.2.6 Exosomal RNA purification....30
2.2.7 Exosomal protein purification....30
2.2.8 Dual-luciferase reporter assays....31
2.2.8.1 Dual-luciferase reporter assays with reporter constructs stable expression....31
2.2.8.2 Dual-luciferase reporter assays with luciferase reporter transfection....31
2.2.9 Fluorescence-activated cell sorting....32
2.2.10 Real-time PCR....32
2.2.10.1 Real-time PCR of miRNA (miScript)....32
2.2.10.2 Real-time PCR of miRNA (miRCURY LNA)....34
2.2.10.3 Real-time PCR of total RNA....35
2.2.11 Western blot of total protein....37
2.2.12 Statistical analysis....37
3. RESULTS....38
3.1 *Let-7* levels alter in an *in vitro* co-culture system....38
3.1.1 The differential expression of *let-7* in normal and tumor cells....38
3.1.2 The generation of a dual-luciferase reporter-based co-culture system....38
3.1.3 The measurement of *let-7* levels in the co-culture system....41
3.1.4 Paragraph summary....43

3.2 Non-contact co-culture leads to alteration of *let-7* levels 44
3.2.1 The generation of a microporous insert-based co-culture system 44
3.2.2 The assessment of *let-7* levels during non-contact co-culture 45
3.2.3 Paragraph summary 46
3.3 LIN28B-dependent alteration of *let-7* expression during co-culture 47
3.3.1 The generation of LIN28B knockout cells 47
3.3.2 LIN28B-dependent alteration of *let-7* expression during contact co-culture 48
3.3.3 LIN28B-dependent alteration of *let-7* expression during non-contact co-culture 49
3.3.4 Paragraph summary 50
3.4 The incubation of tumor cells with LIN28B KO-conditioned medium results in an increase of *let-7* level 50
3.4.1 The generation of a cell culture-conditioned medium system 50
3.4.2 The examination of LIN28B-mediated *let-7* level in the cell-culture conditioned medium system 51
3.4.3 Paragraph summary 53
3.5 The investigation of *let-7* transfer via cell-free exosomes 54
3.5.1 The exosomes collection from serum-free conditional medium 54
3.5.2 The validation of exosomal markers. 55
3.5.3 Exosome-rich conditioned medium assay 55
3.5.4 LIN28B-mediated intercellular transfer of *pre-let-7* via exosomes 57
3.5.5 Paragraph summary 59
3.6 The observation of cell morphology regulated by LIN28B 59
3.6.1 The generation of LIN28B overexpressing cells 59
3.6.2 The generation of a fluorescence-based co-culture system 60
3.6.3 Live cell imaging in fluorescence-based co-culture system 61
3.6.4 Paragraph summary 62
4. DISCUSSION 63
5. SUMMARY 71
6. ZUSAMMENFASSUNG 72
7. BIBLIOGRAPHY 73

8. DECLARATION OF CONTRIBUTION 86
9. ACKNOWLEDGEMENT 87

List of Figures

Figure 1. The inefficiency process of the invasion-metastasis cascade 2
Figure 2. The complex process of miRNA production 7
Figure 3. The process of *let-7* miRNA regulated by the RNA-binding protein LIN28 13
Figure 4. The differential expression of *let-7* in normal and tumor cells 38
Figure 5. The generation of a dual-luciferase reporter-based co-culture system 39
Figure 6. The measurement of luminescence activity in co-culture 40
Figure 7. The alteration of *let-7* levels during co-culture between NIH 3T3 and BE2C 41
Figure 8. The alteration of *let-7* levels during co-culture between NIH 3T3 and Kelly 42
Figure 9. The alteration of *let-7* levels during co-culture between HDF and Kelly 43
Figure 10. The generation of a microporous insert-based co-culture system 44
Figure 11. The assessment of *let-7* levels in the non-contact co-culture of NIH 3T3 and BE2C 45
Figure 12. The assessment of *let-7* levels in the non-contact co-culture of NIH 3T3 and Kelly 46
Figure 13. The generation of CRISPR/Cas9-mediated LIN28B KO cells 47
Figure 14. The measurement of luminescence activity in co-culture 48
Figure 15. LIN28B-mediated *let-7* transfer in the non-contact co-culture system 49
Figure 16. The workflow of cell culture-conditioned medium assay 51
Figure 17. The examination of LIN28B-mediated *let-7* level in CCM system 52
Figure 18. The luciferase activity of LIN28B knockout and control cells in cell culture-conditioned medium assay 53
Figure 19. The workflow of exosomes collection from serum-free conditional medium 54
Figure 20. The validation of exosomal markers 55
Figure 21. Exosome-rich conditioned medium assay 56
Figure 22. The measurement of exosomal markers in cell-free exosomes 56
Figure 23. The examination of *let-7* transfer in exosome-rich CCM assay 57
Figure 24. The expression of precursor *let-7s* in exosomes 58
Figure 25. Reexpression of LIN28B in LIN28B KO BE2C cells 60
Figure 26. The generation of fluorescence-based co-culture system 61
Figure 27. Live cell imaging in a fluorescence-based co-culture system 62

List of Tables

Table 1. Parental and gene-edited cell lines 17
Table 2. Cell culture reagents 18
Table 3. Materials for mRNA and miRNA assays 19
Table 4. Materials for protein assays 20
Table 5. Antibodies for protein assays 21
Table 6. Materials for exosome isolation 21
Table 7. Materials for molecular assays 22
Table 8. Main experimental equipments 23
Table 9. Cell culture medium 24
Table 10. Lentiviral packaging components 25
Table 11. Retroviral packaging components 25
Table 12. Antibiotic selection concentration 26
Table 13. Rotor application for UC (Beckman Coulter) 28
Table 14. Rotor application for OptiPrep-UC (Beckman Coulter) 29
Table 15. OptiPrep density gradient medium preparation 29
Table 16. Rotor application for ExoQuick (Jouan) 30
Table 17. RT reaction components (miScript, miRNA) 32
Table 18. RT procedure (miScript, miRNA) 33
Table 19. Real-time PCR reaction components (miScript, miRNA) 33
Table 20. Real-time PCR cycling conditions (miScript, miRNA) 33
Table 21. RT reaction components (miRCURY LNA, miRNA) 34
Table 22. RT procedure (miRCURY LNA, miRNA) 34
Table 23. Real-time PCR reaction components (miRCURY LNA, miRNA) 34
Table 24. Real-time PCR cycling conditions (miRCURY LNA, miRNA) 35
Table 25. RT reaction components (miScript, total RNA) 35
Table 26. RT procedure (miScript, total RNA) 36
Table 27. Real-time PCR reaction components (miScript, total RNA) 36
Table 28. Real-time PCR cycling conditions (miScript, total RNA) 36

List of abbreviations

AGO	Argonaute
CCM	cell culture medium
CMV	cytomegalovirus
CSC	cancer stem cells
CSD	cold shock domain
CTC	circulating tumor cell
CRC	colorectal cancer
EMT	epithelial-mesenchymal transition
ESC	embryonic stem cell
EV	extracellular vesicle
EXO	exosome
FACS	fluorescence-activated cell sorting
GFP	green fluorescent protein
HGP	Human Genome Project
hnRNP	heterogeneous nuclear ribonucleoprotein
ILV	intraluminal vesicle
KH	K homology domain
KO	knockout
let-7	*lethal-7*
LNP	lipid nanoparticle
LUC	luciferase
LV	lentivirus
MET	mesenchymal-epithelial transition
MIC	metastasis-initiating cell
miRNA, miR	microRNA
mRNA	messenger RNA
MUT	mutant

MVB	multivesicular body
ncRNA	non-coding RNA
NPC	nuclear pore complexes
OE	overexpression
oncomiR	oncogenic miRNA
PMN	pre-metastatic niche
pre-miRNA	precursor miRNA
pri-miRNA	primary miRNA
RBD	RNA-binding domain
RBP	RNA-binding protein
RFP	red fluorescent protein
RISC	RNA-induced silencing complex
RNase	ribonuclease
RNP	ribonucleoprotein
rRNA	ribosomal RNA
RT	reverse transcription
RV	retrovirus
SEER	Surveillance, Epidemiology, and End Results
TDMD	target-directed miRNA degradation
tRNA	transfer RNA
TUTase	terminal uridylyltransferase
UC	ultracentrifugation
UTR	untranslated region
WT	wildtype
XPO5	Exportin 5
ZKD	zinc knuckles domain

1. Introduction

1.1 Cancer metastasis

Cancer is the leading cause of mortality in most countries. In 2021, there is estimated 608,570 cancer deaths in the United States (Siegel et al., 2021). Up-to-date statistics across Europeon countries reveal 4 million new cancer cases and 1.9 million cancer-related mortality (Dyba et al., 2021). Data from the Surveillance, Epidemiology, and End Results (SEER) program of the National Cancer Institute indicates that patients diagnosed with metastatic diseases have extremely low overall 5-year survival rates (Steeg, 2016, Siegel et al., 2021). Tumor metastasis is responsible for about 90% of tumor related deaths (Esposito et al., 2021, Spano et al., 2012).

Metastasis is a hallmark of malignant disease with complex multistep processes (Hanahan and Weinberg, 2011). Single circulating tumor cells (CTCs) or clusters disseminate from primary lesions and interact with host cells, such as leukocytes, platelets, etc. Cancer cells derived from metastatic lesion also show capabilities to return into circulation, which terms as tumor cell recirculation (Pachmann, 2005) or self-seeding (Kim et al., 2009). The recirculated tumor cells contribute to further metastases and promote recurrence of cancer (Keller and Pantel, 2019). It is diffificult for disseminated CTCs to reside in a distant organ due to the defense from immune cells including macrophages, dendritic cells, natural killer cells and others (Hiam-Galvez et al., 2021, Dianat-Moghadam et al., 2021). The metastatic niches arise after metastasis-initiating cells (MICs) survive and gain the ability to regenerate tumors, leading to final micrometastases and macrometastases in distant organs (Ganesh and Massague, 2021). The metastatic niches with various components regulate MICs dormancy and metastasis growth (Ganesh and Massague, 2021). Furthermore, MICs are important for tumor treatment, because they are able to drive the resistance and relapse of tumor metastases (Massague and Ganesh, 2021).

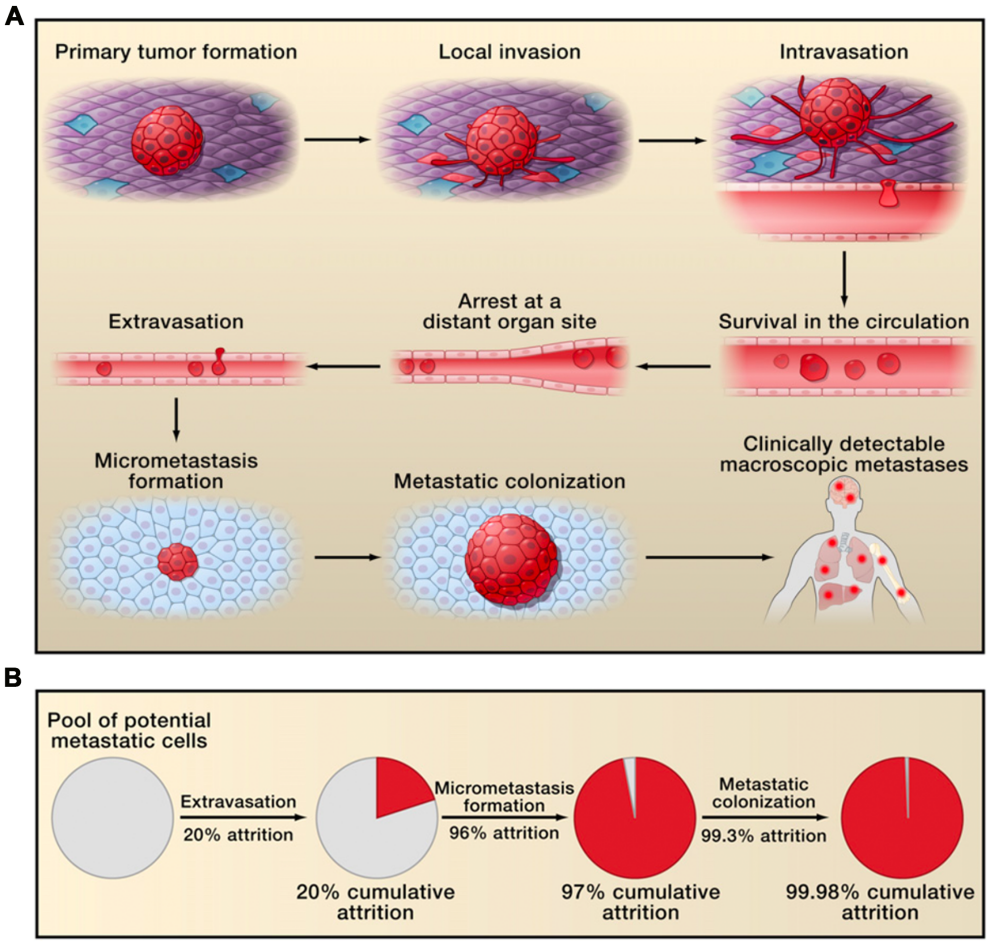

Figure 1. The inefficiency process of the invasion-metastasis cascade. (**A**) The invasion-metastasis cascade. (Valastyan and Weinberg, 2011, *pp*. 276). (**B**) The inefficient multistages in the invasion-metastasis cascade. (Valastyan and Weinberg, 2011, *pp*. 283).

Although the natural progression of metastasis varies among different malignant tumors, they follow the principle of the invasion-metastasis cascade (**Figure 1A**) (Zhang et al., 2009, Valastyan and Weinberg, 2011). CTCs represent an intermediate stage in the process of tumor metastasis (Schuster et al., 2021). Single-cell profiling of CTCs provides insights into cancer metastasis. In particular, CTCs are released from primary lesions and disseminate into circulation, allowing the formation of macroscopic metastases with stepwise progression (Keller and Pantel, 2019). Although CTCs are the

source of metastasis, only a tiny proportion of them eventually succeed in colonizing distant organs (**Figure 1B**) (Taftaf et al., 2021, Valastyan and Weinberg, 2011). Over 80 % of cancer cells that escape from primary lesions are successful in extravasating. Less than 3 % of those cells that exit the microcirculation are actually capable of generating micrometastasis. The subsequent step is even much less efficient, that only 0.02 % of those surviving cells lead to macroscopic metastasis (Valastyan and Weinberg, 2011). Metastatic colonization is the rate-limiting step in the invasion-metastasis cascade. However, the mechanisms are still uncertain.

1.2 Post-transcriptional gene regulation

The central dogma of molecular biology was formulated in 1957 and published in 1958 by Francis Crick (Crick, 1970). DNA is replicated from existing DNA, that is DNA replication. Then, the enzymes such as RNA polymerase and transcription factors (TF) facilitate the production of messenger RNA (mRNA) by utilizing the information in DNA, that is the process of transcription. The newly assembled pieces of RNA produce DNA, which is the reverse transcription. The translate is the process that proteins are synthesized by using mRNA (Cobb, 2017). The regulatory processes between transcription and translation are known as post-transcriptional gene regulation, controlling subsequent gene expression or degradation (Zhao et al., 2017). Post-transcriptional gene regulation plays important roles in cell differentiation and development (Zhao et al., 2017), immunity (Carpenter et al., 2014), cancer and other diseases (Kim and Kyung Lee, 2012).

The conventional post-transcriptional gene regulation in eukaryotes includes 5’ end capping (Corbett, 2018, Jiao et al., 2013), 3’ end polyadenylation (addition of poly(A) tail) (Corbett, 2018, Ren et al., 2020), RNA splicing (Corbett, 2018, Witten and Ule, 2011), RNA editing (Behm and Ohman, 2016, Xu et al., 2022), mRNA stability (McGary et al., 1997, Feigerlova and Battaglia-Hsu, 2017) and nuclear export (Reddy

et al., 2000, Li et al., 1999). 5' end capping protects mRNA from degradation by 5' exonuclease and contributes to ribosomal binding, assisting in the selection of the correct mRNA that will be translated (Jiao et al., 2013, Shuman, 2002). 3' end polyadenylation protects the mRNA from 3' exonuclease to retain mRNA decay (Slomovic and Schuster, 2011) and increases translation (Erson-Bensan and Can, 2016). RNA splicing eliminates introns and noncoding regions to facilitate the transform from precursor mRNAs transcript into mature mRNAs (Wilkinson et al., 2020, Cao et al., 2020). RNA editing is an enzyme-catalyzed process such as addition or deletion of uracil, that influences the localization, activity and stability of RNAs (Maydanovych and Beal, 2006, Feigerlova and Battaglia-Hsu, 2017). The nuclear export of RNA is important for gene expression. Different RNA species are synthesized in the nucleus and are exported to the cytoplasm through the nuclear pore complexes (NPCs) (Stewart, 2010). For examples, small RNAs such as transfer RNA (tRNA) and microRNA (miRNA) directly bind to export receptors for nuclear export. Large RNAs such as ribosomal RNA (rRNA) and mRNA are exported by assembling into ribonucleoprotein (RNP) complexes (Kohler and Hurt, 2007).

The central dogma of molecular biology has been refined since it was formulated (Cobb, 2017). The post-transcriptional gene regulation of mRNA is mainly driven by mRNA interaction of RNA-binding proteins (RBPs) and non-coding RNAs (ncRNAs) (Filipowicz et al., 2008, Briata and Gherzi, 2020, Franks et al., 2017). The ncRNAs post-transcriptionally regulate mRNA degradation or mediate translational repression, with different functional types including tRNA, rRNA and small RNA (miRNA, siRNA, lncRNAs, piRNA, snoRNA, snRNA and others) (Filipowicz et al., 2008, Mattick and Makunin, 2006). In addition, the distribution and stability of transcripts is post-transcriptionally regulated by RBPs, which can modulate almost all processes of post-transcriptional regulation in cells such as alternative splicing (Hu et al., 2020) or nuclear export (Hsu et al., 2019) for RNA maturation, translocation, degradation and translation. The nuclear polyadenylation complex containing RBP promotes RNA degradation by

the exosome (LaCava et al., 2005). RBPs also affect mRNA stability (McGary et al., 1997) and participate in RNA editing (Xu et al., 2022),.

1.3 RNA-binding protein

RBPs are proteins that contain single or multiple globular RNA-binding domains (RBDs) to bind RNAs and regulate the biological function of the bound RNAs (Hentze et al., 2018). Some RBPs recognize mRNA at the 5' cap or the 3' poly(A) tail, and some recognize the specific sequence motifs or secondary structures in mRNA (van Kouwenhove et al., 2011). RBDs may include RNA-recognition motif (Hentze et al., 2018), double-stranded RNA-binding motif (St Johnston et al., 1992), cold shock domain (CSD) (Samsonova et al., 2021), zinc knuckles domain (ZKD) (Wang et al., 2017), heterogeneous nuclear ribonucleoprotein (hnRNP) K homology domain (KH) (Hentze et al., 2018) and DEAD box helicase domain (Hentze et al., 2018). RBPs assemble in RNP complexes with mRNAs and ncRNAs (Kafasla et al., 2014).

RNA transcripts are instantly covered with RBPs as nuclear RNA emerges from RNA polymerase, regulating biosynthesis (Lopez de Silanes et al., 2004), maturation (Cuadrado et al., 2002), metabolism (Castello et al., 2015), transport (Gerstberger et al., 2014), subcellular localization (Gerstberger et al., 2014) and stability (Mukherjee et al., 2011) of RNA in cells. RBPs bind RNA with RNA-sequence specificity and affinity, targeting mRNAs and plenty of functional ncRNAs such as miRNAs (Gerstberger et al., 2014, Vos et al., 2019).

The Cancer Genome Atlas project reviewed dysregulation of RBPs in variety of cancer (Kechavarzi and Janga, 2014). Furthermore, aberrant expression of RBPs is detected in various human cancers, highly associated with advanced tumor stage and poor prognosis (He et al., 2021). As an example, high levels of the RNA binding proteins LIN28A and LIN28B are associated with malignant behaviors and poor prognosis of

cancer (Wang et al., 2015). Further, ERα (a potent non-canonical RBP) regulates post-transcriptional expression of stress response genes by alternative splicing of *XBP1*, which promotes cancer cell survival and maintains tamoxifen resistance in breast cancer progression (Xu et al., 2021). TIP30, a tumor suppressor RBP, inhibits metastasis by repressing transcription of *OPN* through interaction with ETS-1 in hepatocarcinogenesis (Zhang and Li, 2021).

1.4 Biogenesis and homeostasis of miRNA

MiRNAs are small non-coding RNAs of 20 to 22 nucleotides in length, regulating target genes by base-pairing to partially complementary sites in the 3' untranslated region (3' UTR) of mRNA (Kasinath et al., 2006). The complementary binding sites in the 3' UTR of mRNAs can be predicted for the interaction between miRNA and mRNA (Didiano and Hobert, 2006, Bartel, 2009). Moreover, the stability of miRNAs is also affected by ncRNAs (Chipman and Pasquinelli, 2019). For example, a rapid decay of miR-7 is caused by pairing to lncRNA Cyrano through target-directed miRNA degradation (TDMD) in mice (Chipman and Pasquinelli, 2019). MiRNAs regulate the expression of numerous protein coding genes in the human genome that affect cellular phenotype (Gosline et al., 2016). To date, roughly 1872 miRNA precursors are annotated, encoding apropriate 2600 mature miRNAs in human (Hussen et al., 2021, Plotnikova et al., 2019) and targeting around 5,300 human genes (Shenouda and Alahari, 2009).

The maturation of miRNA is a complicated process (**Figure 2**). The miRNA gene is transcribed by RNA polymerase II to produce the primary miRNA (pri-miRNA) in the nucleus, which includes a stem loop. Drosha, a class 2 ribonuclease (RNase) III enzyme, cleaves pri-miRNA to generate the precursor miRNA (pre-miRNA), which is transported to the cytoplasm via Exportin 5 (XPO5). Then, the endoribonuclease Dicer cleaves the stem loop of pre-miRNA, producing a double-stranded miRNA. The

complex that double-stranded miRNA couples to Argonaute (AGO) 2 is loaded into RNA-induced silencing complex (RISC). After the passage strand is discarded, the single-stranded miRNA partially complementary binds to the "seed region" of the 3' UTR in mRNA. Then the target mRNA is inhibited, resulting in mRNA degradation or translation repression (Rupaimoole et al., 2016).

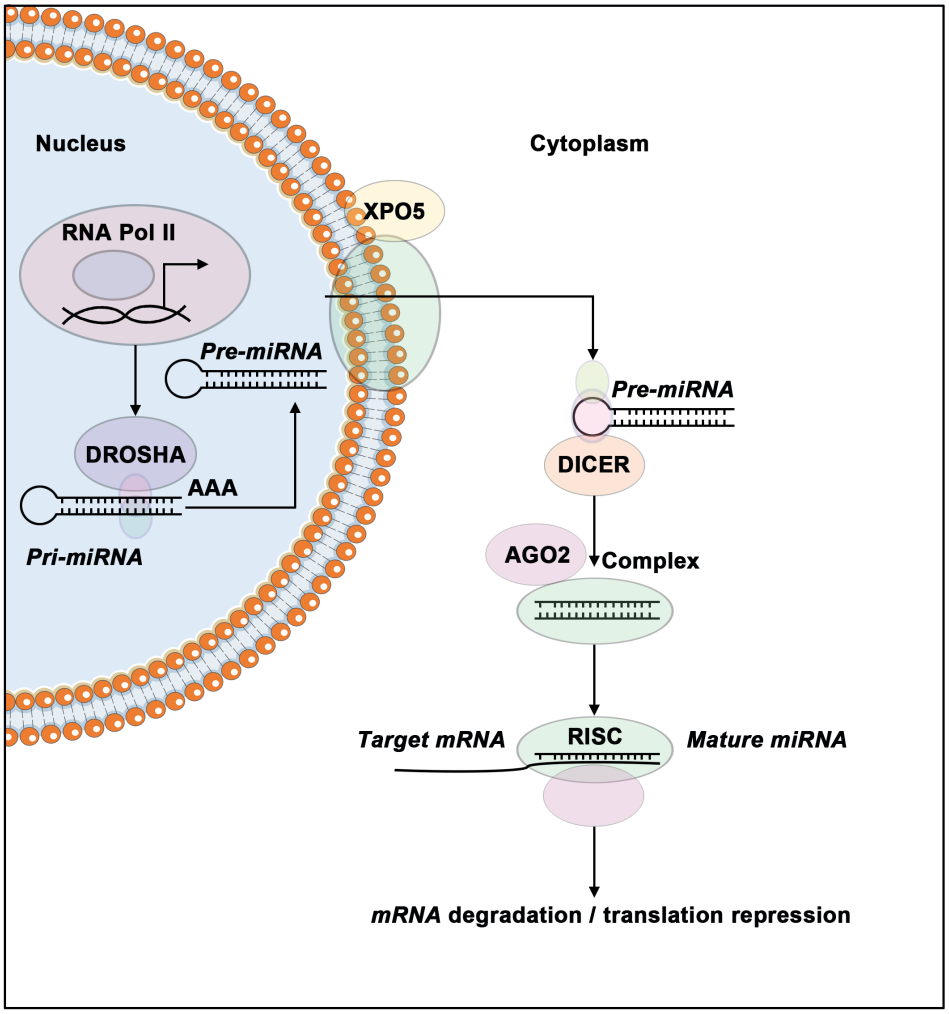

Figure 2. The complex process of miRNA production. RNA Pol II, RNA polymerase II; pri-miRNA, primary miRNA; pre-miRNA, precursor miRNA; XPO5, Exportin 5; AGO 2, Argonaute 2; RISC, RNA-induced silencing complex.

MiRNAs regulate target genes, that behave as 'switch', 'tuning' or 'neutral' regulation (Flynt and Lai, 2008). MiRNAs negatively regulate target genes to an inconsequential

level, which is known as ‘off’ switch (Hobert, 2004, Bartel and Chen, 2004). For example, *lin-4* reduces *lin-14* and *lin-28 lin-14* and *let-7* silences *lin-41* (Lee et al., 1993, Reinhart et al., 2000). Tuning targets still have biological activity and function even in presence of miRNAs (Flynt and Lai, 2008). These miRNAs can fine-tune a potential class of mRNAs to optimize protein expression in particular cell types (Bartel and Chen, 2004). Neutral targets, that have no special impact on the cells, are involved in species-specific regulatory interactions (Flynt and Lai, 2008). These miRNAs pair with mRNAs occasionally, whereas the subsequent downregulation of protein is neutralized or counteracted by feedback mechanisms (Bartel and Chen, 2004).

1.5 MiRNA in cancer

MiRNAs comprise one of the most abundant classes of regulatory genes during the whole process of cancer development (Shenouda and Alahari, 2009). The dysregulation of miRNAs is associated with tumorigenesis (Garo et al., 2021), progression and metastasis (Huang et al., 2021, Shenouda and Alahari, 2009). Cancer associated miRNAs, including oncogenic miRNAs (oncomiR) and tumor suppressor miRNAs (Shenouda and Alahari, 2009), can serve as a driver of metastasis depending on their target genes (Shi et al., 2010, Nicoloso et al., 2009).

OncomiRs promote tumorigenesis and improve malignant progression (Inoue and Inazawa, 2021). As an example, *miR-21* is found in a wide range of human cancer (Si et al., 2007), which directly targets *RAS/MEK/ERK* pathways to drive tumorigenesis and suppress apoptosis (Hatley et al., 2010). Oncogene *miR-21* promoted invasion and metastasis by targeting *PDCD4* and maspin in metastatic breast cancer cells (Kim et al., 2018). Inhibiton of *miR-21* suppressed invasion of breast cancer cells and metastasis formation in lungs (Zhu et al., 2008). *miR-21* also downregulated *JAM-A* to activate progression and metastasis in colorectal cancer (CRC) (Lampis et al., 2021). *miR-9*, a second metastasis promoting miRNA, improved metastatis in breast cancer cells by

targeting *CDH1* in the presence of E-cadherin (Ma et al., 2010) and targeting *LIFR* in the absence of E-cadherin (Chen et al., 2012). The *miR-17-92* cluster (*miR-17*, *miR-18a*, *miR-19a*, *miR-19b-1*, *miR-20a*, and *miR-92-1*) inhibits apoptosis and promotes proliferation of cancer cells, and induces tumor angiogenesis (Mendell, 2008). It has been reported that *miR-17-92* negatively regulated c-myc by HIF-1α (Taguchi et al., 2008).

On the contrary, tumor suppressor miRNA is a class of miRNAs that promote anti-tumor properties, negatively regulating oncogenes to improve the differentiation of tumor cells or to suppress the maliganant behaviors (Salimimoghadam et al., 2021). *MiR-29* activates the tumor suppressor *p53* by targeting *p85α* and *CDC42*, inducing apoptosis of cancer cells (Salimimoghadam et al., 2021). Underexpression of tumor suppressor miRNAs results in invasion and metastasis (Otmani and Lewalle, 2021). A liver-specific tumor suppressor miRNA *miR-122* is downregulated in liver cancers with intrahepatic metastastasis. Restoration of *miR-122* impedes intrahepatic metastasis by regulating *ADAM17* in hepatocellular carcinoma (HCC) (Tsai et al., 2009). *MiR-140* inhibits tumor progression and liver metastasis by targeting *BCL9*/*BCL2* axis in CRC (Liu et al., 2021a). *MiR-34a*, a p53 target, is underexpressed in $CD44^{+}$ prostate cancer cells. Overexpression of *miR-34a* represses clonogenic expansion and metastasis by inhibiting *CD44* (Liu et al., 2011). *MiR-30a*, as a tumor suppressor gene, suppresses tumor development and metastasis by targeting metadherin in breast cancer (Zhang et al., 2014).

MiRNA network functions as a regulator in tumor metastasis by regulating the metastasis-associated genes or modifying epigenetic alterations (Zhang et al., 2010). In 2007, Li Ma and colleagues reported the dysregulation of miRNAs in tumor metastases (Ma et al., 2007). They identified miRNA *miR-10b*, the first metastasis-associated miRNA (metastamiR), highly expressed in metastatic cancer cells. The overexpression of *miR-10b* increased the expression of pro-metastatic gene *RHOC* to promote lung

metastases in non-metastatic cancer cell-derived orthotopic *xenograft* mice (Ma et al., 2007). Hereafter, more and more experimental evidence has been achieved on the significant roles of miRNAs in tumor metastasis (Kim et al., 2018). MiRNAs function as both metastasic activators and suppressors by participating in various steps of migration and invasion, particularly in cancer invasion-metastasis cascade (Le et al., 2010, Li et al., 2021). MiRNAs can also modulate tumor microenvironment of metastasis (Sole and Lawrie, 2021) and reprogram the formation of metastatic niche (Zeng et al., 2018, Feng et al., 2019). In addition, identified miRNA signatures from body fluids such as circulating blood (Cai et al., 2021) and urine (Aftab et al., 2021) are used as potential non-invasive biomarkers for diagonosis and prognosis in different types of cancer (Izumi et al., 2021). Prostasomes are extracellular vesicles derived from the prostate, participating in tumor metastasis. The prostate cancer cells secret prostasomes containing miRNAs to the extracellular environment (Valentino et al., 2017). MiRNAs in plasma and serum microvesicles can potentially be utilized in the diagnosis and prognosis of prostate cancer, such as miR-16, miR-34b, miR-92a, *miR-92b*, *miR-103*, *miR-107*, *miR-197* and *miR-328.* (Lodes et al., 2009).

1.6 *Let-7* miRNA

The *lethal-7* (*let-7*) family of microRNAs were first discovered as heterochronic regulators in *Caenorhabditis elegans* (*C. elegans*), *Drosophila* (late larval stages), zebrafish (48 hours after fertilization), and in annelids and molluscs (adult stages) (Pasquinelli et al., 2000). It is well conserved in a variety of species (e.g., mammals) and governs temporal transitions during development in phylogeny (Roush and Slack, 2008, Pasquinelli et al., 2000). In *C. elegans*, increase of *let-7* leads to precocious expression of adult fates during the larval stages, whereas *let-7* deficiency results in reiteration of larval cell fates during the adult stage (Reinhart et al., 2000). In humans, the *let-7* family includes *let-7a*, *let-7b*, *let-7c*, *let-7d*, *let-7e*, *let-7f*, *let-7g*, *let-7i* and *miR-98*. They are abundantly expressed in embryonic and differentiated cells

(Boyerinas et al., 2010). The high expression level of *let-7* promotes differentiation in both normal and tumor cells (Boyerinas et al., 2010). *Let-7* deficiency may enhance transformation from proliferative or differentiated normal cells to cancer stem cells (CSCs) that are dedifferentiated (Bussing et al., 2008).

So far, *let-7* is generally regarded as a tumor suppressor miRNA (Qian et al., 2011). Decreased expression of *let-7* is associated with lymph node metastasis and poor prognosis (Bussing et al., 2008). Various oncogenes are targeted by *let-7*, such as *RAS* (Shui et al., 2022), *HMGA2*, *IMP-1* (Boyerinas et al., 2010), *CDC34*, *ARID3A* (Boyerinas et al., 2008), *MYC* (Wang et al., 2015), *LIN28B* (Qian et al., 2011) and others (Balzeau et al., 2017). The crosstalk between *let-7* and its targets contributes to tumor progression (Wang et al., 2015, Kassam et al., 2013). For instance, *let-7* targets *IGF1R* and *AKT2* to suppress the activity of PI3K/AKT pathway and targets *RAS* to the activity of inhibit MAPK pathway (Wang et al., 2015). The expression of mature *let-7s* is attenuated or absent during tumorigenesis (Wang et al., 2015, Chen et al., 2011), while transcripts of the primary *let-7* (*pri-let-7*) and the hairpin precursor *let-7* (*pre-let-7*) can be detected in undifferentiated cells (Bussing et al., 2008). This expression pattern of *let-7* indicates distinct post-transcriptional regulation of mature *let-7*, such as RBPs-mediated regulation.

1.7 LIN28 and LIN28-mediated regulation

LIN28 was originally found in *C. elegans* (Ambros and Horvitz, 1984, Shyh-Chang and Daley, 2013). Mammalian LIN28 highly expressed in embryonic stem cells (ESCs), while decreases upon differentiation (Shyh-Chang and Daley, 2013). LIN28 family includes homolog A (LIN28A) and homolog B (LIN28B) (Zhang et al., 2016). The human LIN28A gene encodes for the 209-amino acid proteins, and LIN28B gene encodes for the 250-amino acid proteins (Balzeau et al., 2017). LIN28A and LIN28B share the RNA binding domains that are N-terminal CSD (Piskounova et al., 2011) and

C-terminal ZKD (Cys-Cys-His-Cys [CCHC]-type CCHCx2) (Wang et al., 2017). LIN28 CSD recognizes a (U)GAU motif and ZKD binds a GGAG-like element. Both binding domains are involved in recognition of *pre-let-7* through the terminal loop structure (Ustianenko et al., 2018).

LIN28 regulates *let-7* expression (**Figure 3**). LIN28 recognizes and binds to the stem loop of *pri-let-7* and *pre-let-7* to prevent the maturation of *let-7*. In the absence of LIN28, *pre-let-7* will be processed properly, leading to high level of mature *let-7* (Roush and Slack, 2008). In addition, LIN28 can recruit terminal uridylyltransferases (TUTases) to *pre-let-7* to block the cleavage by Dicer in cytoplasm (Heo et al., 2009), initiating the degradation of *let-7* precursors (Wang et al., 2017). TUTase4 is a noncanonical poly (A) polymerase. LIN28 recognizes the GGAG motif to recruit TUTase4, which acts as a uridylyl transferase for *pre-let-7* to block Dicer processing (Heo et al., 2009).

LIN28B is a homolog of LIN28 in humans. High expression of LIN28B is associated with malignant behaviors and poor prognosis in cancer (Wang et al., 2015, Feng et al., 2012). LIN28B/*let-7* pathway modulates several hallmarks of cancer, including proliferation, metabolism, cell death, invasion, and metastasis (Wang et al., 2015). LIN28B promotes cell proliferation and maintains pluripotent cells by binding to *cyclinB* and *CDK4* in human and mouse ESCs (Xu et al., 2009). In human ESCs, LIN28B enhances metabolism through interaction with glycolysis enzymes such as HK1, PDHA1 and PDHB (Peng et al., 2011). The interaction of LIN28B and *let-7* also regulates cell apoptosis (Attali-Padael et al., 2021), induces the differentiation of CSCs (Zhou et al., 2013) and contributes to the therapeutic sensitivity or resistance (Wang et al., 2013). For example, overexpression of LIN28 suppresses radiation-induced apoptosis in breast cancer cells, whereas LIN28-induced radioresistance can be decreases by transfection of *let-7a* (Wang et al., 2013). LIN28 is associated with tumor size and HER2 expression in breast cancer, and promotes cancer cell growth by

regulating HER2 (Feng et al., 2012). Furthermore, the LIN28B/*let-7* pathway regulates invasion and metastasis via epithelial-mesenchymal transition (EMT) in various cancer cells (Liu et al., 2013). Overexpression of LIN28B promotes angiogenesis and EMT in KRAS-driven lung adenocarcinomas, inducing phosphor-AKT and nuclear c-MYC expression (Meder et al., 2018).

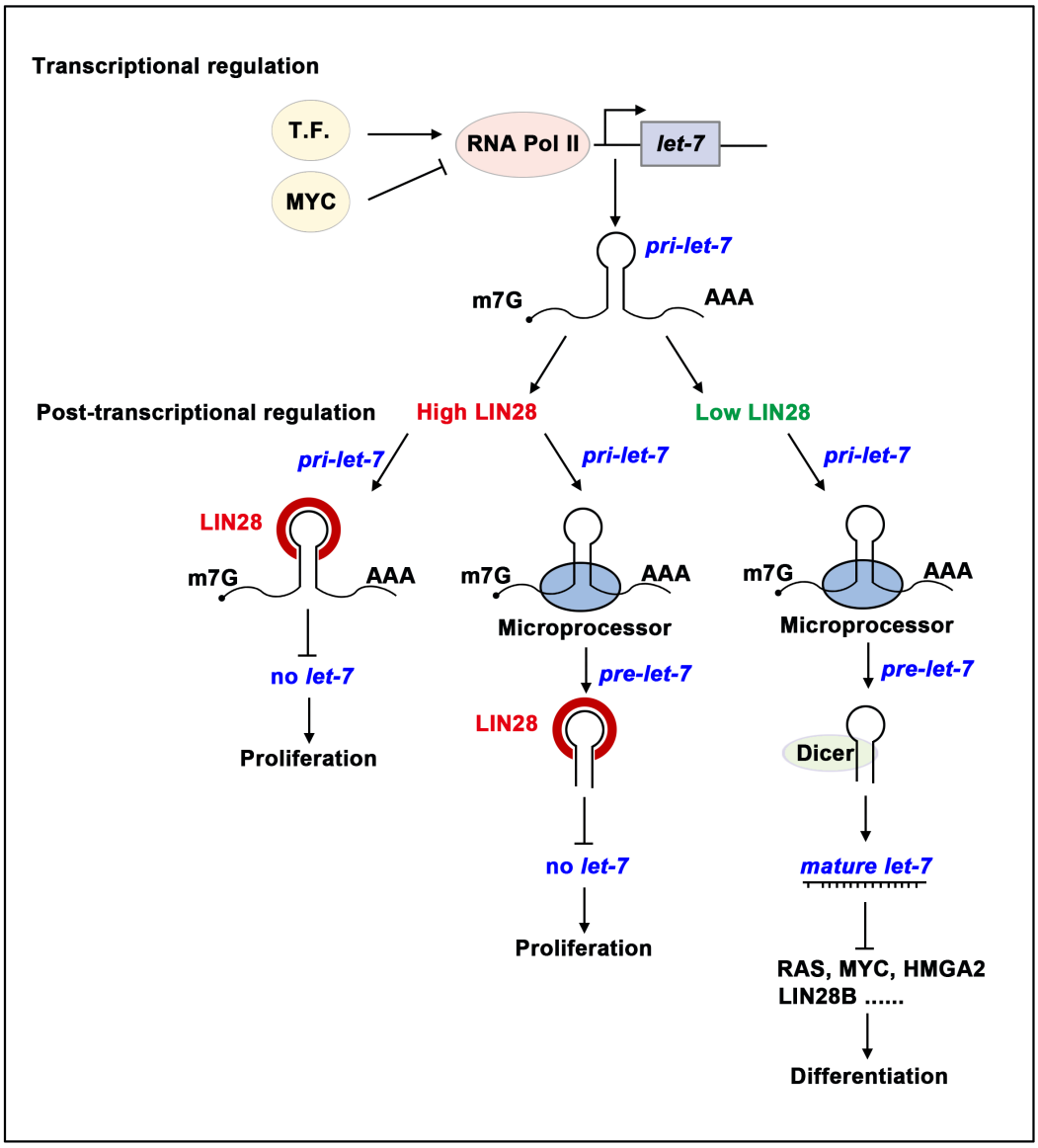

Figure 3. The process of *let-7* miRNA regulated by the RNA-binding protein LIN28. T.F., transcription factors; RNA Pol II, RNA polymerase II; *pri-let-7*, primary *let-7*; *pre-let-7*, precursor *let-7*.

1.8 Cell-to-cell communication

Stephen Paget proposed that tumor metastasis depended on cross-talk between the "seeds" and the "soil", which is the conventional pathogenesis of tumor metastases (Fidler, 2003). The "seed" represents disseminated tumor cells, and the "soil" indicates the microenvironment of tumor metastasis (Fidler and Poste, 2008). The tumor microenvironment is composed of cancerous and non-cancerous cells such as fibroblasts, as well as molecules and mediators (Oktay et al., 2015). The interaction between cancerous and neighbouring cells regulates metastatic processes through direct cell-to-cell contact or non-contact procedures (O'Driscoll, 2015). In this process, intercellular communication mediated by extracellular vesicles (EVs) plays an essential role in the education of the metastatic microenvironment (Xu et al., 2018, Fares et al., 2020). The metastatic tumor cell-derived EVs transfer bioactive cargoes and educate the foreign microenvironment to promote the metastatic colonization and formation (Peinado et al., 2017, Liu et al., 2017, Fares et al., 2020).

Cell-to-cell communication mediated by EVs in the microenvironment of distant organs is important for pre-metastatic niche (PMN) formation and metastasis (Mathieu et al., 2019). EVs, including microvesicles (Wang et al., 2014), exosomes (Feng et al., 2019), ectosomes (O'Driscoll, 2015) and oncosomes (Di Vizio et al., 2012), are lipid bilayer-enclosed extracellular particles that arise from the fusion of surface membrane invaginations with the products of Golgi apparatus (Xu et al., 2018). Tumor-derived EVs play an important role in intercellular communication between stromal and tumor cells in both local and distant microenvironments (Becker et al., 2016). The circulating EVs isolated from cancer patients have been identified to be related with metastasis or relapse in clinic (Lener et al., 2015, Becker et al., 2016).

1.9 Exosomes and exosomal miRNAs

Exosomes are intraluminal vesicles (ILVs) of multivesicular bodies (MVBs) with a diameter of 30 nm to 150 nm (Becker et al., 2016). Exosomes are fused from cellular membranes loading bioactive compounds including DNA, RNA, amino acids, protein, metabolites and others to facilitate intercellular communication (Mathieu et al., 2019, LeBleu and Kalluri, 2020). Exosomes can be released by a variety of cell types such as cancer cells, epithelial cells, immune cells, neural stem cells and mesenchymal cells, enabling intercellular communication (Kalluri and LeBleu, 2020). The transfer of exosomal RNAs (mRNA, miRNA, lncRNA and others) between donor and recipient cells modifies intercellular function and behavior (Becker et al., 2016, Matei et al., 2017) (Mashouri et al., 2019). For example, tumor-derived exosomal *miR-106b-5p* activates intercellular communication of EMT-CRC cell and tumor-associated macrophages mediating CRC metastasis (Yang et al., 2021). Cancer-associated fibroblasts-derived exosomal *miR-500a* increased metastasis by targeting USP28 in breast cancer cell (Chen et al., 2021). Exosomal *miR-210* from human colon cancer cells altered the adhesive ability of neighboring metastatic cells by regulating the process between EMT and mesenchymal-epithelial transition (MET) (Bigagli et al., 2016).

EVs, particularly exosomes, have received a great attention as non-invasive indicators for diagnosis and prognosis of cancers (Hosseini et al., 2022). Tumour-derived cell-free miRNAs are detected in body fluids including plasma, serum, urine and saliva, serving as potential biomarkers for early diagnosis and predict prognosis in various cancers such as gastrointestinal cancer, lung cancer and breast cancer (Schwarzenbach et al., 2014). The major components of exosomal miRNAs derived from cancer cells include pri-miRNAs, pre-miRNAs and mature miRNAs (Tran, 2016, Rupaimoole et al., 2016). *Let-7* is enriched in the extracellular exosomes derived from human stomach cancer cells with high peritoneal-metastatic potential (AZ-P7a cell line) to maintain invasiveness (Ohshima et al., 2010). *Let-7* transcripts is also identified in ovarian cancer cells and corresponding exosomes, which is associated with invasive potential of ovarian cancer cells (Kobayashi et al., 2014).

1.10 Aim of the work

Up to date, there is only little known about extracellular *let-7* in cancer biology. Although the expression of *let-7s* was detected in tumor cell-derived exosomes, the influence of intercellular transfer of *let-7s* through exosomes remains unclear. The aim of this study is to generate simplified *in vitro* co-culture systems to simulate the metastases and examine the roles of *let-7* transfer in the metastatic niche.

2. Materials and methods

2.1 Materials

2.1.1 Cells

BE2C (human neuroblastoma cell), Kelly (human neuroblastoma cell), CHP-212 (human neuroblastoma cell), PANC-1 (human pancreatic cancer cell), HDF (human dermal fibroblasts), NIH 3T3 (mouse embryonic fibroblasts), AML12 (alpha mouse liver cell) and HEK 293T (human embryonic kidney cell) cells were used in this dissertation. LIN28B knockout (LIN28B KO) cell lines were generated based on CRISPR Cas9/sgRNA system in BE2C, Kelly and PANC-1. LIN28B wildtype (LIN28B KO+LIN28B WT) or mutant (LIN28B KO+LIN28B MUT) cell lines were generated based on LIN28B KO cells. Dual-luciferase reporter (dual Luc, dLuc) expressed cell lines were generated in BE2C, BE2C KO, Kelly, HDF and NIH 3T3. HEK 293T was used for virus amplification and delivery of genome engineering, including the production of lentivirus (LV), retrovirus (RV) and cytomegalovirus (CMV). Parental and gene-edited cell lines are listed in **Table 1**.

Table 1. Parental and gene-edited cell lines

Cell line	Genotype (LIN28B)	*let-7*	Pool/ single clone	Tag
BE2C	-	low	-	-
BE2C-GFP	-	low	pool	GFP
BE2C-LIN28B KO	knockout	low	pool	GFP
BE2C-LIN28B KO +LIN28B WT	knockout+wildtype	high	pool	GFP
BE2C-CTRL (0301)	-	low	single clone	GFP
BE2C-LIN28B KO (0303)	knockout	high	single clone	GFP
BE2C-LIN28B KO +LIN28B WT	knockout+wildtyp	low	pool	GFP
BE2C-dLUC	dual-luciferase reporter	low	pool	-
BE2C-CTRL-dLUC	dual-luciferase reporter	low	pool	-

BE2C-LIN28B KO-dLUC	dual-luciferase reporter	high	pool	-
Kelly	-	low	-	-
Kelly-CTRL (0201)	-	low	single clone	-
Kelly-LIN28B KO (0202)	knockout	high	single clone	-
Kelly-dLUC	dual-luciferase reporter	low	pool	-
CHP-212	-	low	-	-
PANC1-LIN28B KO	knockout	low	pool	-
HDF	-	high (relatively)	-	-
NIH 3T3	-	high	-	-
NIH 3T3-RFP	-	high	pool	RFP
NIH 3T3-dLUC	dual-luciferase reporter	high	pool	-

2.1.2 Cell culture reagents

The reagents for cell culture are listed in **Table 2**.

Table 2. Cell culture reagents

Reagent	Cat. No.	Supplier
DMEM, high glucose	41965-039	Gibco
Advanced DMEM/F-12	12634028	Gibco
DPBS, no calcium, no magnesium	14190-094	Gibco
Fetal Bovine Serum Superior	S0615	Biochrom, Merck
Penicillin-Streptomycin-Glutamine (100X)	10378016	Gibco
Penicillin-Streptomycin	DE17-603E	Lonza
Trypsin/EDTA 10x 100ml	BE02-007E	Lonza
X-tremeGENE 9 DNA Transfection Reagent	06365787001	Roche
Opti-MEM reduced-serum medium	31985062	Gibco
Protamine sulfate for biochemistry	1101230005	Merck
Puromycin	ant-pr-1	Invivogen
Blasticindin (solution)	ant-bl-05	Invivogen
G418	G8168	Sigma-Aldrich
Plasmocin prophylactic	ant-mpp	Invivogen
Dual-Glo Luciferase Assay System	E2940	Promega
Doxycycline hydrochloride	D3447-500MG	Sigma-Aldrich
DAPI	D3571	Invitrogen

Insert, 6 Well, PET 0.4μm, TP	83.3930.041	Sarstedt
Insert, 6 Well, PET 1μm, TP	83.3930.101	Sarstedt
Insert, 6 Well, PET 3μm, TL	83.3930.300	Sarstedt
Insert, 6 Well, PET 5μm, TL	83.3930.500	Sarstedt
Insert, 6 Well, PET 8μm, TL	83.3930.800	Sarstedt
C-Chip Disposable Hemocytometer	DHC-N01	Incyto

2.1.3 Materials for mRNA and miRNA assays

The materials for mRNA and miRNA assays are listed in **Table 3**.

Table 3. Materials for mRNA and miRNA assays

Reagent	Cat. No.	Supplier
QuantiTect SYBR Green PCR Kit	204143	Qiagen
miScript SYBR Green PCR Kit	218076	Qiagen
miScriptII RT Kit	218161	Qiagen
RNeasy Mini Kit (250)	74106	Qiagen
miRCURY LNA SYBR Green PCR Kit	339347	Qiagen
miRCURY LNA RT Kit	339340	Qiagen
miScript Primer Assay *Hs_Snord48_11*	218300 (MS00007511)	Qiagen
miScript Primer Assay *Hs_Snord68_11*	218300 (MS00033712)	Qiagen
miScript Primer Assay *Hs_RNU6-2_11*	218300 (MS00033740)	Qiagen
miScript Primer Assay *Hs_let-7g_2*	218300 (MS00008337)	Qiagen
miScript Primer Assay *Hs_let-7i_1*	218300 (MS00003157)	Qiagen
miScript Precursor Assay *Hs_let-7b_1_PR*	3014105 (MP00000028)	Qiagen
miScript Precursor Assay *Hs_let-7i_1_PR*	3014105 (MP00000077)	Qiagen
miRCURY LNA miRNA PCR Array Precursor *Hs_let-7g_1*	339317 (YCP1831343)	Qiagen
U6 snRNA miRCURY LNA miRNA PCR Assay	339306 (YP00203907)	Qiagen

Snord68 miRCURY LNA miRNA PCR Assay	339306 (YP00203911)	Qiagen
hsa-let-7a-5p miRCURY LNA miRNA PCR Assay	339306 (YP00205727)	Qiagen
hsa-let-7b-5p miRCURY LNA miRNA PCR Assay	339306 (YP00204750)	Qiagen
hsa-let-7c-5p miRCURY LNA miRNA PCR Assay	339306 (YP00204767)	Qiagen
hsa-let-7d-5p miRCURY LNA miRNA PCR Assay	339306 (YP00204124)	Qiagen
hsa-let-7e-5p miRCURY LNA miRNA PCR Assay	339306 (YP00205711)	Qiagen
hsa-let-7f-5p miRCURY LNA miRNA PCR Assay	339306 (YP00204359)	Qiagen
hsa-let-7g-5p miRCURY LNA miRNA PCR Assay	339306 (YP00204565)	Qiagen
hsa-let-7i-5p miRCURY LNA miRNA PCR Assay	339306 (YP00204394)	Qiagen
dre-let-7h miRCURY LNA miRNA PCR Assay	339306 (YP02104276)	Qiagen
Trizol Reagent	15596018	Invitrogen
Buffer RWT	1067933	Qiagen
Buffer RPE	1018013	Qiagen
RNase AWAY™ Decontamination Reagent	10328011	Invitrogen
DNAZap™ PCR DNA Degradation Solutions	AM9890	Invitrogen
Chloroform anhydrous	288306	Sigma-Aldrich
Ethanol 200 Proof	BP2818-500	Fisher Bioreagents
TE, pH 8.0, RNase-free	AM9849	Invitrogen

2.1.4 Materials for protein assays

The materials for protein assays are listed in **Table 4**.

Table 4. Materials for protein assays

Reagent	Cat. No.	Supplier
Intercept® T20 (PBS) Antibody Diluent	927-75001	LI-COR

Intercept® (PBS) Blocking Buffer	927-70001	LI-COR
Pierce™ BCA Protein Assay Kit	23227	Thermo Fisher Scientific
Halt™ Protease and Phosphatase Inhibitor	78442	Thermo Fisher Scientific
Nupage Sample Reducing Agent	NP0009	Thermo Fisher Scientific
Nupage LDS Sample Buffer	NP0007	Thermo Fisher Scientific
Amersham™ ECL™ Rainbow™ Marker - Full range	GERPN800E	Merck
Immobilon-FL PVDF Membrane	IPFL00005	Merck
4-15% Mini-Protean TGX Precast Gels	4561085	BIO-RAD
10X Tris/Tricine/SDS Buffer	1610744	BIO-RAD
Thick Blot Filter Paper	1703932	BIO-RAD

2.1.5 Antibodies for protein assays

The antibodies for protein assays are listed in **Table 5**.

Table 5. Antibodies for protein assays

Antibody	Cat. No.	Supplier
LIN28B Antibody	#4196	Cell Signaling Technology
CD9 Monoclonal Antibody (Ts9)	10626D	Invitrogen
CD63 Monoclonal Antibody (Ts63)	10628D	Invitrogen
IRDye® 800CW Goat anti-Mouse IgG Secondary Antibody	926-32210	LI-COR Biosciences
IRDye® 680LT Goat anti-Rabbit IgG Secondary Antibody	926-68021	LI-COR Biosciences
Rb pAb to alpha Tubulin	ab4074	Abcam

2.1.6 Materials for exosome isolation

The materials for exosome isolation are listed in **Table 6**.

Table 6. Materials for exosome isolation

Reagent	Cat. No.	Supplier
OptiPrep™ Density Gradient Medium	92339-11-2 D1556-250ml	Sigma-Aldrich
SeraMir Exosome RNA Purification Kit	RA806TC	System Biosciences
Total Exosome Isolation Reagent	4478359	Invitrogen
Total Exosome RNA & Protein Isolation Kit	4478545	Invitrogen
UltraPure 1M Tris-HCL pH 7.5	15567027	Invitrogen
UltraPure™ DNase/ RNase-Free Distilled Water	10977035	Invitrogen
Sucrose	S0389	Sigma-Aldrich
11.2 mL, OptiSeal™ Polypropylene Tube, 16 x 70mm	362181	Beckman Coulter
14 mL, Open-Top Thinwall Ultra-Clear Tube, 14 x 95mm	344060	Beckman Coulter

2.1.7 Materials for molecular assays

The materials for molecular assays are listed in **Table 7**.

Table 7. Materials for molecular assays

Reagent	Cat. No.	Supplier
pCIneo-RL-*let7*-perf	115367	Addgene
pCIneo-RL-*let7*-3xBulgeB	115368	Addgene
pCIneo-RL-*let7*-3xBulgeB-mut	115369	Addgene
psiCHECK2-*let-7* MT	78261	Addgene
psiCHECK2-*let-7* WT	78260	Addgene
pLenti-pHluorin_M153R-CD63	172117	Addgene
pLenti-pHluorin_M153R-CD63-mScarlet	172118	Addgene
gag/pol	14887	Addgene
lentiCRISPR v2	52961	Addgene
pBS-CMV-gagpol	35614	Addgene
pRRLsin-SV40 T antigen-IRES-mCherry	58993	Addgene
pBABE-puro-hTERT	1771	Addgene
One Shot™ Stbl3™ Chemically Competent E. coli	C737303	Thermo Fisher
One Shot™ TOP10 Chemically Competent E. coli	C404010	Invitrogen
ZymoPURE II Plasmid Maxiprep Kit	D4202	Zymo Research

ZR Plasmid Miniprep - Classic (100 Preps)	D4015	Zymo Research
Zymo-Gel Purification Kit	D4007	Zymo Research
quikchange II XL site-directed mutagenesis kit	200521	Agilent

2.1.8 Experimental equipments

The main experimental equipments are listed in **Table 8**.

Table 8. Main experimental equipments

Equipment	Cat. No.	Supplier
LightCycler	LightCycler 480	Roche
Thermal Cyclers	Mastercycler Pro	Eppendorf
Fluorometer	Qubit 4	Invitrogen
Spectrophotometer	Nanodrop 2000	Thermo Scientific
Ultrocentrifuge	Optima LE-80K	Beckman Coulter
Centrifuge	KR 22 i	Jouan
Laboratory centrifuge	Heraeus Multifuge X3R	Thermo Scientific
Laboratory centrifuge	Mikro 200	Hettich
CO_2 Incubator	BB 15	Thermo Scientific
Luminescence MultiMode Microplate Reader	Spark 10M	Tecan
Multi-Detection Microplate Reader	Synergy HT	BioTek
Microscope platform	Axio Observer	ZEISS
Biosafety Cabinet	MAXISAFE 2030i	Thermo Scientific
TermoMixer	TermoMixer C	Eppendorf
Flow Cytometer	LSR II	BD

2.2 Methods

2.2.1 Cell culture

Human and murine cells were purchased from ATCC (Manassas, VA) and were cultured at 37 °C in an atmosphere of 95% air and 5% CO_2. BE2C, Kelly and CHP-212 cells were cultured in Advanced Dulbecco's Modified Eagle Medium/Ham's F-12 medium (DMEM/F-12, Gibco) supplemented with 10% fetal bovine serum (Gibco) and 1% Penicillin-Streptomycin-Glutamin (Gibco, 100X). PANC-1, HDF, NIH 3T3, AML12 and HEK 293T cells were cultured in Dulbecco's modified Eagle's medium (DMEM, Gibco) supplemented with 10% fetal bovine serum (FBS, Gibco) and 1% Penicillin-Streptomycin (P/S, Gibco). Cell culture media for different cell lines are listed in **Table 9**.

Table 9. Cell culture medium

Cell line	Medium	FBS (%)	P/S (%)	Glutamine (%)
BE2C	DMEM/F12	10	1	1
Kelly	DMEM/F12	10	1	1
CHP-212	DMEM/F12	10	1	1
PANC-1	DMEM	10	1	-
HDF	DMEM	10	1	-
NIH 3T3	DMEM	10	1	-
AML12	DMEM	10	1	-
HEK 293T	DMEM	10	1	-

2.2.2 Viral packaging and production

HEK 293T cells were plated at a density of 11×10^6 in a 15 cm cell culture dish. The plasmid DNA was transfected in HEK 293T cells by X-tremeGENE 9 DNA Transfection Reagent (Roche) in Penicillin-Streptomycin free DMEM with 10% FBS. 24 h after transfection, changed 25 mL fresh medium containing 20% FBS. 12 h later, changed 12.5 mL fresh medium containing 20% FBS. Another 12 h later, collected supernantant containing virus and filtered through a 0.2 μm filter. Then changed another 12.5 mL fresh medium containing 20% FBS. 12 h later, collected supernantant containing virus and filtered through a 0.2 μm filter. Virus suspensions were ready to

use or freezed at -80 °C. The components for lentiviral packaging are listed in **Table 10**.

Table 10. Lentiviral packaging components

Reagent	Amount
Opti-MEM	750 µL
Plasmid DNA	16.5 µg
pMD2.G	8.25 µg
pPAX2	12.75 µg
Opti-MEM	750 µL
X-tremeGENE 9	90 µL
Incubation time	20 min

The components for retroviral packaging are listed in **Table 11**.

Table 11. Retroviral packaging components

Reagent	Amount
Opti-MEM	750 µL
Plasmid DNA	12 µg
pMD2.G	6 µg
gag/pol	12 µg
Opti-MEM	750 µL
X-tremeGENE 9	90 µL
Incubation time	20 min

2.2.3 Generation of stable cell line with constitutive gene expression

Cells were plated at a density of 5×10^6 in a 10 cm cell culture dish or 2×10^5 in a 6-well plate. Cells were infected with 1 mL virus suspension by protamine sulfate (12 µg/mL). 16 h after virus infection, removed medium and washed with PBS for three times. Cells were cultured with fresh medium for 24 h, and then selected by antibiotics. The optimal concentration for antibiotic selection is listed in **Table 12**.

Table 12. Antibiotic selection concentration

Cell line	Puromycin (μg/mL)	Blasticidin (μg/mL)	G418/Neomycin (μg/mL)
BE2C	2.5	10	800
Kelly	1.2	-	800
NIH 3T3	2	4	500
HDF	-	10	500

2.2.4 Cell co-culture

2.2.4.1 The generation of a dual-luciferase reporter-based co-culture system

A dual-luciferase reporter-based co-culture system was generated. First, dual-luciferase reporter constructs harboring eight fully complementary *let-7* target elements were generated based on pmirGLO vector (Promega). Then we generated dual-luciferase reporter stabley expressing recipient cells and performed co-culture with donor cells. The luciferase activity was measured at day 3, 5 and 10 respectively. The renilla luciferase was the testing reporter, which could be activated in the absence of *let-7*. The firefly luciferase reporter was internal reference control. The co-cultured cells were collected to measure the intercellular transfer of *let-7*.

2.2.4.2 The generation of a microporous insert-based co-culture system

A microporous insert-based co-culture system was generated. The tissue culture-treated (TC) inserts (Sarstedt) with a pore diameter of 1.0 μm or 3.0 μm were validated to be suitable for co-culture system for 6 well-plates (all pore sizes included 0.4 μm, 1.0 μm, 3.0 μm, 5.0 μm and 8.0 μm). We plated recipient cells (e.g., dual-luciferase reporter stabely expressing NIH 3T3 cell, NIH 3T3-dual Luc) in the bottom chambers and donor cells (e.g., NIH 3T3, BE2C or Kelly) in the top inserts of 6-well plates. The recipient and donor cells were collected to measure *let-7* transfer after co-culture for 5 days.

2.2.4.3 The generation of a cell culture conditioned medium system

A cell culture conditioned medium system was generated. The recipient cells were seeded at a density of 2×10^6 in 15 cm tissue dishes with 30 mL media for 3 days. The supernantant (cell culture conditioned media, CCM) were collected and centrifuged at 300 g_{avg} for 10 min at 4 °C respectively. After filtering with 0.22 μm filter, the CCM were ready to use. The donor cells were plated at a density of 25×10^3 in 6-well plates and incubated with different CCM for 3 or 5 days. Fresh CCM were changed every 2 days. The recipient cells were collected to measure *let-7* transfer after co-culture.

2.2.4.4 The generation of an exosome-rich conditioned medium system

An exosome-rich conditioned medium system was generated. The recipient cells were seeded at a density of 2×10^6 in 15 cm tissue dishes (8 dishes for each cell) with 15 mL serum-free medium for 24 h. The supernantant (CCM) were collected and centrifuged at 300 g_{avg} for 10 min at 4 °C respectively. After filtering with 0.22 μm filter, the CCM were used for exosome isolation (see 2.2.4). The isolated exosomes were resuspended and then exosome-rich CCM were ready to use. The donor cells were plated at a density of 25×10^3 in 6-well plates and incubated with exosome-rich CCM for 5 days. Fresh exosome-rich CCM were changed every 2 days. The recipient cells were collected to measure *let-7* transfer after co-culture.

2.2.4.5 The generation of a fluorescence-based co-culture system

A fluorescence-based co-culture system was generaged between fibroblasts and tumor cells. First, red fluorescent protein (RFP) expressing NIH 3T3 cells (NIH 3T3-RFP) and green fluorescent protein (GFP) expressing BE2C cells (BE2C-GFP, BE2C-LIN28B KO-GFP and BE2C-LIN28B KO+LIN28B WT-GFP) were generated. BE2C-GFP at a density of 50×10^3 and NIH 3T3-RFP at a density of 50×10^3 were co-cutured. Cell morphologies were dynamically observed under fluorescence microscopy.

2.2.5 Cell-free exosome isolation

2.2.5.1 Exosome isolation with ultracentrifugation

We collocted sufficient CCM from cells (~100 mL for each sample) and performed ultracentrifugation (UC) at 100,000 g_{avg} for 90 min with NVT65 rotor at 4°C. The supernatant was carefully removed, and crude exosome-containing pellets were resuspended in ice-cold PBS and repeated ultracentrifugation at 100,000 g_{avg} for 90 min with NVT65 rotor at 4°C. Rotors applied for UC are listed in **Table 10**.

Table 13. Rotor application for UC (Beckman Coulter)

Step	Rotor	Speed (g)	Speed (rpm)	Duration (time)	Tm (°C)	Centrifuge tube
1	NVT65	100,000	40,000	90 min	4	OptiSeal
2	NVT65	100,000	40,000	90 min	4	OptiSeal

2.2.5.2 Exosome isolation with OptiPrep-UC

We collocted sufficient CCM from cells (~100 mL for each sample) and performed ultracentrifugation at 100,000 g_{avg} for 90 min with NVT65 rotor at 4°C. The supernatant was carefully removed, and crude exosome-containing pellets were resuspended in ice-cold PBS and repeated ultracentrifugation at 100,000 g_{avg} for 90 min with NVT65 rotor at 4°C. Exosomes were purified using OptiPrep™ density gradient media at 100,000 g_{avg} (28,000 rpm) with SW40 rotor for 18 h (over night) at 4°C. Top layer media of 3~4 mL were removed and the four fractions (~3 mL for each fraction) were collected from the top of the gradient respectively. The exosomes from each fraction were resuspended in ice-cold PBS and ultracentrifuged at 100,000 g_{avg} (40,000 rpm) for 90 min with NVT65 rotor at 4°C. The pure exosomes were collected after supernatant was removed. Positive fractions were resuspended in ice-cold PBS and ultracentrifuged at 100,000 g_{avg} (40,000 rpm) for 90 min at 4°C with a NVT65 rotor. The final pellets were pure exosomes and were ready to use.

Table 14. Rotor application for OptiPrep-UC (Beckman Coulter)

Step	Rotor	Speed (g)	Speed (rpm)	Duration (time)	Tm (°C)	Centrifuge tube
1	NVT65	100,000	40,000	90 min	4	OptiSeal
2	NVT65	100,000	40,000	90 min	4	OptiSeal
3	SW40	100,000	28,000	18 h	4	Ultra-Clear
4	NVT65	100,000	40,000	90 min	4	OptiSeal

Briefly, a discontinuous iodixanol gradient was prepared by diluting a stock solution of OptiPrep™ (60% w/v) with 0.25 M sucrose/10 mM Tris, pH 7.5 to generate 40%, 20%, 10% and 5% w/v iodixanol solutions (Lobb et al., 2015, Witwer et al., 2013). With care, the discontinuous iodixanol gradient was generated by sequentially layering 3 mL each of 40%, 20% and 10% (w/v) iodixanol solutions, followed by 2.5 mL of the 5% iodixanol solution in 14 x 89 mm Ultra-Clear™ Beckman Coulter centrifuge tubes at 4°C overnight. Rotors applied for OptiPrep-UC are listed in **Table 11**. The components of OptiPrep density gradient medium are listed in **Table 12**.

Table 15. OptiPrep density gradient medium preparation

Layer	Iodixanol solution (%, w/v)	Volum (mL)
1	5	2.5
2	10	3
3	20	3
4	40	3

2.2.5.3 Exosome isolation with ExoQuick

CCM were collected and centrifuged at 3000 g_{avg} for 15 minutes to remove cells and cell debris. 5 ml media conbined with 1 ml ExoQuick-TC (System Biosciences) were mixed well and placed at 4°C overnight. The supernatant was removed, and the exosome pellets were collected following centrifugation at 13,000 rpm for 2 min. Rotors applied for ExoQuick are listed in **Table 13**.

Table 16. Rotor application for ExoQuick (Jouan)

Rotor	Speed (rpm)	Duration (time)	Tm (°C)
AK 16-205	13,000	2 min	4

2.2.6 Exosomal RNA purification

RNA of exosomes pelleting by ExoQuick kit (System Biosciences) was extracted following the instructions of SeraMir (System Biosciences). 350 µl LYSIS Buffer were added into the exosome pellets and placed at room temperature for 5 min to allow complete lysis. Adding 200µl of 100% Ethanol, the solution was transferred to spin columns and centrifuged at 13,000 rpm for 1 min. The supernantant was discared and the spin columns were washed by WASH Buffer twice. Then, discard flow-through and centrifuged at 13,000 rpm for 2 min to dry. Discarded collection tube and assembled spin column with a fresh, RNase-free 1.5ml elution tube. Added 30µl ELUTION Buffer directly to membrane in spin column and centrifuged at 2,000 rpm for 2 minutes to load buffer in membrane. Increase speed to 13,000 rpm and centrifuge for 1 min to elutes exoRNAs. 30-40µl exosome RNA were recovered and the concentration was measured using with the Qubit 4 Fluorometer (Thermo Fisher Scientific).

2.2.7 Exosomal protein purification

Protein was extracted from exosomes pelleting by OptiPrep™ density gradient ultracentrifugation. The exosome pellets were resuspended by RIPA buffer containing Halt™ Protease and Phosphatase Inhibitor (100X, Thermo Fisher Scientific) and placed on ice for 30 min for complete lysis. Centrifuged the lysate at 12,000 g_{avg} for 15 minutes and immediately transferred the supernatant to a fresh tube. The protein concentration was measured by BCA Protein Assay kit (Thermo Fisher Scientific). The exosome lysate was added with 4x Nupage LDS sample buffer (Invitrogen, Thermo Fisher Scientific) and heated for 9 min at 95°C in thermocycler. The exosomal protein was ready for immediate use, or stored at -20°C.

2.2.8 Dual-luciferase reporter assays

2.2.8.1 Dual-luciferase reporter assays with reporter constructs stable expression

Dual-luciferase reporter constructs were generated. The renilla luciferase reporter construct contained 8 *let-7* binding sites, that could bind to *let-7* to inactivate the luciferase reporter. The firefly luciferase reporter construct was reference control. Then the dual-luciferase reporter constructs stably expressed cells were generated for the co-culture assays. The luminescence activities of both firefly and renilla luciferase were analyzed using Dual-Luciferase Reporter Assay System (Promega) following the instruction. Cell pellets were resuspended by media and plated into 96-well plates (75 μL for each well). 75 μL Dual-Glo® Luciferase Assay Reagent was added to each well, incubating at room temperature for 15 min. Measured firefly luminescence (control reporter) intermittently (15 min, 30 min and 45 min respectively) using luminometer instrument. Then added 75 μL Dual-Glo® Stop & Glo® Reagent to each well, incubating at room temperature for 15 min. Measured Renilla (experimental reporter) luminescence intermittently (15 min, 30 min and 45 min respectively) using luminometer instrument. 5 technical replicates for each sample. Calculated ratio of Renilla: firefly luminescence for each well.

2.2.8.2 Dual-luciferase reporter assays with luciferase reporter transfection

The pCIneo-RL-*let7*-perf, pCIneo-RL-*let7*-3xBulgeB, pCIneo-RL-*let7*-3xBulgeB-mut, psiCHECK2-*let-7* MT and psiCHECK2-*let-7* WT constructs were purchased from Addgene (see 2.1.7). Briefly, firefly luciferase reporter (reference control) and luciferase renilla reporter (psiCHECK2-*let-7* WT was used for co-culture assays) were transfected in recipient cells by X-tremeGENE 9 DNA Transfection Reagent (Roche, Sigma-Aldrich) simultaneously before luciferase reporter assay performing. The

luminescence activities of both firefly and renilla luciferase were analyzed using Dual-Luciferase Reporter Assay System (Promega) following the instruction (see 2.2.7.1).

2.2.9 Fluorescence-activated cell sorting

Briefly, cell co-culture was performed between NIH 3T3-RFP and BE2C-GFP (parental BE2C-GFP, BE2C-LIN28B KO-GFP or BE2C-LIN28B KO+LIN28B WT-GFP). After co-cultured, fluorescence-activated cell sorting (FACS) were performed using Flow Cytometry to collect co-cultured NIH 3T3-RFP and BE2C-GFP respectively. FACS-sorted cells were cultured or ready to use.

2.2.10 Real-time PCR

2.2.10.1 Real-time PCR of miRNA (miScript)

Tissue cells were homogenized in TRIzol Reagent (Invitrogen). Chloroform was added to separate the homogenate into a clear upper aqueous layer, an interphase, and an organic layer. The aqueous layer was collected to recover RNA using RNeasy Mini Kit (Qiagen). First-strand cDNA was synthesized using miScriptII RT Kit (Qiagen). Real-time PCR was performed using miScript SYBR Green PCR Kit (Qiagen). The components for reverse transcription (RT) reaction (miScript, miRNA) are listed in **Table 14**.

Table 17. RT reaction components (miScript, miRNA)

Component	Volume / reaction
5x miScript HiSpec Buffer	4 µl
10x miScript Nucleics Mix	2 µl
RNase-free water	8 µl
miScript Reverse Transcriptase Mix	1 µl
Template RNA	5 µl
Total volume	20 µl

The procedures for RT reaction (miScript, miRNA) are listed in **Table 15**.

Table 18. RT procedure (miScript, miRNA)

Step	Time	Temperature
Reverse transcription step	60 min	37°C
Inactivation of reaction	5 min	95°C
Storage	Hold	4°C

The components for real-time PCR (miScript, miRNA) are listed in **Table 16**.

Table 19. Real-time PCR reaction components (miScript, miRNA)

Component	Volume / reaction (96-well)
2x QuantiTect SYBR Green PCR Master Mix	12.5 µl
10x miScript Universal Primer	2.5 µl
10x miScript Primer Assay	2.5 µl
RNase-free water	5 µl
Template cDNA	2.5 µl
Total volume	25 µl

The procedures for real-time PCR (miScript, miRNA) are listed in **Table 17**.

Table 20. Real-time PCR cycling conditions (miScript, miRNA)

Step	Time	Temperature
Initial activation	15 min	95°C
3-step cycling		
Denaturation	15 s	94°C
Annealing	30 s	55°C
Extension	30 s	70°C
Cycle number	45 cycles	

2.2.10.2 Real-time PCR of miRNA (miRCURY LNA)

Tissue cells were homogenized in TRIzol Reagent (Invitrogen). Chloroform was added to separate the homogenate into a clear upper aqueous layer, an interphase, and an organic layer. The aqueous layer was collected to recover RNA using RNeasy Mini Kit (Qiagen). First-strand cDNA was synthesized using miRCURY LNA RT Kit (Qiagen). Real-time PCR was performed using miRCURY LNA SYBR Green PCR Kit (Qiagen). The components for RT reaction (miRCURY LNA, miRNA) are listed in **Table 18**.

Table 21. RT reaction components (miRCURY LNA, miRNA)

Component	Volume / reaction
5x miRCURY RT Reaction Buffer	2 µl
10x miRCURY RT Enzyme Mix	1 µl
RNase-free water	5 µl
Template RNA (5 ng/µl)	2 µl
Total volume	10 µl

The procedures for RT reaction (miRCURY LNA, miRNA) are listed in **Table 19**.

Table 22. RT procedure (miRCURY LNA, miRNA)

Step	Time	Temperature
Reverse transcription step	60 min	42°C
Inactivation of reaction	5 min	95°C
Storage	Hold	4°C

The components for real-time PCR (miRCURY LNA, miRNA) are listed in **Table 20**.

Table 23. Real-time PCR reaction components (miRCURY LNA, miRNA)

Component	Volume / reaction (96-well)
2x miRCURY SYBR® Green Master Mix	5 µl
Resuspended PCR primer mix	1 µl
RNase-free water	1 µl
Template cDNA	3 µl
Total volume	10 µl

The procedures for real-time PCR (miRCURY LNA, miRNA) are listed in **Table 21**.

Table 24. Real-time PCR cycling conditions (miRCURY LNA, miRNA)

Step	Time	Temperature
PCR Initial activation step	2 min	95°C
2-step cycling		
Denaturation	10 s	95°C
Combined annealing/ extension	60 s	56°C
Number of cycles	45 cycles	
Melting curve analysis		60°C - 95°C

2.2.10.3 Real-time PCR of total RNA

Tissue cells were homogenized in TRIzol Reagent (Invitrogen). Chloroform was added to separate the homogenate into a clear upper aqueous layer, an interphase, and an organic layer. The aqueous layer was collected to recover RNA using RNeasy Mini Kit (Qiagen). First-strand cDNA was synthesized using miScriptII RT Kit (Qiagen). Real-time PCR was performed using miScript SYBR Green PCR Kit (Qiagen). The components for RT reaction (miScript, total RNA) are listed in **Table 22**.

Table 25. RT reaction components (miScript, total RNA)

Component	Volume / reaction
5x miScript HiFlex Buffer	4 µl
10x miScript Nucleics Mix	2 µl
RNase-free water	8 µl

miScript Reverse Transcriptase Mix	1 µl
Template RNA	5 µl
Total volume	20 µl

The procedures for RT reaction (miScript, total RNA) are listed in **Table 23**.

Table 26. RT procedure (miScript, total RNA)

Step	Time	Temperature
Reverse transcription step	60 min	37°C
Inactivation of reaction	5 min	95°C
Storage	Hold	4°C

The components for real-time PCR (miScript, total RNA) are listed in **Table 24**.

Table 27. Real-time PCR reaction components (miScript, total RNA)

Component	Volume / reaction (96-well)
2x QuantiTect SYBR Green PCR Master Mix	12.5 µl
Forward Primer	2.5 µl
Reverse Primer	2.5 µl
RNase-free water	5 µl
Template cDNA	2.5 µl
Total volume	25 µl

The procedures for real-time PCR (miScript, total RNA) are listed in **Table 25**.

Table 28. Real-time PCR cycling conditions (miScript, total RNA)

Step	Time	Temperature
Initial activation	15 min	95°C
3-step cycling		
Denaturation	15 s	94°C
Annealing	30 s	55°C
Extension	30 s	70°C

Cycle number	45 cycles

2.2.11 Western blot of total protein

Total proteins were extracted from cells using RIPA buffer with Halt™ Protease and Phosphatase Inhibitor (100X, Thermo Fisher Scientific) and placed on ice for 30 min for complete lysis. Centrifuged the lysate at 12,000 g_{avg} for 15 minutes and immediately transferred the supernatant to a fresh tube. The protein concentration was determined by BCA Protein Assay kit (Thermo Fisher Scientific). The cell lysate was added with 4x Nupage LDS sample buffer (Invitrogen, Thermo Fisher Scientific) and heated for 9 min at 95°C in thermocycler. Loaded samples into Mini-Protean TGX Precast Gels (4-15%, BIO-RAD). Protein gel electrophoresis was performed with SDS running buffer and then transferred to polyvinylidene fluoride (PVDF) membrane in protein transfer buffer. Next, the membrane was incubated with primary antibodies at 4 °C overnight, followed by blocked using Intercept® (PBS) Blocking Buffer (LI-COR). After washing four times with PBST, the membrane was incubated with secondary antibodies at room temperature for 1 h. After washing four times with PBST, western blots were imaged on Odyssey Imaging System (LI-COR).

2.2.12 Statistical analysis

Statistical analysis was performed using SPSS 21.0 software (SPSS Inc.). Data between two groups were compared by using Student's t-test. Two-way ANOVA analysis was used for the comparison between multiple groups. The values are expressed as the mean ± standard deviation of at least three independent experiments. $P < 0.05$ was statistically different. Graphs were plotted using GraphPad Prism 9.0 (GraphPad Software Inc.).

3. Results

3.1 *Let-7* levels alter in an *in vitro* co-culture system

3.1.1 The differential expression of *let-7* in normal and tumor cells

To evaluate *let-7* microRNA family expression, we collected a variety of cell lines, including the alpha mouse liver cell (AML12), mouse embryonic fibroblasts (NIH 3T3), human dermal fibroblasts (HDF), and human neuroblastoma cells (BE2C, Kelly and CHP-212). Real-time PCR was performed to measure relative expression of *let-7* and demonstrated that *let-7a* (**Figure 4A**) and *let-7g* (**Figure 4B**) were strongly expressed in NIH 3T3 in comparison to BE2C ($P < 0.0001$), Kelly ($P < 0.0001$) and CHP-212 ($P < 0.0001$). The results also showed that *let-7a* (**Figure 4A**) and *let-7g* (**Figure 4B**) were highly expressed in HDF compared to Kelly ($P < 0.0001$).

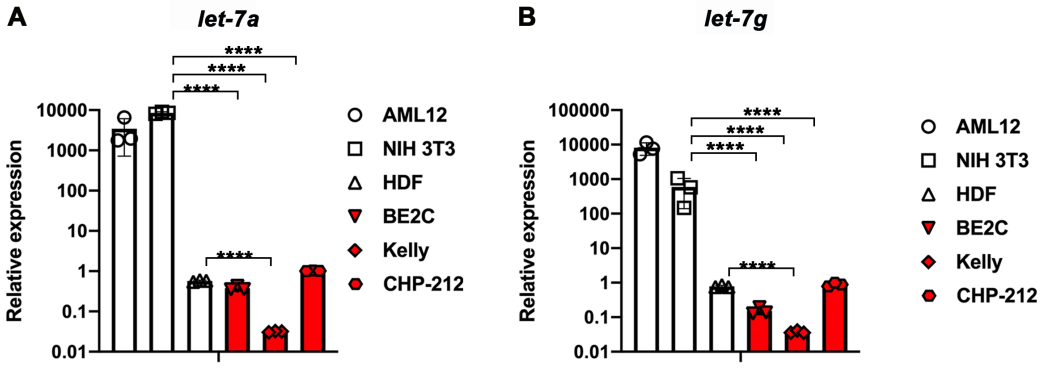

Figure 4. The differential expression of *let-7* in normal and tumor cells. (**A**) The relative expression of *let-7a* was examined by real-time PCR in normal and tumor cells. (**B**) The relative expression of *let-7g* was examined by real-time PCR in normal and tumor cells. **** $P < 0.0001$.

3.1.2 The generation of a dual-luciferase reporter-based co-culture system

In order to elucidate the *let-7* transfer between cells, we designed and generated a dual-luciferase reporter-based co-culture system. We generated constitutive expression of dual-luciferase reporter with *let-7* target binding sites (**Figure 5A**) in NIH 3T3 (NIH 3T3-dual Luc), Kelly (Kelly-dual Luc) and BE2C (BE2C-dual Luc) cells. Renilla luciferase was the testing reporter having *let-7* binding sites, which was activated in the absence of *let-7*. The presence of *let-7* inactivatd the reporter by blocking renilla luciferase translation (**Figure 5B**). The firefly luciferase reporter was internal reference control. The dual-luciferase reporter-based co-culture system was used to examine the alteration of *let-7s* during *in vitro* co-culture (**Figure 5C**).

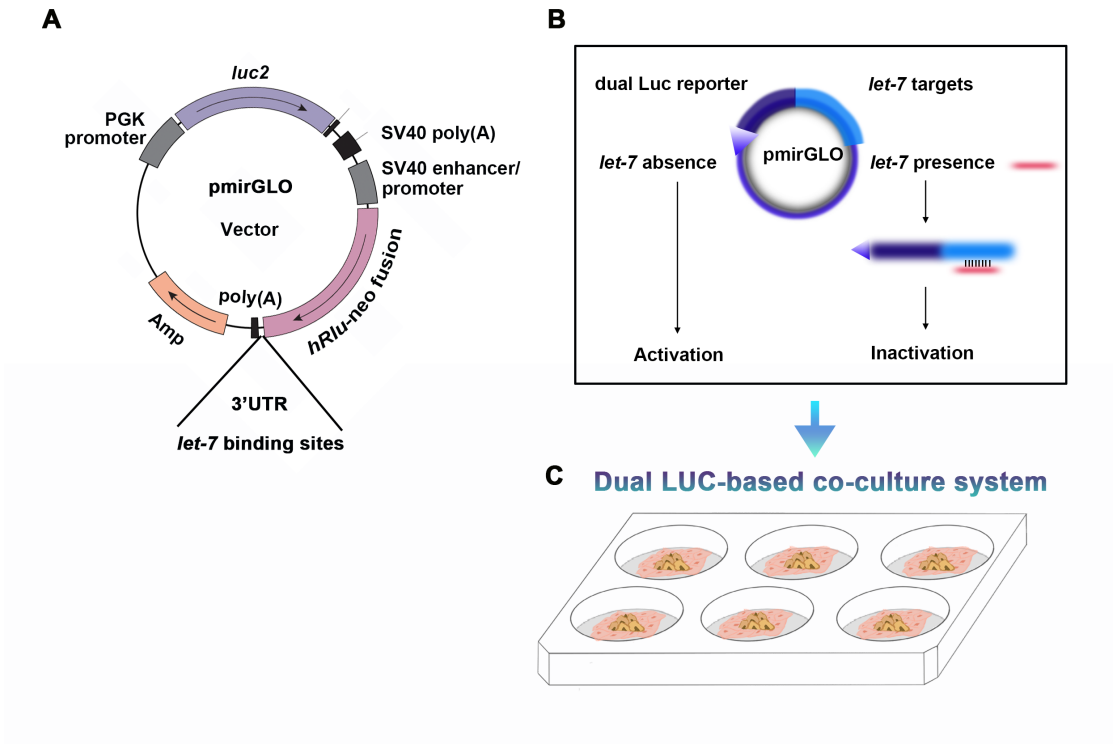

Figure 5. The generation of a dual-luciferase reporter-based co-culture system. (**A**) The map of pmirGLO dual-luciferase miRNA target expression vector. (**B**) The schematic diagram of activated/inactivated mechanism of a constitutively expressing dual-luciferase reporter system with *let-7* binding sites based on pmirGLO vector. (**C**) The generation of a dual-luciferase reporter-based co-culture system.

We co-cultured Kelly-dual Luc with either NIH 3T3 or Kelly and measured dual-luciferase reporter activities respectively. The results showed that luciferase reporter activities were reduced in Kelly-dual Luc co-cultured with Kelly for 3 and 5 days in comparison to co-culture with NIH 3T3 (**Figure 6A**). Then we performed co-culture between NIH 3T3-dual Luc and either NIH 3T3 or BE2C and found that the luciferase activity of recipient NIH 3T3 was dramatically decreased after co-culturing with BE2C in comparison to NIH 3T3 for 5 ($P < 0.0001$) and 10 ($P < 0.0001$) days (**Figure 6B**). These results indicated that *let-7* levels in recipient cells were increased during co-culture with tumor cells (Kelly and BE2C) compared to embryonic fibroblasts (NIH 3T3). Hereby, we successfully generated a dual-luciferase reporter-based co-culture system *in vitro*.

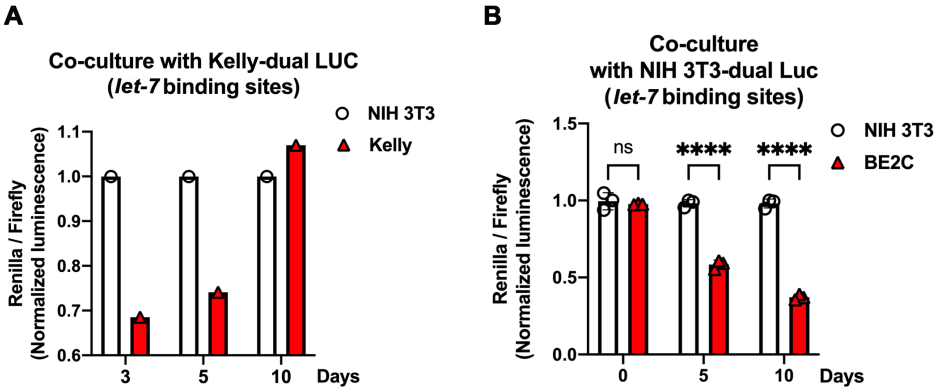

Figure 6. The measurement of luminescence activity in co-culture. (**A**) The measurement of luciferase activities in co-culture of NIH 3T3 and Kelly cells for 3, 5 and 10 days. Dual-luciferase reporters were expressed in Kelly with *let-7* binding sites. The experiment was independently performed once with five technical replicates. (**B**) The measurement of luciferase activity in co-culture of NIH 3T3 and BE2C cells for 0, 5 and 10 days. Dual-luciferase reporters were expressed in NIH 3T3 with *let-7* binding sites. The experiments were independently performed three times with five technical replicates for each biological replicate. **** $P <$ 0.0001; ns, no significant difference.

3.1.3 The measurement of *let-7* levels in the co-culture system

We performed further co-culture assays to investigate the alteration of *let-7* levels during co-culture. The expression level of *let-7i* was validated by real-time PCR in input cells, which confirmed that *let-7i* was abundently expressed in NIH 3T3 compared to BE2C cells (**Figure 7A**, $P < 0.001$). BE2C-dual Luc and either NIH 3T3 or BE2C were co-cultured for 3 and 5 days respectively. The results of luminescence measurement indicated that the activity of luciferase reporter in recipient BE2C was significantly diminished after co-culturing with donor BE2C compared to donor NIH 3T3 for 3 ($P < 0.001$) and 5 ($P < 0.01$) days (**Figure 7B**). Then, we performed co-culture between NIH 3T3-dual Luc and either NIH 3T3 or BE2C. Correspondingly, the activity of luciferase reporter in recipient NIH 3T3 was significantly decreased after co-culturing with donor BE2C compared to donor NIH 3T3 for 3 ($P < 0.001$) and 5 ($P < 0.0001$) days (**Figure 7C**). As a result, *let-7* levels of recipient cells were augmented during co-culture with donor BE2C compared to donor NIH 3T3.

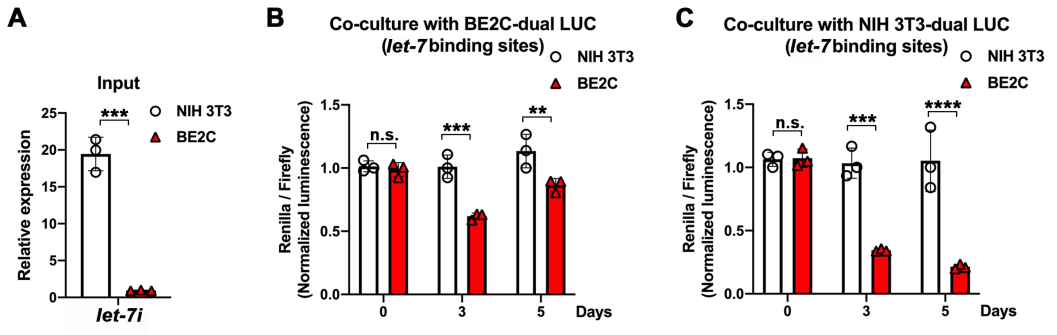

Figure 7. The alteration of *let-7* levels during co-culture between NIH 3T3 and BE2C. (**A**) The relative expression of *let-7i* in input BE2C and NIH 3T3 cells respectively by real-time PCR. (**B**) The measurement of luciferase activity in co-culture of NIH 3T3 and BE2C cells for 0, 3 and 5 days. Dual-luciferase reporters were expressed in BE2C with *let-7* binding sites. (**C**) The measurement of luciferase activity in co-culture of NIH 3T3 and BE2C cells for 0, 3 and 5 days. Dual-luciferase reporters were expressed in NIH 3T3 with *let-7* binding sites. All experiments were independently performed three times with five technical replicates for each biological replicate. ** $P < 0.01$; *** $P < 0.001$; **** $P < 0.0001$; n.s, no significant difference.

We also validated the expression level of *let-7a* by real-time PCR in input cells and comfirmed that *let-7a* was highly expressed in NIH 3T3 compared to Kelly cells (**Figure 8A**, $P < 0.0001$). Kelly-dual Luc were co-cultured with either NIH 3T3 or Kelly for 5 days. The results of luminescence measurement indicated that the activity of luciferase reporter in recipient Kelly was significantly diminished after co-culturing with donor Kelly compared to donor NIH 3T3 for 3 days (**Figure 8B**, $P < 0.0001$). Then we co-culture NIH 3T3-dual Luc with either NIH 3T3 or Kelly. Correspondingly, the activity of luciferase reporter in recipient NIH 3T3 was significantly decreased after co-culturing with donor Kelly compared to donor NIH 3T3 for 3 days (**Figure 8C**, $P < 0.0001$). Thus, *let-7* levels of recipient cells were elevated during co-culture with donor Kelly compared to donor NIH 3T3.

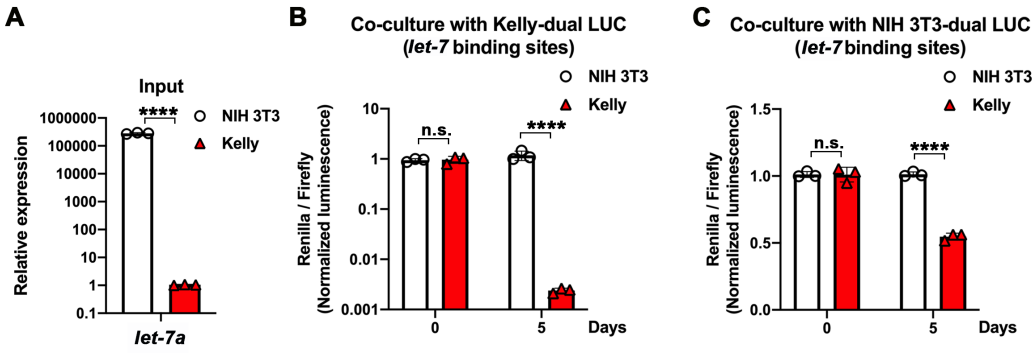

Figure 8. The alteration of *let-7* levels during co-culture between NIH 3T3 and Kelly. (**A**) The relative expression of *let-7a* in input NIH 3T3 and Kelly cells respectively by real-time PCR. (**B**) The measurement of luciferase activity in co-culture of NIH 3T3 and Kelly cells for 0 and 5 days. Dual-luciferase reporters were expressed in Kelly with *let-7* binding sites. (**C**) The measurement of luciferase activity in co-culture of NIH 3T3 and Kelly cells for 0 and 5 days. Dual-luciferase reporters were expressed in NIH 3T3 with *let-7* binding sites. All experiments were independently performed three times with five technical replicates for each biological replicate. **** $P < 0.0001$; n.s, no significant difference.

After all, considerring that NIH 3T3 cells are mouse embryonic fibroblasts, we repeated the co-culture assays using HDF cells, which are human fibroblasts. We measured the expression levels of *let-7* by real-time PCR in input cells and validated that *let-7a* ($P < 0.001$) and *let-7g* ($P < 0.001$) were highly expressed in HDF compared to Kelly cells (**Figure 9A**). Then we performed co-culture assays and found that the activity of luciferase reporter in recipient Kelly was significantly diminished after co-culturing with donor Kelly compared to donor HDF for 3 ($P < 0.001$), 4 ($P < 0.0001$) and 5 ($P < 0.0001$) days (**Figure 9B**). As a result, *let-7* levels of recipient cells were augmented during co-culture with donor Kelly compared to donor HDF.

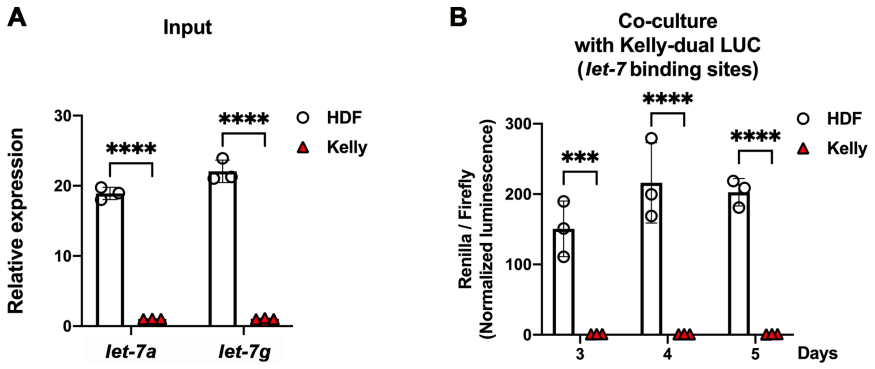

Figure 9. The alteration of *let-7* levels during co-culture between HDF and Kelly. (**A**) The relative expression of *let-7a* and *let-7g* in input HDF and Kelly cells respectively by real-time PCR. (**B**) The measurement of luciferase activity in co-culture of HDF and Kelly cells for 3, 4 and 5 days. Dual-luciferase reporters were expressed in Kelly with *let-7* binding sites. All experiments were independently performed three times with five technical replicates for each biological replicate. **** $P < 0.0001$.

3.1.4 Paragraph summary

In this section, the results showed that the expression levels of *let-7* miRNAs were significantly differential between normal and tumor cells. We generated a dual-luciferase reporter-based co-culture system to elucidate the altered level of *let-7* between fibroblasts and tumor cells *in vitro*. The results from cell co-culture

demonstrated that *let-7* levels of recipient cells, regardless of the initiating expression level of mature *let-7s*, were increased during co-culture with low *let-7* expressing donor cells (BE2C and Kelly) compared to high *let-7* expressing donor cells (NIH 3T3 and HDF).

3.2 Non-contact co-culture leads to alteration of *let-7* levels

3.2.1 The generation of a microporous insert-based co-culture system

In order to explore the alteration of *let-7* levels due to intercellular contact or non-contact during co-culture, we generated a non-contact co-culture system based on microporous inserts (**Figure 10**). We plated donor cells onto the top microporous inserts, while seeded dual-Luc expressing cells in the bottom chambers as recipient cells. After co-cultre for 3 or 5 days, the recipient cells were harvested for the measurement of the luciferase reporter activity.

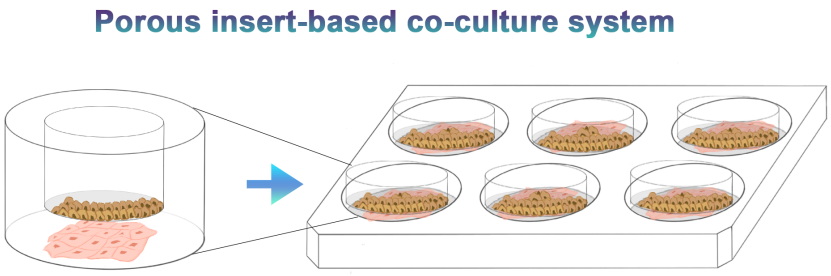

Figure 10. The generation of a microporous insert-based co-culture system. The schematic diagram of a microporous insert-based co-culture system. Donor cells were plated onto the top microporous inserts and recipient cells were seeded in the bottom chambers respectively. The donor and recipient cells could be co-cultured without contact.

3.2.2 The assessment of *let-7* levels during non-contact co-culture

We plated recipient NIH 3T3-dual Luc in the bottom chambers of 6-well plates and plated either donor NIH 3T3 or BE2C cells onto the top microporous inserts (**Figure 11A**). After co-culturing for 5 days, the recipient cells were collected, and the luciferase activities were measured (**Figure 11B**). The results demonstrated that the luciferase activity of recipient NIH 3T3-dual Luc (bottom chambers) was significantly reduced during non-contact co-culture with donor BE2C (top inserts) compared to donor NIH 3T3 (top inserts) via microporous inserts of 1.0 μm ($P < 0.01$) and 3.0 μm ($P < 0.01$).

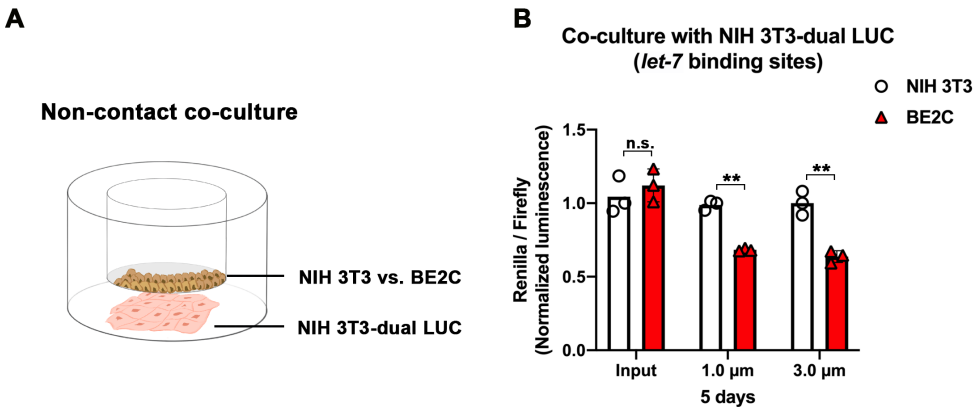

Figure 11. The assessment of *let-7* levels in the non-contact co-culture of NIH 3T3 and BE2C. (**A**) The schematic diagram of a microporous insert-based co-culture system. The donor NIH 3T3 or BE2C cells were plated onto the top microporous inserts (1.0 μm and 3.0 μm). The recipient NIH 3T3-dual Luc cells were seeded in the bottom chambers. Dual-luciferase reporters were expressed in NIH 3T3 with *let-7* binding sites. (**B**) The measurement of luciferase activity of recipient NIH 3T3 after co-culturing with donor NIH 3T3 or donor BE2C for 5 days. The experiments were independently performed three times with five technical replicates for each biological replicate. ** $P < 0.01$; n.s, no significant difference.

In addition, we plated recipient NIH 3T3-dual Luc in the bottom chambers of 6-well plates and plated donor NIH 3T3 or Kelly cells onto the top microporous inserts (**Figure 12A**). After co-culturing for 5 days, the recipient cells were collected, and the luciferase

activities were measured (**Figure 12B**). The results demonstrated that the luciferase activity of recipient NIH 3T3-dual Luc (bottom chambers) was significantly reduced during non-contact co-culture with donor Kelly (top inserts) compared to donor NIH 3T3 (top inserts) via microporous inserts of 1.0 μm ($P < 0.05$). As a result, the *let-7* levels in recipient NIH 3T3 cells were augmented during non-contact co-culture with donor tumor cells (BE2C and Kelly) compared to donor embryonic fibroblasts (NIH 3T3).

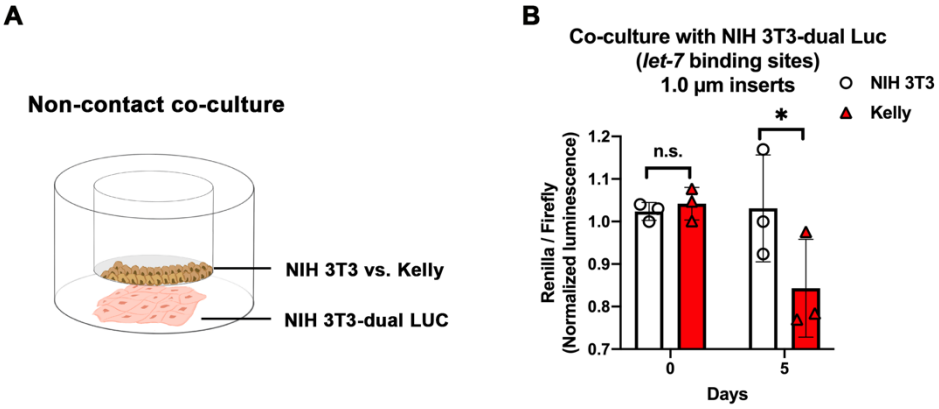

Figure 12. The assessment of *let-7* levels in the non-contact co-culture of NIH 3T3 and Kelly. (**A**) The schematic diagram of a microporous insert-based co-culture system. The donor NIH 3T3 or Kelly cells were plated onto the top microporous inserts (1.0 μm). The recipient NIH 3T3-dual Luc cells were seeded in the bottom chambers. Dual-luciferase reporters were expressed in NIH 3T3 with *let-7* binding sites. (**B**) The measurement of luciferase activity of recipient NIH 3T3 after co-culturing with donor NIH 3T3 or donor Kelly for 5 days. The experiments were independently performed three times with five technical replicates for each biological replicate. * $P < 0.05$; n.s, no significant difference.

3.2.3 Paragraph summary

In this section, we generated a microporous insert-based co-culture system to explore the alteration of *let-7* levels due to intercellular contact or non-contact during co-culture. In the non-contact co-culture system, the *let-7* levels in recipient NIH 3T3 cells were

increased during non-contact co-culture with donor tumor cells (BE2C and Kelly) compared to donor embryonic fibroblasts (NIH 3T3). These results indicated that the alteration of *let-7* levels during cell co-culture was in a non-contact manner.

3.3 LIN28B-dependent alteration of *let-7* expression during co-culture

3.3.1 The generation of LIN28B knockout cells

We generated LIN28B knockout (LIN28B KO) based on CRISPR/Cas9 system in BE2C and Kelly cells respectively. After sorted by FACS, we collected single clones of GFP-positive BE2C and Kelly cells, as well as control cells. GFP-positive BE2C and Kelly cells were the candidates of LIN28B KO cells. Western blot was performed to validate the efficiency of LIN28B KO in BE2C (**Figure 13A**) and Kelly (**Figure 13B**) cells.

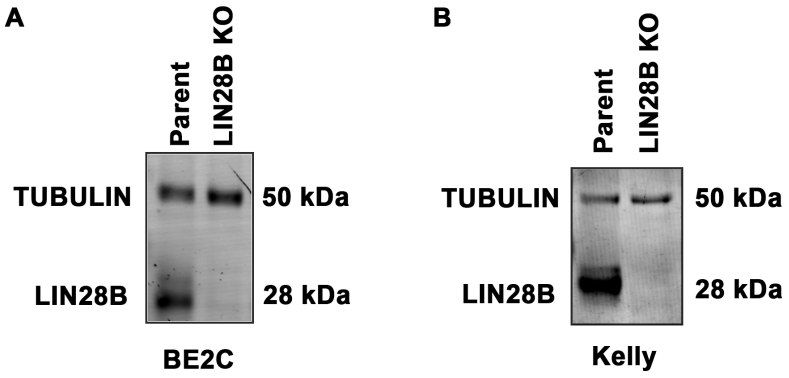

Figure 13. The generation of CRISPR/Cas9-mediated LIN28B KO cells. (**A**) The measurement of LIN28B expression at protein level in parental and LIN28B KO BE2C cells. (**B**) The measurement of LIN28B expression at protein level in parental and LIN28B KO Kelly cells. TUBULIN was used as internal reference control.

3.3.2 LIN28B-dependent alteration of *let-7* expression during contact co-culture

We generated constitutive dual luciferase reporter expression in LIN28B KO BE2C (LIN28B KO BE2C-dual Luc) and control BE2C (CTRL BE2C-dual Luc) cells. We validated the expression levels of *let-7s* by real-time PCR in input cells. *Let-7b*, *let-7g* and *let-7i* were highly expressed in LIN28B KO BE2C-dual Luc compared to CTRL BE2C-dual Luc cells (**Figure 14A**). CTRL BE2C-dual Luc or LIN28B KO BE2C-dual Luc was co-cultured with NIH 3T3 for 3, 5 and 10 days. The results of the luminescence measurement indicated that luciferase reporter activity was decreased in LIN28B KO BE2C-dual Luc compared to CTRL BE2C-dual Luc after co-culture with NIH 3T3 (**Figure 14B**).

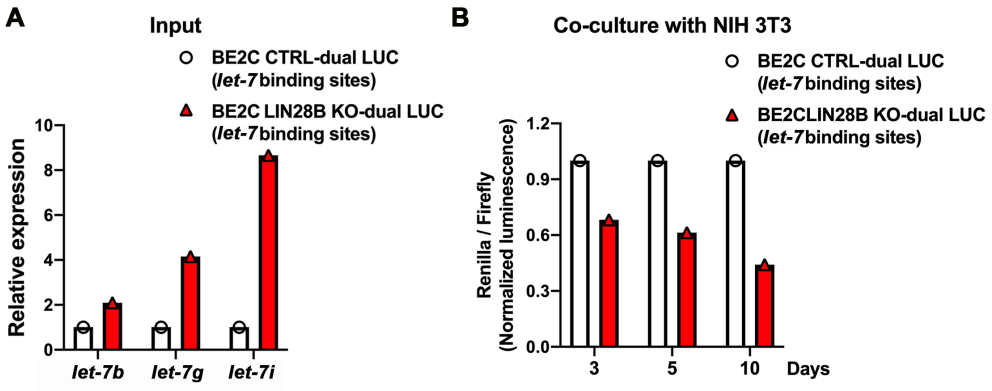

Figure 14. The measurement of luminescence activity in co-culture. (**A**) The measurement of *let-7 b*, *let-7g* and *let-7i* expression in input CTRL BE2C-dual Luc and LIN28B KO BE2C-dual Luc cells by real-time PCR. (**B**) The measurement of luciferase activity in co-culture of NIH 3T3 with either CTRL BE2C-dual Luc or LIN28B KO BE2C-dual Luc for 3, 5 and 10 days. Dual-luciferase reporters were expressed in CTRL BE2C and LIN28B KO BE2C with *let-7* binding sites. The experiment was independently performed once with five technical replicates.

3.3.3 LIN28B-dependent alteration of *let-7* expression during non-contact co-culture

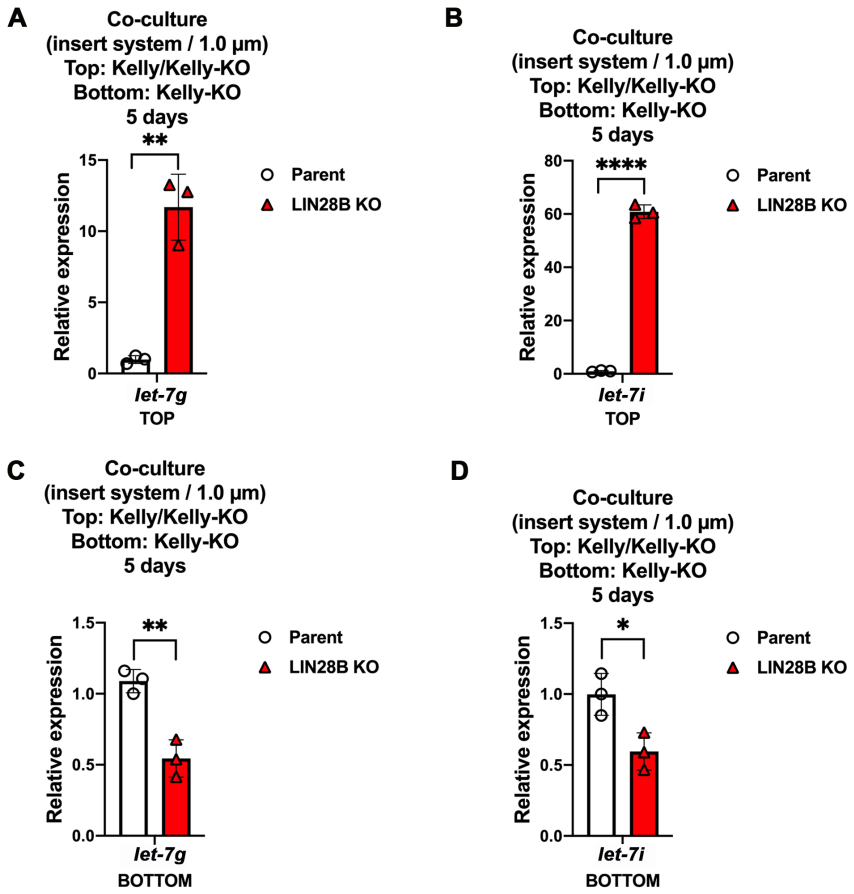

Figure 15. LIN28B-mediated *let-7* transfer in the non-contact co-culture system. (**A**) The measurement of *let-7g* expression in donor Kelly (top inserts) and donor LIN28B KO Kelly (top inserts). (**B**) The measurement of *let-7i* expression in donor Kelly (top inserts) and donor LIN28B KO Kelly (top inserts). (**C**) The measurement of *let-7g* expression in recipient LIN28B KO Kelly (bottom chambers) co-cultured with parental or LIN28B KO Kelly. (**D**) The measurement of *let-7i* expression in recipient LIN28B KO Kelly (bottom chambers) co-cultured with parental or LIN28B KO Kelly. The experiments were independently performed three times. * $P < 0.05$; ** $P < 0.01$; **** $P < 0.0001$.

We also performed microporous insert-based co-culture between parental Kelly and LIN28B knockout Kelly (LIN28B KO Kelly). LIN28B KO Kelly cells were seeded in the bottom chambers as recipient cells. Parental or LIN28B KO Kelly cells were respectively plated onto the top microporous inserts (1.0 μm) as donor cells. After co-culturing for 5 days, we collected recipient and donor cells to measure relative expression of *let-7s*, respectively. The results demonstrated that LIN28B KO increased the expression of *let-7g* (**Figure 15A**, $P < 0.01$) and *let-7i* (**Figure 15B**, $P < 0.0001$) in donor cells (top inserts) compared to parental Kelly (top inserts). However, the expression levels of *let-7g* (**Figure 15C**, $P < 0.01$) and *let-7i* (**Figure 15D**, $P < 0.05$) were significantly decreased in recipient cells (bottom chambers) co-cultured with donor LIN28B KO Kelly (top inserts) compared to recipient cells (bottom chambers) co-cultured with donor parental Kelly (top inserts). As a result, *let-7* levels were altered in cell co-culture, which might be mediated by LIN28B.

3.3.4 Paragraph summary

In this section, we generated LIN28B KO cells and perfermed intercellular contact and non-contact co-culture to evaluate the expression level of *let-7s*. The results indicated that the expression levels of *let-7s* in recipient cells (LIN28B KO Kelly) were reduced after co-culturing with donor LIN28B KO Kelly compared to donor parental Kelly.

3.4 The incubation of tumor cells with LIN28B KO-conditioned medium results in an increase of *let-7* level

3.4.1 The generation of a cell culture-conditioned medium system

In order to investigate LIN28B-mediated intercellular transfer of *let-7* in cell-to-cell communication, we generated a cell culture-conditioned medium system. Cell culture-conditioned media (CCM) were collected from donor cells after culturing for 3 days

(**Figure 16A**). Centrifugation was performed to remove cell debris (**Figure 16B**). Then recipient cells were incubated with CCM to evaluate *let-7* levels (**Figure 16C**).

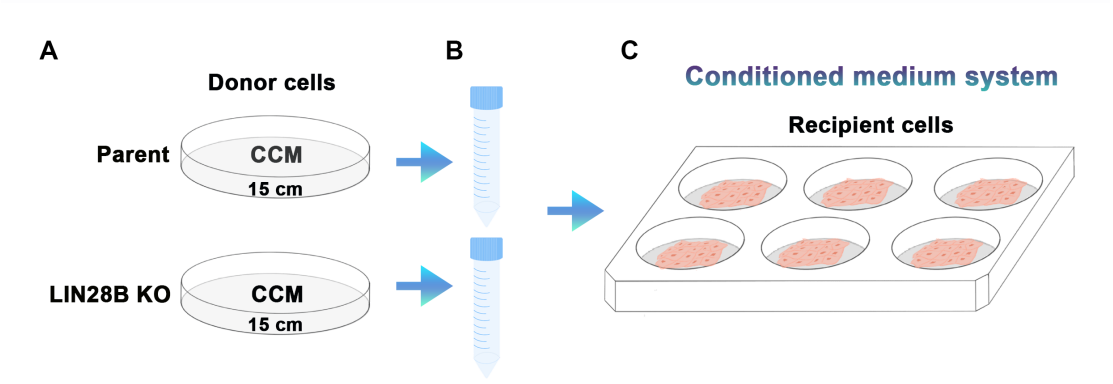

Figure 16. The workflow of cell culture-conditioned medium assay. (**A**) The preparation and collection of CCM. (**B**) The centrifugation to remove cell debris. (**C**) The generation of CCM system.

3.4.2 The examination of LIN28B-mediated *let-7* level in the cell-culture conditioned medium system

We plated parental BE2C and LIN28B KO BE2C as donor cells for three days, and then collected CCM respectively. The expression of LIN28B and *let-7i* was measured at RNA level in input cells before CCM assay was performed. The results from real-time PCR showed that LIN28B was downregulated (**Figure 17A**) while *let-7i* was upregulated (**Figure 17B**) in LIN28B KO BE2C compared to parental BE2C. LIN28B KO BE2C-dual Luc was prepared in 6-well plates as recipient cells and incubated with CCM from either parental BE2C (CCM-BE2C parent) or LIN28B KO BE2C (CCM-BE2C-LIN28B KO) cells. The luciferase activities were measured at day 3 and day 5. The results demonstrated that luciferase activity of recipient LIN28B KO BE2C-dual Luc incubated with CCM-BE2C parent was significantly decreased compared to recipient cells incubated with CCM-BE2C-LIN28B KO (**Figure 17C**). The results from CCM assays implicated that LIN28B KO reduced *let-7* secretion from BE2C cells.

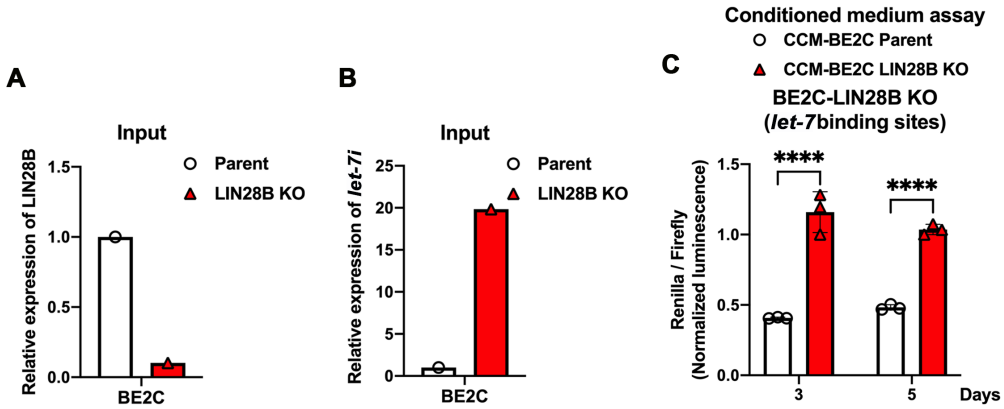

Figure 17. The examination of LIN28B-mediated *let-7* level in CCM system. (**A**) The relative expression of LIN28B in input BE2C and LIN28B KO BE2C cells. (**B**) The relative expression of *let-7i* in input BE2C and LIN28B KO BE2C cells. (**C**) The measurement of luciferase activity in LIN28B KO BE2C-dual Luc with CCM incubation for 3 and 5 days. Dual-luciferase reporters were expressed in recipient LIN28B KO BE2C with *let-7* binding sites. The experiments were independently performed three times. **** $P < 0.0001$.

In order to avoid the biological function of *let-7* binding sites per se in constitutive dual luciferase reporters, we then performed transient transfection of both renilla luciferase reporter psiCHECK2-*let-7*-WT (construct with a complementary *let-7* target element) and firefly luciferase reporter (reference control) into recipient cells incubated with CCM to evaluate *let-7* levels.

We plated parental Kelly and LIN28B KO Kelly as donor cells for three days, and then collected CCM respectively. The expression of LIN28B and *let-7i* was measured at RNA level in input cells before CCM assay was performed. The results from real-time PCR showed that LIN28B was downregulated (**Figure 18A**) while *let-7i* was upregulated (**Figure 18B**) in LIN28B KO Kelly compared to parental Kelly. Kelly was plated in 6-well plates as recipient cells and incubated with CCM from either parental Kelly (CCM-Kelly parent) or LIN28B KO Kelly (CCM-Kelly-LIN28B KO) cells for 5 days. Both renilla and firefly luciferase reporters were transfected into recipient Kelly

cells incubated with CCM to evaluate *let-7* transfer. Then the luciferase activities were measured. The results demonstrated that luciferase activity of recipient Kelly incubated with CCM-Kelly parent was significantly reduced compared to recipient cells incubated with CCM-Kelly-LIN28B KO (**Figure 18C**).

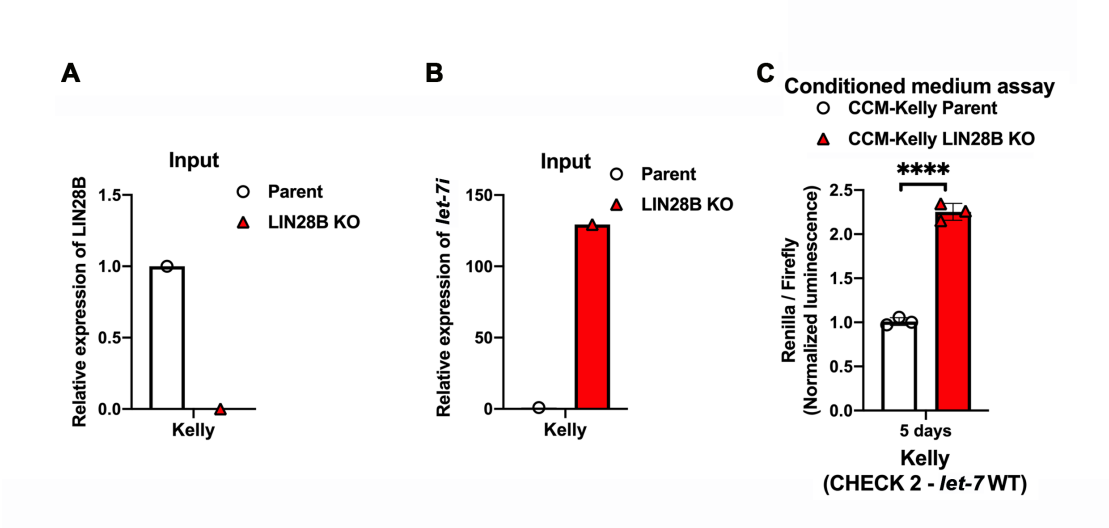

Figure 18. The luciferase activity of LIN28B knockout and control cells in cell culture-conditioned medium assay. (**A**) The relative expression of LIN28B in input Kelly and LIN28B KO Kelly cells. (**B**) The relative expression of *let-7i* in input Kelly and LIN28B KO Kelly cells. (**C**) The measurement of luciferase activity in CCM incubated recipient Kelly with transfection of renilla (psiCHECK2-*let-7*-WT) and firefly luciferase reporters at day 5. The renilla luciferase reporter construnct had a fully complementary *let-7* target element (psiCHECK2-*let-7*-WT). The firefly luciferase reporter construnct was used as reference control. The experiments were independently performed three times. **** $P < 0.0001$.

3.4.3 Paragraph summary

In this section, we collected CCM from donor cells to incubate recipient cells. Compared to CCM from LIN28B KO cells, CCM from parental cells resulted in a significant decrease of luciferase activity in recipient cells. The results from these CCM assays demonstrated that LIN28B KO reduced *let-7* secretion from donor BE2C and Kelly cells.

3.5 The investigation of *let-7* transfer via cell-free exosomes

3.5.1 The exosomes collection from serum-free conditional medium

In oder to elucidate the intercellular transfer of *let-7*, we isolated extracellular vesicles, identified exosomes and performed exosome-rich cell co-culture. We collected sufficient conditional media (~100 mL for each sample) from cells (**Figure 19A**). After performing OptiPrep-ultracentrifugation, we isolated four fractions (F1, F2, F3 and F4) of pure cell-free exosomes respectively (**Figure 19B**).

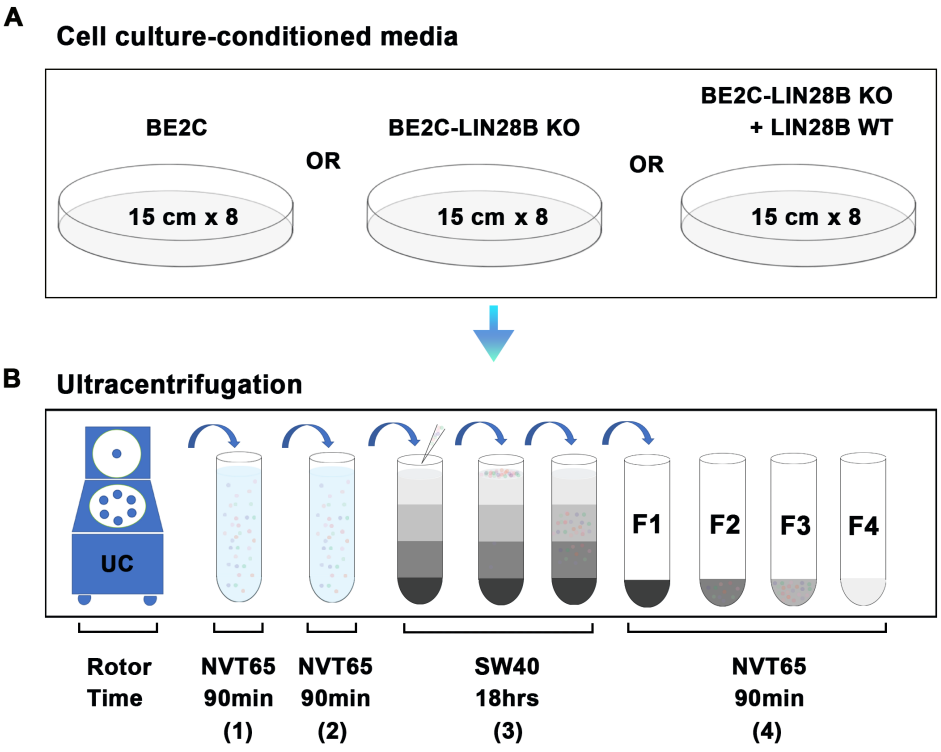

Figure 19. The workflow of exosomes collection from serum-free conditional medium. (**A**) Cells were cultured with serum-free media in 15 cm plates for 24 h. Then the conditional media were collected for ultracentrifugation using Beckman system. (**B**) The workflow of cell-free exosome isolation with Backman ultracentrifuge.

3.5.2 The validation of exosomal markers.

We identified exosomes by measuring the exosomal biomarkers at protein level. We performed western blot in pure exosomes from each fraction and found that CD9 and CD63 were expressed in exosomes of fraction 2 (F2) and fraction 3 (F3) (**Figure 20A**). LIN28B and TUBULIN did not show expression in any fractions (**Figure 20B**). This indicated successful isolation of exosomes from serum-free cell culture medium.

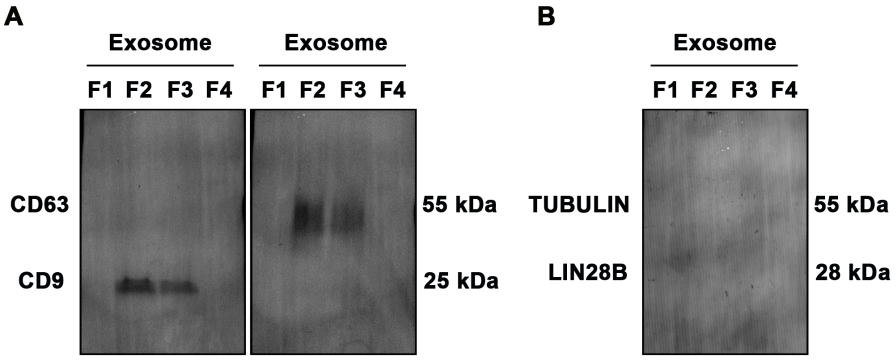

Figure 20. The validation of exosomal markers. (**A**) The measurement of exosome markers CD63 (55 kDa) and CD9 (25 kDa) in four fractions of isolated exosomes by western blot. (**B**) The measurement of TUBULIN (55 kDa) and LIN28B (28 kDa) in four fractions of isolated exosomes by western blot.

3.5.3 Exosome-rich conditioned medium assay

Donor parental and LIN28B KO cells were cultured in serum-free medium for 24 h (**Figure 21A**). CCM were collected respectively and isolated exosomes by ultracentrifugation to obtain exosome-rich conditioned media (**Figure 21B**). Recipient cells with dual-luciferase reporter expression were prepared in 6-well plates with density of 25×10^3. Then we incubated recipient cells with either exosome-rich CCM-BE2C or exosome-rich CCM-BE2C-LIN28B KO for 5 days, and then measured the luciferase activities (**Figure 21C**).

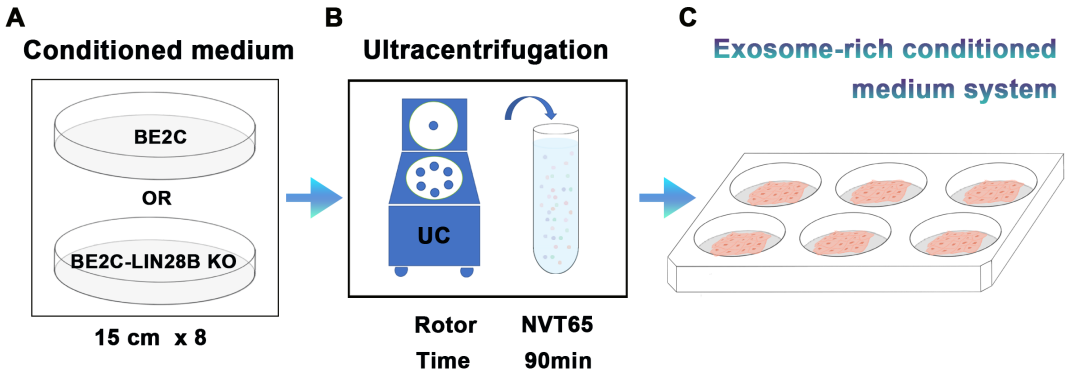

Figure 21. Exosome-rich conditioned medium assay. (**A**) The preparation of serum-free conditioned media from parental and LIN28B KO BE2C cells. (**B**) The isolation of cell-free exosomes derived from parental and LIN28B KO BE2C cells by ultracentrifugation. (**C**) The generation of exosome-rich CCM assays.

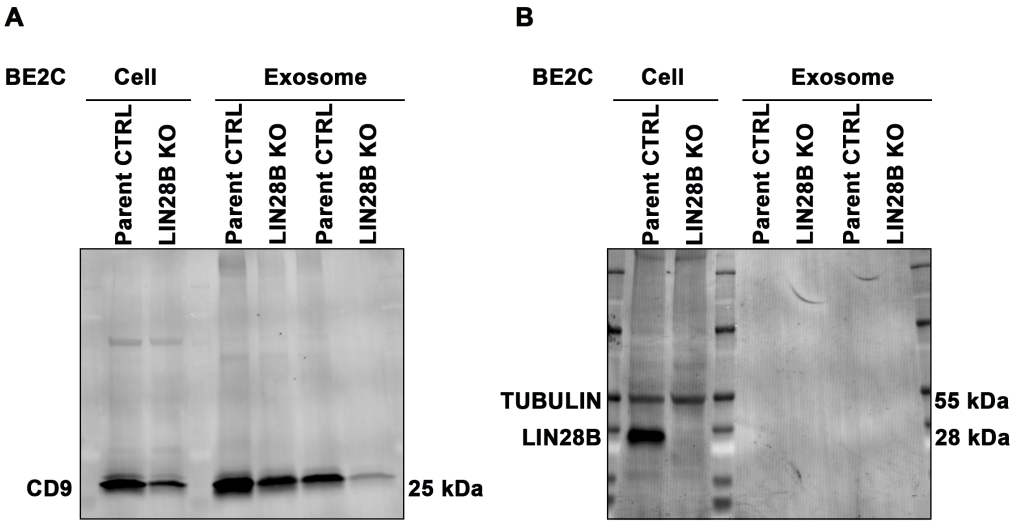

Figure 22. The measurement of exosomal markers in cell-free exosomes. (**A**) The measurement of exosomal marker CD9 (25 kDa) in cells and cell-free exosomes derived from parental and LIN28B KO BE2C cells isolated by ultracentrifugation. (**B**) The measurement of LIN28B (28 kDa) and TUBULIN (55 kDa) in cells and cell-free exosomes derived from parental and LIN28B KO BE2C cells isolated by ultracentrifugation.

We collected exosome pellets to measure exosomal marker CD9 at protein level. The results demonstrated that CD9 was highly expressed in input parental and LIN28B KO BE2C cells and isolated exosomes derived from parental and LIN28B KO BE2C cells (**Figure 22A**). Meanwhile, we tested for LIN28B expression and found that LIN28B was expressed in input parental BE2C cells, while being abscent in LIN28B KO BE2C cells as well as in isolated exosomes derived from control and LIN28B KO BE2C (**Figure 22B**).

3.5.4 LIN28B-mediated intercellular transfer of *pre-let-7* via exosomes

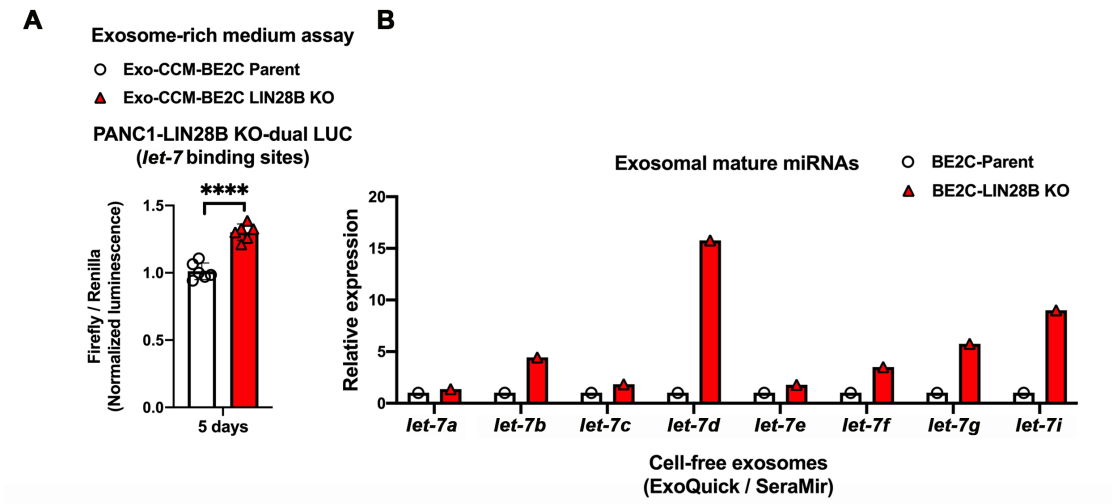

Figure 23. The examination of *let-7* transfer in exosome-rich CCM assay. (**A**) The measurement of luciferase activity in LIN28B KO PANC1-dual Luc incubated by exosome-rich CCM from parental BE2C and LIN28B KO BE2C cells. Dual-luciferase reporters were expressed in LIN28B KO PANC1 with *let-7* binding sites. The experiments were independently performed six times with five technical replicates for each biological replicate. (**B**) The expression of mature *let-7s* in cell-free exosomes derived from parental BE2C and LIN28B KO BE2C cells. Exo-CCM, exosome-rich conditioned medium. **** $P < 0.0001$.

We cultivated parental BE2C and LIN28B KO BE2C cells in serum-free medium for 24 h. CCMs were collected respectively and isolated exosomes by ultracentrifugation

to obtain exosome-rich conditioned media. We generated LIN28B KO PANC1 with dual-luciferase reporter expression (LIN28B KO PANC1-dual Luc) and incubated recipient cells with either exosome-rich CCM-BE2C or exosome-rich CCM-BE2C-LIN28B KO for 5 days. At the end of the exosome-rich CCM assay, the luciferase activity was measured to evaluate the intercellular transfer of *let-7*. The results demonstrated that luciferase activity of LIN28B KO PANC1-dual Luc cells was significantly reduced after incubation with parental BE2C-derived exosome-rich CCM compared to LIN28B KO BE2C-derived exosome-rich CCM (**Figure 23A**). We measured relative expression of mature *let-7s* in cell-free exosomes and found most mature *let-7s* highly expressed in exosomes derived from LIN28B KO BE2C compared to parental BE2C cells (**Figure 23B**).

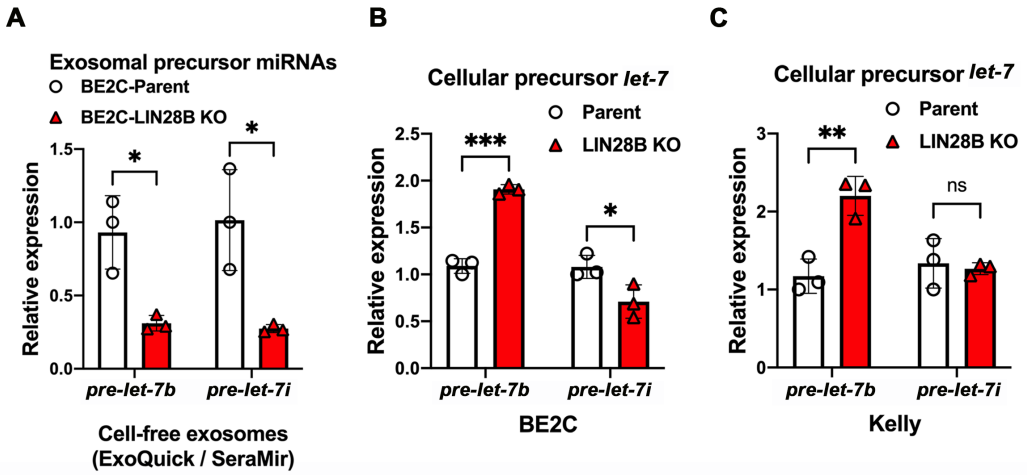

Figure 24. The expression of precursor *let-7s* in exosomes. (**A**) The expression of *pre-let-7b* and *pre-let-7i* in cell-free exosomes derived from parental BE2C and LIN28B KO BE2C cells isolated by ExoQuick/SeraMir kit. (**B**) The expression of *pre-let-7b* and *pre-let-7i* in parental and LIN28B KO BE2C cells. (**C**) The expression of *pre-let-7b* and *pre-let-7i* in parental and LIN28B KO Kelly cells. The experiments were independently performed three times. Exo-CCM, exosome-rich conditioned medium. * $P < 0.05$; ** $P < 0.01$; *** $P < 0.001$; n.s, no significant difference.

We recovered RNA from exosomes derived from parental BE2C and LIN28B KO BE2C cells by using ExoQuick SeraMir kit and performed real-time PCR. The results demonstrated that LIN28B KO dramatically decreased the expression levels of precursor *let-7b* and precursor *let-7i* in exosomes (**Figure 24A**). Further, we extracted RNA from input cells to measure intracellular *pre-let-7* and found that *pre-let-7b* was significantly upregulated by LIN28B KO in both BE2C (**Figure 24B**) and Kelly (**Figure 24C**) cells.

3.5.5 Paragraph summary

In this section, we isolated cell-free exosomes and performed exosome-rich CCM assays to elucidate the intercellular transfer of *let-7*. We found that the *let-7* levels of recipient cells were significantly elevated after incubation with CCM derived from parental BE2C compared to LIN28B KO BE2C. We measured both mature and precursor *let-7s* in exosomes and found that the expression of *pre-let-7* was significantly decreased in exosomes derived from LIN28B KO cells, even mature *let-7s* were upregulated. LIN28B might mediate intercellular transfer of *let-7* via exosomes in cell-to-cell communication.

3.6 The observation of cell morphology regulated by LIN28B

3.6.1 The generation of LIN28B overexpressing cells

In order to observe the cell morphology regulated by LIN28B, we reexpressed LIN28B expression in LIN28B KO BE2C cells (LIN28B KO + LIN28B WT). Western blot was performed to confirm the efficiency of LIN28B overexpression (**Figure 25**).

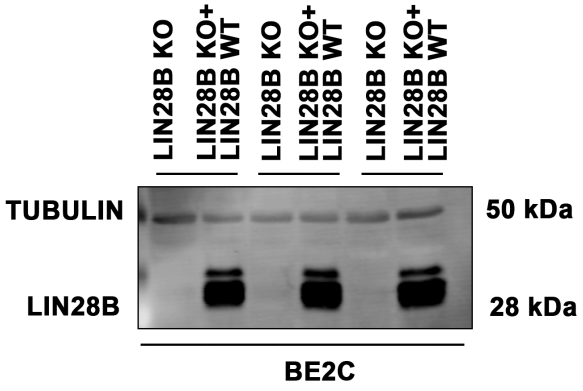

Figure 25. Reexpression of LIN28B in LIN28B KO BE2C cells. The generation of LIN28B expression in LIN28B KO BE2C cells. KO, knockout; WT, wildtype. TUBULIN was used as internal reference control.

3.6.2 The generation of a fluorescence-based co-culture system

Fibroblasts are an integral part of the metastatic microenvironment. In order to simulate metastatic tumor microenvironment *in vitro*, we generated a fluorescence-based co-culture system with fibroblasts and tumor cells. We generated green fluorescent protein (GFP) expressing BE2C cells (BE2C-LIN28B CTRL-GFP, BE2C-LIN28B KO-GFP and BE2C-LIN28B KO+LIN28B WT-GFP cells) and red fluorescent protein (RFP) expressing NIH 3T3 cells (NIH 3T3-RFP). Then we co-cultured BE2C and NIH 3T3 cells at a density of 25×10^3 for each cell line in 6-well plates (**Figure 26A**) and performed live cell imaging of co-culture through fluorescence microscopy (**Figure 26B**). LIN28B KO BE2C cells displayed a stem cell-like morphology, whereas parental BE2C and BE2C-LIN28B KO+LIN28B WT cells had a compact shape.

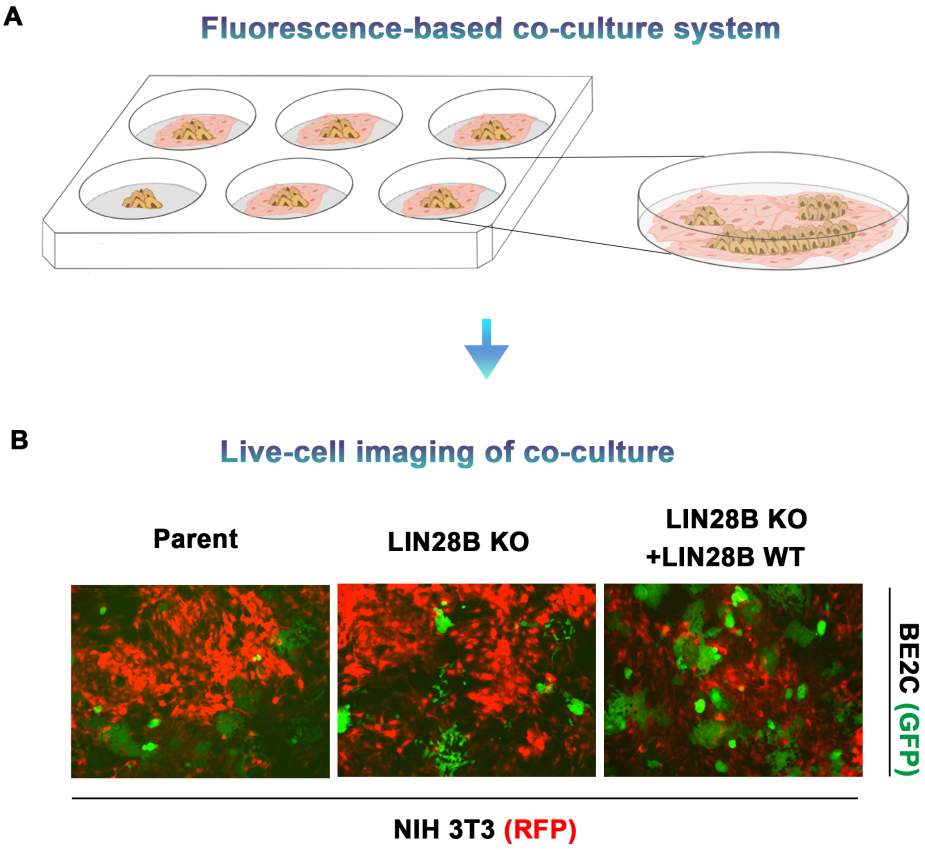

Figure 26. The generation of fluorescence-based co-culture system. (**A**) The schematic diagram of fluorescence-based co-culture system. (**B**) Live cell imaging of co-culture through fluorescence microscopy. Cells were distinguished based on fluorescence. GFP represented BE2C cells and RFP represented NIH 3T3 cells.

3.6.3 Live cell imaging in fluorescence-based co-culture system

We observed the morphology of living cells using fluorescence microscopy daily (**Figure 27**). Cells were distinguished based on fluorescence, with GFP representing BE2C cells and RFP representing NIH 3T3 cells. BE2C cells exhibited a cobblestone-like morphology. However, LIN28B KO BE2C cells displayed a spindle-like morphology. On the contrary, LIN28B was reexpressed in LIN28B KO BE2C cells (BE2C-LIN28B KO+LIN28B WT) and reversed cells to a cobblestone-like

morphology. LIN28B deficiency resulted in a significant increase in *let-7* expression, whereas LIN28B overexpression suppessed *let-7* expression.

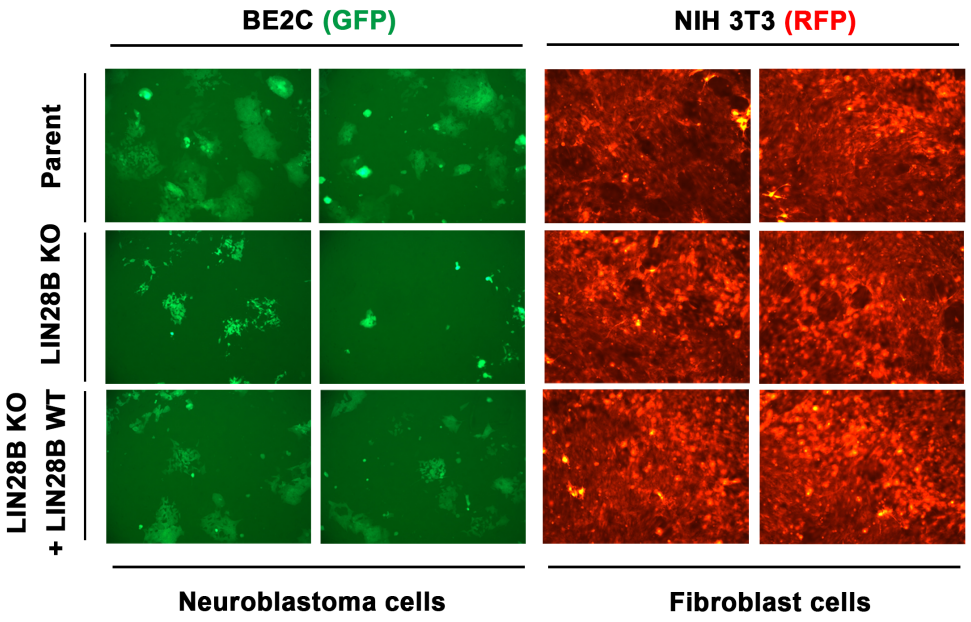

Figure 27. Live cell imaging in a fluorescence-based co-culture system. The observation of cell morphology in fluorescence-based co-culture system between BE2C and NIH 3T3 cells. GFP represented BE2C cells and RFP represented NIH 3T3 cells.

3.6.4 Paragraph summary

In this section, we explored a fluorescence-based co-culture system. We generated BE2C cell lines constitutively expressing GFP, and NIH 3T3 cell line constitutively expressing RFP. Then we plated NIH 3T3-RFP with BE2C-GFP. During the co-culture, we observed the cell morphology controlled by LIN28B expression.

4. Discussion

Tumor suppressor miRNA *let-7* serves as a potential player in cancer physiology, but could potentially be used for treatment of cancer (Bussing et al., 2008, Zhang et al., 2020). However, the role of *let-7* microRNA transfer in the metastatic niche remains unclear. In this dissertation, we measured the relative expression of *let-7* in both tumor and normal cells and found that *let-7* was strongly expressed in mouse embryonic fibroblasts NIH 3T3 in comparison to human neuroblastoma cells BE2C, Kelly and CHP-212. In addition, *let-7* was highly expressed in human dermal fibroblasts HDF compared to human neuroblastoma cell Kelly. The expression levels of *let-7* miRNAs were significantly differential between normal and tumor cells. Our results are consistent with published results that *let-7* highly expresses in embryonic cells, while decreases in tumor cells (Boyerinas et al., 2010, Divisato et al., 2020).

Tumor metastasis to distant organs is a a hallmark of most cancers (Hanahan and Weinberg, 2011). The majority of cancer deaths are caused by distant metastasis of tumor cells (Esposito et al., 2021). Metastatic dissemination has generally been defined as the final stage in multistep tumor progression (Bergers and Fendt, 2021, Campbell et al., 2010). In general, there is an invasion-metastasis cascade in metastasis that tumor cells disseminate from local neoplasma to distant organs (Nguyen et al., 2009) and subsequently educate foreign microenvironment to develop metastases (Zhang et al., 2009, Valastyan and Weinberg, 2011, Tannock and Hickman, 2016). It has been demonstrated that fibroblastic cells derived from normal tissues could enhance tumor phenotypes such as metastasis (Hanahan and Weinberg, 2011) . In order to investigate the roles of *let-7* in metastatic niche, we established a simplified *in vitro* cell co-culture system of fibroblasts and tumor cells to simulate metastatic tumor microenvironment. We generated a dual-luciferase reporter-based co-culture system based on either a constitutively expressed dual-luciferase reporter construct, or the transfection of firefly and renilla luciferase reporters. Our previous hypothesis was that *let-7* levels in

recipient cells should be increased after co-culture with donor cells with high *let-7* expression. However, the results of direct cell co-culture assays are opposite to what we expected. NIH 3T3 has a high level of *let-7* expression in comparison to BE2C and Kelly cells. However, it was surprising that recipient cells did not show higher *let-7* level after co-culture with high *let-7* expressing donor fibroblasts NIH 3T3, HDF. On the contrary, *let-7* levels in recipient cells were increased during co-culture with low *let-7* expressing donor neuroblastoma cells BE2C and Kelly.

To clarify whether the alterations of *let-7* levels were independent of direct cell contact or non-contact behavior, we generated a microporous insert-based non-contact co-culture system. We seeded recipient embryonic fibroblasts NIH 3T3 with constitutively expressed dual-luciferase reporters in the bottom chambers and plated donor cells onto the top microporous inserts. The results of the non-contact co-culture indicated that *let-7* levels in recipient cells was elevated during non-contact co-culture with donor neuroblastoma cells BE2C or Kelly compared to donor embryonic fibroblasts NIH 3T3. These results demonstrated that the alterations of *let-7* levels were independent of direct cell contact.

So far, the direct contact co-culture and non-contact co-culture systems consistently illustrated that *let-7* level altered during co-culture. There might be a unique regulatory mechanism to control the alteration of *let-7* level in the co-culture system. We would like to overexpress *let-7s* in donor cells to investigate the roles of *let-7* during co-culture. *Let-7* mimics only upregulate mature *let-7s* that might lose the effects of precursor *let-7s*. RNA-binding protein LIN28B recognizes and binds the stem loop of primary and precursor *let-7s* to prevent the maturation of *let-7* (Roush and Slack, 2008). Thus, we knocked out LIN28B to regulate *let-7* expression in neuroblastoma cells. We found that the expression level of *let-7* in recipient cells was diminished after co-culturing with donor malignant neuroblastoma cell lines in the absence of LIN28B by performing intercellular contact and non-contact co-culture.

These results provided us a hint there might be *let-7* transfer during cell co-culture. Thus, we further generated a CCM system to test the cell-free *let-7* transfer via extracellular supernatant. The incubation with extracellular supernatant derived from donor neuroblastoma cells in the absence of LIN28B led to a decrease of *let-7* levels in recipient cells. MiRNAs can be transferred between neighbouring cells via extracellular exosomes (Ghoshal et al., 2021). Subsequently, we isolated four fractions (F1, F2, F3 and F4) of cell-free exosomes by performing OptiPrep-ultracentrifugation. CD9 and CD63 are the exosomal markers which are commonly used for the identification of exosomes (Mathieu et al., 2021). Thus, we detected the expression of exosomal markers CD9 and CD63 at protein level and found that the pure exosomes were enriched in fractions that CD9 and CD63 highly expressed. We collected enriched exosomes to further generate an exosome-rich CCM system. We found that *let-7* levels in recipient cells were diminished after incubation with exosome-rich CCM derived from donor neuroblastoma cells in the absence of LIN28B. These results point towards intercellular transfer of *let-7* via cell-free exosomes.

Furthermore, we measured the expression of mature *let-7s* in neuroblastoma cell-derived exosomes. Most mature *let-7s* highly expressed in exosomes derived from LIN28B KO BE2C compared to parental BE2C cells. However, these results couldn't explain our previous results that *let-7* levels in recipient cells were decreased during co-culture with LIN28B absent donor cells. Therefore, we further measured the *pre-let-7s* in neuroblastoma cell-derived exosomes. Interestingly, the expressions of *pre-let-7s* were diminished in exosomes derived from LIN28B absent neuroblastoma cells compared to parental cells. We also examined that the intracellular expressions of *pre-let-7b* were upregulated in the absence of LIN28B in neuroblastoma cells. We also observed cell morphology by generating a fluorescence-based co-culture system through fluorescence microscopy. Parental BE2C cells exhibited a cobblestone cell-like morphology, whereas LIN28B KO BE2C cells displayed a spindle-like morphology.

Once LIN28B was reexpressed in LIN28B KO BE2C, cells were reversed to a cobblestone-like morphology. LIN28B deficiency resulted in a significant increase in *let-7* expression, whereas LIN28B overexpression suppessed *let-7* expression. These results hint that LIN28B expression may mediates morphological alteration in *in vitro* cell co-culture. These results indicated an important role of LIN28B in this process.

Over the past three decades, advanced sequencing technologies have greatly facilitated the Human Genome Project (HGP) to achieve a wealth of research results, revealing the molecular signature of many cancers (Rood and Regev, 2021, Lander et al., 2001, Venter et al., 2001). The development and application of molecular-targeted agents for cancer has been progressed from the bench to the bed, guiding both scientific researchers and clinicians (Stratton et al., 2009, Rood and Regev, 2021). In recent years, miRNA-based therapeutics have been applicated against tumor (Inoue and Inazawa, 2021). For example, Inoue and Inazawa reported a double-stranded *miR-634* mimic promoted the antitumor effects of cisplatin in esophageal squamous cell carcinoma cells and *xenograft* mice (Inoue and Inazawa, 2021, Fujiwara et al., 2015). Overexpression of *miR-634* induced cell apoptotic death in cutaneous squamous cell carcinoma (A431), pancreatic cancer (BxPC-3) and breast cancer (MDA-MB-468) cell lines (Inoue and Inazawa, 2021). Gokita et al. developed a lipid nanoparticle (LNP) mediated delivery of synthetic ds-*miR-634* mimic (*miR-634*-LNP). The administration of *miR-634*-LNP resulted in anti-tumor effects in pancreatic cancer-derived *xenograft* mice (Gokita et al., 2020). Inoue et al. also formulated a therapeutic ointment incorporating ds-*miR-634* mimics (*miR-634* ointment) that improved the efficacy of EGFR inhibitors gefitinib in cutaneous squamous cell carcinoma (Inoue et al., 2020). In addition, the safety, activity and efficacy of tumor suppressor miRNAs-related agents has been studied by Phase 1/2 clinical trials such as the treatment of *miR-16* mimic-loaded minicells targeted to EGFR (Clinical trial registration: NCT02369198, ACTRN12614001248651) in patients with recurrent malignant pleural mesothelioma (van Zandwijk et al., 2017) and the administration of a liposomal *miR-34a* mimic MRX34 (Clinical trial registration:

NCT01829971) with solid tumors (Beg et al., 2017, Hong et al., 2020). These remind us that replacement of tumor suppressor miRNAs has therapeutic potential, and the tumor suppressor miRNAs are expected to be a prospective drug seed for cancer therapy (Kwok et al., 2017, Reid et al., 2016).

Let-7s may serve as appealing potential therapeutic candidates for cancer, particularly in cancers that underexpress *let-7s* (Barh et al., 2010) such as CRC, breast cancer and neuroblastoma (Powers et al., 2016). In CRC, *let-7e* enhanced the radiosensitivity of CRC cells by directly targeting IGF1R (Samadi et al., 2019). *Let-7f* promoted chemotherapeutic resistance by repressing p53 (Tie et al., 2018). Overexpression of *let-7a*, *let-7b*, and *let-7i* by transfected with miRNA mimics inhibited cell proliferation and induced cell apoptosis in ER-positive breast cancer cells (Zhao et al., 2011). Restoration of *let-7* in tumor-initiating cells from breast cancers via *let-7*-lentivirus inhibited tumorogenesis and metastasis in NOD/SCID mice (Yu et al., 2007). Systemic delivery of *let-7* mimics Using a neutral lipid emulsion reduced tumor burden in KRAS-activated autochthonous non-small cell lung cancer mice (Trang et al., 2011). Although miRNA mimic-based replacement therapy with *let-7* attempts to be effective (Barh et al., 2010, Gilles and Slack, 2018), there are still some potential problems such as the specificity and efficiency of delivery, the instability of mimics and the control of mimics release (Mizuno et al., 2018, Bussing et al., 2008). Transfection of synthesized *let-7* mimics only rescues the expression of specific mature *let-7* (Kuhn et al., 2008). In this project, we regulated *let-7s* expression by modifying the expression of LIN28B instead of directly utilizing *let-7* mimics, so that we could detect almost all mature *let-7s* (*let-7a*, *let-7b*, *let-7c*, *let-7d*, *let-7e*, *let-7f*, *let-7g*, *let-7i* and *miR-98*), as well as the precursor *let-7s*.

MiRNAs are involved in cell-to-cell communication, which is essential for pre-metastatic niche formation in tumor microenvironment of metastasis (Mathieu et al., 2019, Becker et al., 2016, Matei et al., 2017). During the process of PMN formation

and metastasis, cell-to-cell communication via extracellular vesicles (exosomes and microvesicles, *etc.*) between primary tumor cells and the microenvironment of distant organs plays crucial effects, which transfers bioactive contents including miRNAs between cells. The tumor progression is not only autonomous with genetic mutations, but also a non-autonomous process under the influence of the tumor microenvironment. It is reported that oncogenic niche cells trigger neighboring cells and metastasis, contributing to the progression and recurrence of tumor (Enomoto et al., 2015, Hanahan and Weinberg, 2011). *Let-7a* was elevated in serum EVs from CRC patients and was enriched in CRC cell-derived EVs. Forced expression of *let-7a* transfected by miRNA mimics suppressed EV secretion by regulating mitochondrial oxidative phosphorylation through LIN28/SDHA pathway in CRC cells (Liu et al., 2021b). Ohshima et al. revealed that *let-7s* were enriched in the exosomes from metastatic gastric cancer cells. Metastatic gastric cancer cells release *let-7s* via exosomes into the extracellular environment to maintain their oncogenesis (Ohshima et al., 2010). These literatures support our findings that *let-7* may transfer between cells via cell-free exosomes.

Kobayashi et al. pointed out that *let-7* transcripts were detected in ovarian cancer cells and corresponding exosomes. They found that *let-7* low expressed in high invasive tumour cell SKOV-3 compared to low invasive tumour cell OVCAR-3, whereas *let-7* transcripts were more plentiful in SKOV-3-derived exosomes compared to OVCAR-3-derived exosomes (Kobayashi et al., 2014). Although they demonstrated that the releases of exosomes correlated with invasive potential of tumor cells, they did not explore the molecular mechanism in their reserach. In our project, we found the expression of precursor *let-7s* was significantly reduced in cell-free exosomes in the absence of LIN28B, that points towards an important role of LIN28B in this process. We also measured the expression of exosomal protein. However, LIN28B and TUBULIN did not show expression in neuroblastoma cell-derived exosomes. Zhang et al. suggested that the exosomes derived from pancreatic cancer cells enhanced the

recruitment of cancer-associated fibroblasts and improved the formation of metastases (Zhang et al., 2019). Zhang et al. demonstrated that exosomes from pancreatic cancer cells transfered exosomal LIN28B protein into the recipient cells to activate the LIN28B/*let-7*/HMGA2/PDGFB pathway (Zhang et al., 2019). The differential expression of LIN28B protein in exosomes derived from different tumor cells imply that exosomal protein transfer may be cell type-dependent.

We conducted literature research about *let-7* secretion via EVs and found only mature *let-7s* were examined in those studies (Zhang et al., 2019, Kobayashi et al., 2014, Ohshima et al., 2010). In our study, we indicated that *let-7* levels in recipient cells were decreased during co-culture with LIN28B absent donor cells. We isolated cell-free exosomes and found that most mature *let-7s* highly expressed in exosomes derived from LIN28B-deficient neuroblastoma cells, which couldn't explain our previous results. Thus, we further measured the *pre-let-7s* in the corresponding exosomes and found that the expressions of *pre-let-7s* were diminished in exosomes derived from LIN28B-deficient neuroblastoma cells. It is known that TUTase4 acts as the uridylyl transferase of *pre-let-7*. LIN28 can recognize a tetra-nucleotide sequence motif to recruit TUTase4 to *pre-let-7*. TUTase4 can block the cleavage by Dicer by adding an oligouridine tail to *pre-let-7* (Wang et al., 2017). Moreover, it is reported that 3' end uridylation is significantly increased in exosomes compared to corresponding cells (Koppers-Lalic et al., 2014). Therefore, LIN28B may mediate intercellular transfer of *let-7* via exosomes in cell-to-cell communication.

In conclusion, we examined the roles of *let-7* transfer by establishing simplified cell co-culture systems to simulate the metastatic niche *in vitro*. Interestingly, *let-7* levels in recipient cells were increased after co-culturing with low *let-7* expressing tumor cells compared to high *let-7* expressing embryonic fibroblasts. In addition, *let-7* levels in recipient cells were diminished after co-culturing with donor malignant neuroblastoma cell lines in the absence of LIN28B. The alterations of *let-7s* activities were independent

of direct cell contact. Furthermore, *let-7* levels in recipient cells were downregulated after incubation with CCM and exosome-rich CCM derived from LIN28B-deficient BE2C. The expression of precursor *let-7s* was significantly reduced in cell-free exosomes in the absence of LIN28B pointing towards an important role of LIN28B in this process. Taken together, our results indicate an active *let-7* transfer in the micrometastatic niche with LIN28B as a potential mediator. Nevertheless, investigation of LIN28B-dependent *let-7* transfer in tumor-bearing mouse models remains to be further explored.

5. Summary

Metastasis is a hallmark of malignant disease and still accounts for the majority of cancer related deaths. The term metastasis describes a multistep process. One of the most important steps is the formation of micrometastases in the distant soil. The intercellular transfer of cellular bioactive compounds, like mRNAs and miRNAs, has emerged as an important factor within this process. Tumor suppressor microRNA *let-7* serves as a potential player in cancer physiology, but could potentially be used for treatment of cancer. However, the role of *let-7* microRNA transfer in the metastatic niche remains unknown. In this dissertation, I examined the roles of *let-7* transfer by establishing simplified cell co-culture systems to simulate the metastatic niche in vitro. Dual-luciferase reporter-based contact and non-contact co-culture systems were generated to investigate *let-7* level during co-culture of fibroblasts and tumor cells. Interestingly, *let-7* level in recipient cells (NIH 3T3, BE2C and Kelly) was increased after co-culturing with low *let-7* expressing tumor cells (BE2C and Kelly) compared to high *let-7* expressing embryonic fibroblasts (NIH 3T3). In addition, *let-7* level in recipient cells (LIN28B KO Kelly) was diminished after co-culturing with donor malignant neuroblastoma cell lines in the absence of LIN28B. The alterations of *let-7s* activities were independent of direct cell contact. Furthermore, *let-7* levels in recipient cells (LIN28B KO BE2C and LIN28B KO PANC1) were downregulated after incubation with cell culture-conditioned media (CCM) and exosome-rich CCM derived from LIN28B KO BE2C compared to parental BE2C. The expression of precursor *let-7s* was significantly reduced in cell-free exosomes in the absence of LIN28B pointing towards an important role of LIN28B in this process. These results indicate an active *let-7* transfer in the micrometastatic niche with LIN28B as a potential mediator.

6. Zusammenfassung

Die Metastasierung ist ein Hauptmerkmal bösartiger Erkrankungen und ist nach wie vor für die Mehrzahl der krebsbedingten Todesfälle verantwortlich. Der Begriff Metastasierung beschreibt einen mehrstufigen Prozess. Einer der wichtigsten Schritte ist die Ausbildung von Mikrometastasen im entfernten Organ. Der interzelluläre Transfer bioaktiver Verbindungen, wie mRNAs und miRNAs, hat sich als wichtiger Faktor in diesem Prozess herausgestellt. Die Tumorsuppressor-microRNA *let-7* ist ein potenzieller Akteur in der Krebsphysiologie, könnte aber auch zur Behandlung von Krebs eingesetzt werden. Die Rolle von *let-7* im miRNA-Transfer in der metastatischen Nische ist noch nicht geklärt. In dieser Dissertation untersuchte ich die Rolle des *let-7*-Transfers, indem ich vereinfachte Zell-Ko-Kultur-Systeme entwickelte, um die metastatische Nische in vitro zu simulieren. Es wurden kontakt- und kontaktlose Ko-Kultur-Systeme mit Dual-Luciferase-Reporter entwickelt, um die *let-7*-Spiegel während der Ko-Kultur von Fibroblasten und Tumorzellen zu untersuchen. Interessanterweise waren die *let-7*-Spiegel in Empfängerzellen (NIH 3T3, BE2C und Kelly) nach der Ko-Kultur mit niedrig *let-7*-exprimierenden Tumorzellen (BE2C und Kelly) im Vergleich zu hoch exprimierenden embryonalen Fibroblasten (NIH 3T3) erhöht. Darüber hinaus war die *let-7*-Konzentration in Empfängerzellen (LIN28B KO Kelly) nach Ko-Kultivierung mit malignen Neuroblastom-Zelllinien in Abwesenheit von LIN28B vermindert. Die Veränderungen der *let-7*-Aktivitäten waren unabhängig vom direkten Zellkontakt. Darüber hinaus wurden die *let-7*-Spiegel in Empfängerzellen (LIN28B KO BE2C und LIN28B KO PANC1) nach Inkubation mit zellkulturkonditioniertem Medium (CCM) und exosomenreichem CCM aus LIN28B KO BE2C im Vergleich zu Wildtyp BE2C herunterreguliert. Die Expression von pre-*let-7s* war in zellfreien Exosomen in Abwesenheit von LIN28B deutlich reduziert, was auf eine wichtige Rolle von LIN28B in diesem Prozess hindeutet. Diese Ergebnisse deuten auf einen aktiven Transfer der miRNA *let-7* in der mikrometastatischen Nische hin, wobei sich LIN28B als potenzieller Vermittler darstellt.

7. Bibliography

AFTAB, M., POOJARY, S. S., SESHAN, V., KUMAR, S., AGARWAL, P., TANDON, S., ZUTSHI, V. & DAS, B. C. 2021. Urine miRNA signature as a potential non-invasive diagnostic and prognostic biomarker in cervical cancer. *Sci Rep,* 11**,** 10323.

AMBROS, V. & HORVITZ, H. R. 1984. Heterochronic mutants of the nematode Caenorhabditis elegans. *Science,* 226**,** 409-16.

ATTALI-PADAEL, Y., ARMON, L. & URBACH, A. 2021. Apoptosis induction by the stem cell factor LIN28A. *Biol Cell,* 113**,** 450-457.

BALZEAU, J., MENEZES, M. R., CAO, S. & HAGAN, J. P. 2017. The LIN28/let-7 Pathway in Cancer. *Front Genet,* 8**,** 31.

BARH, D., MALHOTRA, R., RAVI, B. & SINDHURANI, P. 2010. MicroRNA let-7: an emerging next-generation cancer therapeutic. *Curr Oncol,* 17**,** 70-80.

BARTEL, D. P. 2009. MicroRNAs: target recognition and regulatory functions. *Cell,* 136**,** 215-33.

BARTEL, D. P. & CHEN, C. Z. 2004. Micromanagers of gene expression: the potentially widespread influence of metazoan microRNAs. *Nat Rev Genet,* 5**,** 396-400.

BECKER, A., THAKUR, B. K., WEISS, J. M., KIM, H. S., PEINADO, H. & LYDEN, D. 2016. Extracellular Vesicles in Cancer: Cell-to-Cell Mediators of Metastasis. *Cancer Cell,* 30**,** 836-848.

BEG, M. S., BRENNER, A. J., SACHDEV, J., BORAD, M., KANG, Y. K., STOUDEMIRE, J., SMITH, S., BADER, A. G., KIM, S. & HONG, D. S. 2017. Phase I study of MRX34, a liposomal miR-34a mimic, administered twice weekly in patients with advanced solid tumors. *Invest New Drugs,* 35**,** 180-188.

BEHM, M. & OHMAN, M. 2016. RNA Editing: A Contributor to Neuronal Dynamics in the Mammalian Brain. *Trends Genet,* 32**,** 165-175.

BERGERS, G. & FENDT, S. M. 2021. The metabolism of cancer cells during metastasis. *Nat Rev Cancer,* 21**,** 162-180.

BIGAGLI, E., LUCERI, C., GUASTI, D. & CINCI, L. 2016. Exosomes secreted from human colon cancer cells influence the adhesion of neighboring metastatic cells: Role of microRNA-210. *Cancer Biol Ther,* 17**,** 1062-1069.

BOYERINAS, B., PARK, S. M., HAU, A., MURMANN, A. E. & PETER, M. E. 2010. The role of let-7 in cell differentiation and cancer. *Endocr Relat Cancer,* 17**,** F19-36.

BOYERINAS, B., PARK, S. M., SHOMRON, N., HEDEGAARD, M. M., VINTHER, J., ANDERSEN, J. S., FEIG, C., XU, J., BURGE, C. B. & PETER, M. E. 2008. Identification of let-7-regulated oncofetal genes. *Cancer Res,* 68**,** 2587-91.

BRIATA, P. & GHERZI, R. 2020. Long Non-Coding RNA-Ribonucleoprotein Networks in the Post-Transcriptional Control of Gene Expression. *Noncoding RNA,* 6.

BUSSING, I., SLACK, F. J. & GROSSHANS, H. 2008. let-7 microRNAs in development, stem cells and cancer. *Trends Mol Med,* 14**,** 400-9.

CAI, S., PATAILLOT-MEAKIN, T., SHIBAKAWA, A., REN, R., BEVAN, C. L., LADAME, S., IVANOV, A. P. & EDEL, J. B. 2021. Single-molecule amplification-free multiplexed detection of circulating microRNA cancer biomarkers from serum. *Nat Commun,* 12**,** 3515.

CAMPBELL, P. J., YACHIDA, S., MUDIE, L. J., STEPHENS, P. J., PLEASANCE, E. D., STEBBINGS, L. A., MORSBERGER, L. A., LATIMER, C., MCLAREN, S., LIN, M. L., MCBRIDE, D. J., VARELA, I., NIK-

ZAINAL, S. A., LEROY, C., JIA, M., MENZIES, A., BUTLER, A. P., TEAGUE, J. W., GRIFFIN, C. A., BURTON, J., SWERDLOW, H., QUAIL, M. A., STRATTON, M. R., IACOBUZIO-DONAHUE, C. & FUTREAL, P. A. 2010. The patterns and dynamics of genomic instability in metastatic pancreatic cancer. *Nature,* 467**,** 1109-13.

CAO, S., ZHOU, D. C., OH, C., JAYASINGHE, R. G., ZHAO, Y., YOON, C. J., WYCZALKOWSKI, M. A., BAILEY, M. H., TSOU, T., GAO, Q., MALONE, A., REYNOLDS, S., SHMULEVICH, I., WENDL, M. C., CHEN, F. & DING, L. 2020. Discovery of driver non-coding splice-site-creating mutations in cancer. *Nat Commun,* 11**,** 5573.

CARPENTER, S., RICCI, E. P., MERCIER, B. C., MOORE, M. J. & FITZGERALD, K. A. 2014. Post-transcriptional regulation of gene expression in innate immunity. *Nat Rev Immunol,* 14**,** 361-76.

CASTELLO, A., HENTZE, M. W. & PREISS, T. 2015. Metabolic Enzymes Enjoying New Partnerships as RNA-Binding Proteins. *Trends Endocrinol Metab,* 26**,** 746-757.

CHEN, A. X., YU, K. D., FAN, L., LI, J. Y., YANG, C., HUANG, A. J. & SHAO, Z. M. 2011. Germline genetic variants disturbing the Let-7/LIN28 double-negative feedback loop alter breast cancer susceptibility. *PLoS Genet,* 7**,** e1002259.

CHEN, B., SANG, Y., SONG, X., ZHANG, D., WANG, L., ZHAO, W., LIANG, Y., ZHANG, N. & YANG, Q. 2021. Exosomal miR-500a-5p derived from cancer-associated fibroblasts promotes breast cancer cell proliferation and metastasis through targeting USP28. *Theranostics,* 11**,** 3932-3947.

CHEN, D., SUN, Y., WEI, Y., ZHANG, P., REZAEIAN, A. H., TERUYA-FELDSTEIN, J., GUPTA, S., LIANG, H., LIN, H. K., HUNG, M. C. & MA, L. 2012. LIFR is a breast cancer metastasis suppressor upstream of the Hippo-YAP pathway and a prognostic marker. *Nat Med,* 18**,** 1511-7.

CHIPMAN, L. B. & PASQUINELLI, A. E. 2019. miRNA Targeting: Growing beyond the Seed. *Trends Genet,* 35**,** 215-222.

COBB, M. 2017. 60 years ago, Francis Crick changed the logic of biology. *PLoS Biol,* 15**,** e2003243.

CORBETT, A. H. 2018. Post-transcriptional regulation of gene expression and human disease. *Curr Opin Cell Biol,* 52**,** 96-104.

CRICK, F. 1970. Central dogma of molecular biology. *Nature,* 227**,** 561-3.

CUADRADO, A., GARCIA-FERNANDEZ, L. F., IMAI, T., OKANO, H. & MUNOZ, A. 2002. Regulation of tau RNA maturation by thyroid hormone is mediated by the neural RNA-binding protein musashi-1. *Mol Cell Neurosci,* 20**,** 198-210.

DI VIZIO, D., MORELLO, M., DUDLEY, A. C., SCHOW, P. W., ADAM, R. M., MORLEY, S., MULHOLLAND, D., ROTINEN, M., HAGER, M. H., INSABATO, L., MOSES, M. A., DEMICHELIS, F., LISANTI, M. P., WU, H., KLAGSBRUN, M., BHOWMICK, N. A., RUBIN, M. A., D'SOUZA-SCHOREY, C. & FREEMAN, M. R. 2012. Large oncosomes in human prostate cancer tissues and in the circulation of mice with metastatic disease. *Am J Pathol,* 181**,** 1573-84.

DIANAT-MOGHADAM, H., MAHARI, A., HEIDARIFARD, M., PARNIANFARD, N., POURMOUSAVI-KH, L., RAHBARGHAZI, R. & AMOOZGAR, Z. 2021. NK cells-directed therapies target circulating tumor cells and metastasis. *Cancer Lett,* 497**,** 41-53.

DIDIANO, D. & HOBERT, O. 2006. Perfect seed pairing is not a generally reliable predictor for miRNA-target interactions. *Nat Struct Mol Biol,* 13**,** 849-51.

DIVISATO, G., PASSARO, F., RUSSO, T. & PARISI, S. 2020. The Key Role of MicroRNAs in Self-Renewal and Differentiation of Embryonic Stem Cells. *Int J Mol Sci,* 21.

DYBA, T., RANDI, G., BRAY, F., MARTOS, C., GIUSTI, F., NICHOLSON, N., GAVIN, A., FLEGO, M., NEAMTIU, L., DIMITROVA, N., NEGRAO CARVALHO, R., FERLAY, J. & BETTIO, M. 2021. The European cancer

burden in 2020: Incidence and mortality estimates for 40 countries and 25 major cancers. *Eur J Cancer,* 157**,** 308-347.

ENOMOTO, M., VAUGHEN, J. & IGAKI, T. 2015. Non-autonomous overgrowth by oncogenic niche cells: Cellular cooperation and competition in tumorigenesis. *Cancer Sci,* 106**,** 1651-8.

ERSON-BENSAN, A. E. & CAN, T. 2016. Alternative Polyadenylation: Another Foe in Cancer. *Mol Cancer Res,* 14**,** 507-17.

ESPOSITO, M., GANESAN, S. & KANG, Y. 2021. Emerging strategies for treating metastasis. *Nat Cancer,* 2**,** 258-270.

FARES, J., FARES, M. Y., KHACHFE, H. H., SALHAB, H. A. & FARES, Y. 2020. Molecular principles of metastasis: a hallmark of cancer revisited. *Signal Transduct Target Ther,* 5**,** 28.

FEIGERLOVA, E. & BATTAGLIA-HSU, S. F. 2017. Role of post-transcriptional regulation of mRNA stability in renal pathophysiology: focus on chronic kidney disease. *FASEB J,* 31**,** 457-468.

FENG, C., NEUMEISTER, V., MA, W., XU, J., LU, L., BORDEAUX, J., MAIHLE, N. J., RIMM, D. L. & HUANG, Y. 2012. Lin28 regulates HER2 and promotes malignancy through multiple mechanisms. *Cell Cycle,* 11**,** 2486-94.

FENG, W., DEAN, D. C., HORNICEK, F. J., SHI, H. & DUAN, Z. 2019. Exosomes promote pre-metastatic niche formation in ovarian cancer. *Mol Cancer,* 18**,** 124.

FIDLER, I. J. 2003. The pathogenesis of cancer metastasis: the 'seed and soil' hypothesis revisited. *Nat Rev Cancer,* 3**,** 453-8.

FIDLER, I. J. & POSTE, G. 2008. The “seed and soil” hypothesis revisited. *The Lancet Oncology,* 9.

FILIPOWICZ, W., BHATTACHARYYA, S. N. & SONENBERG, N. 2008. Mechanisms of post-transcriptional regulation by microRNAs: are the answers in sight? *Nat Rev Genet,* 9**,** 102-14.

FLYNT, A. S. & LAI, E. C. 2008. Biological principles of microRNA-mediated regulation: shared themes amid diversity. *Nat Rev Genet,* 9**,** 831-42.

FRANKS, A., AIROLDI, E. & SLAVOV, N. 2017. Post-transcriptional regulation across human tissues. *PLoS Comput Biol,* 13**,** e1005535.

FUJIWARA, N., INOUE, J., KAWANO, T., TANIMOTO, K., KOZAKI, K. & INAZAWA, J. 2015. miR-634 Activates the Mitochondrial Apoptosis Pathway and Enhances Chemotherapy-Induced Cytotoxicity. *Cancer Res,* 75**,** 3890-901.

GANESH, K. & MASSAGUE, J. 2021. Targeting metastatic cancer. *Nat Med,* 27**,** 34-44.

GARO, L. P., AJAY, A. K., FUJIWARA, M., GABRIELY, G., RAHEJA, R., KUHN, C., KENYON, B., SKILLIN, N., KADOWAKI-SAGA, R., SAXENA, S. & MURUGAIYAN, G. 2021. MicroRNA-146a limits tumorigenic inflammation in colorectal cancer. *Nat Commun,* 12**,** 2419.

GERSTBERGER, S., HAFNER, M. & TUSCHL, T. 2014. A census of human RNA-binding proteins. *Nat Rev Genet,* 15**,** 829-45.

GHOSHAL, B., BERTRAND, E. & BHATTACHARYYA, S. N. 2021. Non-canonical argonaute loading of extracellular vesicle-derived exogenous single-stranded miRNA in recipient cells. *J Cell Sci,* 134.

GILLES, M. E. & SLACK, F. J. 2018. Let-7 microRNA as a potential therapeutic target with implications for immunotherapy. *Expert Opin Ther Targets,* 22**,** 929-939.

GOKITA, K., INOUE, J., ISHIHARA, H., KOJIMA, K. & INAZAWA, J. 2020. Therapeutic Potential of LNP-Mediated Delivery of miR-634 for Cancer Therapy. *Mol Ther Nucleic Acids,* 19**,** 330-338.

GOSLINE, S. J., GURTAN, A. M., JNBAPTISTE, C. K., BOSSON, A., MILANI, P., DALIN, S., MATTHEWS, B. J., YAP, Y. S., SHARP, P. A. & FRAENKEL, E. 2016. Elucidating MicroRNA Regulatory Networks Using Transcriptional, Post-transcriptional, and Histone Modification Measurements. *Cell Rep,* 14**,**

310-9.

HANAHAN, D. & WEINBERG, R. A. 2011. Hallmarks of cancer: the next generation. *Cell,* 144**,** 646-74.

HATLEY, M. E., PATRICK, D. M., GARCIA, M. R., RICHARDSON, J. A., BASSEL-DUBY, R., VAN ROOIJ, E. & OLSON, E. N. 2010. Modulation of K-Ras-dependent lung tumorigenesis by MicroRNA-21. *Cancer Cell,* 18**,** 282-93.

HE, C., HUANG, F., ZHANG, K., WEI, J., HU, K. & LIANG, M. 2021. Establishment and validation of an RNA binding protein-associated prognostic model for ovarian cancer. *J Ovarian Res,* 14**,** 27.

HENTZE, M. W., CASTELLO, A., SCHWARZL, T. & PREISS, T. 2018. A brave new world of RNA-binding proteins. *Nat Rev Mol Cell Biol,* 19**,** 327-341.

HEO, I., JOO, C., KIM, Y. K., HA, M., YOON, M. J., CHO, J., YEOM, K. H., HAN, J. & KIM, V. N. 2009. TUT4 in concert with Lin28 suppresses microRNA biogenesis through pre-microRNA uridylation. *Cell,* 138**,** 696-708.

HIAM-GALVEZ, K. J., ALLEN, B. M. & SPITZER, M. H. 2021. Systemic immunity in cancer. *Nat Rev Cancer,* 21**,** 345-359.

HOBERT, O. 2004. Common logic of transcription factor and microRNA action. *Trends Biochem Sci,* 29**,** 462-8.

HONG, D. S., KANG, Y. K., BORAD, M., SACHDEV, J., EJADI, S., LIM, H. Y., BRENNER, A. J., PARK, K., LEE, J. L., KIM, T. Y., SHIN, S., BECERRA, C. R., FALCHOOK, G., STOUDEMIRE, J., MARTIN, D., KELNAR, K., PELTIER, H., BONATO, V., BADER, A. G., SMITH, S., KIM, S., O'NEILL, V. & BEG, M. S. 2020. Phase 1 study of MRX34, a liposomal miR-34a mimic, in patients with advanced solid tumours. *Br J Cancer,* 122**,** 1630-1637.

HOSSEINI, K., RANJBAR, M., PIRPOUR TAZEHKAND, A., ASGHARIAN, P., MONTAZERSAHEB, S., TARHRIZ, V. & GHASEMNEJAD, T. 2022. Evaluation of exosomal non-coding RNAs in cancer using high-throughput sequencing. *J Transl Med,* 20**,** 30.

HSU, P. J., SHI, H., ZHU, A. C., LU, Z., MILLER, N., EDENS, B. M., MA, Y. C. & HE, C. 2019. The RNA-binding protein FMRP facilitates the nuclear export of N (6)-methyladenosine-containing mRNAs. *J Biol Chem,* 294**,** 19889-19895.

HU, X., HARVEY, S. E., ZHENG, R., LYU, J., GRZESKOWIAK, C. L., POWELL, E., PIWNICA-WORMS, H., SCOTT, K. L. & CHENG, C. 2020. The RNA-binding protein AKAP8 suppresses tumor metastasis by antagonizing EMT-associated alternative splicing. *Nat Commun,* 11**,** 486.

HUANG, X., ZHU, X., YU, Y., ZHU, W., JIN, L., ZHANG, X., LI, S., ZOU, P., XIE, C. & CUI, R. 2021. Dissecting miRNA signature in colorectal cancer progression and metastasis. *Cancer Lett,* 501**,** 66-82.

HUSSEN, B. M., HIDAYAT, H. J., SALIHI, A., SABIR, D. K., TAHERI, M. & GHAFOURI-FARD, S. 2021. MicroRNA: A signature for cancer progression. *Biomed Pharmacother,* 138**,** 111528.

INOUE, J., FUJIWARA, K., HAMAMOTO, H., KOBAYASHI, K. & INAZAWA, J. 2020. Improving the Efficacy of EGFR Inhibitors by Topical Treatment of Cutaneous Squamous Cell Carcinoma with miR-634 Ointment. *Mol Ther Oncolytics,* 19**,** 294-307.

INOUE, J. & INAZAWA, J. 2021. Cancer-associated miRNAs and their therapeutic potential. *J Hum Genet,* 66**,** 937-945.

IZUMI, D., ZHU, Z., CHEN, Y., TODEN, S., HUO, X., KANDA, M., ISHIMOTO, T., GU, D., TAN, M., KODERA, Y., BABA, H., LI, W., CHEN, J., WANG, X. & GOEL, A. 2021. Assessment of the Diagnostic Efficiency of a Liquid Biopsy Assay for Early Detection of Gastric Cancer. *JAMA Netw Open,* 4**,** e2121129.

JIAO, X., CHANG, J. H., KILIC, T., TONG, L. & KILEDJIAN, M. 2013. A mammalian pre-mRNA 5' end capping quality control mechanism and an unexpected link of capping to pre-mRNA processing. *Mol*

Cell, 50**,** 104-15.

KAFASLA, P., SKLIRIS, A. & KONTOYIANNIS, D. L. 2014. Post-transcriptional coordination of immunological responses by RNA-binding proteins. *Nat Immunol,* 15**,** 492-502.

KALLURI, R. & LEBLEU, V. S. 2020. The biology, function, and biomedical applications of exosomes. *Science,* 367.

KASINATH, B. S., MARIAPPAN, M. M., SATARANATARAJAN, K., LEE, M. J. & FELIERS, D. 2006. mRNA translation: unexplored territory in renal science. *J Am Soc Nephrol,* 17**,** 3281-92.

KASSAM, Z., LEE, C. H., YUAN, Y. & HUNT, R. H. 2013. Fecal microbiota transplantation for Clostridium difficile infection: systematic review and meta-analysis. *Am J Gastroenterol,* 108**,** 500-8.

KECHAVARZI, B. & JANGA, S. C. 2014. Dissecting the expression landscape of RNA-binding proteins in human cancers. *Genome Biol,* 15**,** R14.

KELLER, L. & PANTEL, K. 2019. Unravelling tumour heterogeneity by single-cell profiling of circulating tumour cells. *Nat Rev Cancer,* 19**,** 553-567.

KIM, J., YAO, F., XIAO, Z., SUN, Y. & MA, L. 2018. MicroRNAs and metastasis: small RNAs play big roles. *Cancer Metastasis Rev,* 37**,** 5-15.

KIM, M. Y., OSKARSSON, T., ACHARYYA, S., NGUYEN, D. X., ZHANG, X. H., NORTON, L. & MASSAGUE, J. 2009. Tumor self-seeding by circulating cancer cells. *Cell,* 139**,** 1315-26.

KIM, W. & KYUNG LEE, E. 2012. Post-transcriptional regulation in metabolic diseases. *RNA Biol,* 9**,** 772-80.

KOBAYASHI, M., SALOMON, C., TAPIA, J., ILLANES, S. E., MITCHELL, M. D. & RICE, G. E. 2014. Ovarian cancer cell invasiveness is associated with discordant exosomal sequestration of Let-7 miRNA and miR-200. *J Transl Med,* 12**,** 4.

KOHLER, A. & HURT, E. 2007. Exporting RNA from the nucleus to the cytoplasm. *Nat Rev Mol Cell Biol,* 8**,** 761-73.

KOPPERS-LALIC, D., HACKENBERG, M., BIJNSDORP, I. V., VAN EIJNDHOVEN, M. A. J., SADEK, P., SIE, D., ZINI, N., MIDDELDORP, J. M., YLSTRA, B., DE MENEZES, R. X., WURDINGER, T., MEIJER, G. A. & PEGTEL, D. M. 2014. Nontemplated nucleotide additions distinguish the small RNA composition in cells from exosomes. *Cell Rep,* 8**,** 1649-1658.

KUHN, D. E., MARTIN, M. M., FELDMAN, D. S., TERRY, A. V., JR., NUOVO, G. J. & ELTON, T. S. 2008. Experimental validation of miRNA targets. *Methods,* 44**,** 47-54.

KWOK, G. T., ZHAO, J. T., WEISS, J., MUGRIDGE, N., BRAHMBHATT, H., MACDIARMID, J. A., ROBINSON, B. G. & SIDHU, S. B. 2017. Translational applications of microRNAs in cancer, and therapeutic implications. *Noncoding RNA Res,* 2**,** 143-150.

LACAVA, J., HOUSELEY, J., SAVEANU, C., PETFALSKI, E., THOMPSON, E., JACQUIER, A. & TOLLERVEY, D. 2005. RNA degradation by the exosome is promoted by a nuclear polyadenylation complex. *Cell,* 121**,** 713-24.

LAMPIS, A., HAHNE, J. C., GASPARINI, P., CASCIONE, L., HEDAYAT, S., VLACHOGIANNIS, G., MURGIA, C., FONTANA, E., EDWARDS, J., HORGAN, P. G., TERRACCIANO, L., SANSOM, O. J., MARTINS, C. D., KRAMER-MAREK, G., CROCE, C. M., BRACONI, C., FASSAN, M. & VALERI, N. 2021. MIR21-induced loss of junctional adhesion molecule A promotes activation of oncogenic pathways, progression and metastasis in colorectal cancer. *Cell Death Differ,* 28**,** 2970-2982.

LANDER, E. S., LINTON, L. M., BIRREN, B., NUSBAUM, C., ZODY, M. C., BALDWIN, J., DEVON, K., DEWAR, K., DOYLE, M., FITZHUGH, W., FUNKE, R., GAGE, D., HARRIS, K., HEAFORD, A., HOWLAND, J., KANN, L., LEHOCZKY, J., LEVINE, R., MCEWAN, P., MCKERNAN, K., MELDRIM, J., MESIROV, J. P.,

MIRANDA, C., MORRIS, W., NAYLOR, J., RAYMOND, C., ROSETTI, M., SANTOS, R., SHERIDAN, A., SOUGNEZ, C., STANGE-THOMANN, Y., STOJANOVIC, N., SUBRAMANIAN, A., WYMAN, D., ROGERS, J., SULSTON, J., AINSCOUGH, R., BECK, S., BENTLEY, D., BURTON, J., CLEE, C., CARTER, N., COULSON, A., DEADMAN, R., DELOUKAS, P., DUNHAM, A., DUNHAM, I., DURBIN, R., FRENCH, L., GRAFHAM, D., GREGORY, S., HUBBARD, T., HUMPHRAY, S., HUNT, A., JONES, M., LLOYD, C., MCMURRAY, A., MATTHEWS, L., MERCER, S., MILNE, S., MULLIKIN, J. C., MUNGALL, A., PLUMB, R., ROSS, M., SHOWNKEEN, R., SIMS, S., WATERSTON, R. H., WILSON, R. K., HILLIER, L. W., MCPHERSON, J. D., MARRA, M. A., MARDIS, E. R., FULTON, L. A., CHINWALLA, A. T., PEPIN, K. H., GISH, W. R., CHISSOE, S. L., WENDL, M. C., DELEHAUNTY, K. D., MINER, T. L., DELEHAUNTY, A., KRAMER, J. B., COOK, L. L., FULTON, R. S., JOHNSON, D. L., MINX, P. J., CLIFTON, S. W., HAWKINS, T., BRANSCOMB, E., PREDKI, P., RICHARDSON, P., WENNING, S., SLEZAK, T., DOGGETT, N., CHENG, J. F., OLSEN, A., LUCAS, S., ELKIN, C., UBERBACHER, E., FRAZIER, M., et al. 2001. Initial sequencing and analysis of the human genome. *Nature,* 409**,** 860-921.

LE, X. F., MERCHANT, O., BAST, R. C. & CALIN, G. A. 2010. The Roles of MicroRNAs in the Cancer Invasion-Metastasis Cascade. *Cancer Microenviron,* 3**,** 137-47.

LEBLEU, V. S. & KALLURI, R. 2020. Exosomes as a Multicomponent Biomarker Platform in Cancer. *Trends Cancer,* 6**,** 767-774.

LEE, R. C., FEINBAUM, R. L. & AMBROS, V. 1993. The C. elegans heterochronic gene lin-4 encodes small RNAs with antisense complementarity to lin-14. *Cell,* 75**,** 843-854.

LENER, T., GIMONA, M., AIGNER, L., BORGER, V., BUZAS, E., CAMUSSI, G., CHAPUT, N., CHATTERJEE, D., COURT, F. A., DEL PORTILLO, H. A., O'DRISCOLL, L., FAIS, S., FALCON-PEREZ, J. M., FELDERHOFF-MUESER, U., FRAILE, L., GHO, Y. S., GORGENS, A., GUPTA, R. C., HENDRIX, A., HERMANN, D. M., HILL, A. F., HOCHBERG, F., HORN, P. A., DE KLEIJN, D., KORDELAS, L., KRAMER, B. W., KRAMER-ALBERS, E. M., LANER-PLAMBERGER, S., LAITINEN, S., LEONARDI, T., LORENOWICZ, M. J., LIM, S. K., LOTVALL, J., MAGUIRE, C. A., MARCILLA, A., NAZARENKO, I., OCHIYA, T., PATEL, T., PEDERSEN, S., POCSFALVI, G., PLUCHINO, S., QUESENBERRY, P., REISCHL, I. G., RIVERA, F. J., SANZENBACHER, R., SCHALLMOSER, K., SLAPER-CORTENBACH, I., STRUNK, D., TONN, T., VADER, P., VAN BALKOM, B. W., WAUBEN, M., ANDALOUSSI, S. E., THERY, C., ROHDE, E. & GIEBEL, B. 2015. Applying extracellular vesicles based therapeutics in clinical trials - an ISEV position paper. *J Extracell Vesicles,* 4**,** 30087.

LI, J., TANG, H., MULLEN, T. M., WESTBERG, C., REDDY, T. R., ROSE, D. W. & WONG-STAAL, F. 1999. A role for RNA helicase A in post-transcriptional regulation of HIV type 1. *Proc Natl Acad Sci U S A,* 96**,** 709-14.

LI, J., XUE, J., LING, M., SUN, J., XIAO, T., DAI, X., SUN, Q., CHENG, C., XIA, H., WEI, Y., CHEN, F. & LIU, Q. 2021. MicroRNA-15b in extracellular vesicles from arsenite-treated macrophages promotes the progression of hepatocellular carcinomas by blocking the LATS1-mediated Hippo pathway. *Cancer Lett,* 497**,** 137-153.

LIU, C., KELNAR, K., LIU, B., CHEN, X., CALHOUN-DAVIS, T., LI, H., PATRAWALA, L., YAN, H., JETER, C., HONORIO, S., WIGGINS, J. F., BADER, A. G., FAGIN, R., BROWN, D. & TANG, D. G. 2011. The microRNA miR-34a inhibits prostate cancer stem cells and metastasis by directly repressing CD44. *Nat Med,* 17**,** 211-5.

LIU, D., CHEN, C., CUI, M. & ZHANG, H. 2021a. miR-140-3p inhibits colorectal cancer progression and its liver metastasis by targeting BCL9 and BCL2. *Cancer Med,* 10**,** 3358-3372.

LIU, Q., ZHANG, H., JIANG, X., QIAN, C., LIU, Z. & LUO, D. 2017. Factors involved in cancer metastasis: a

better understanding to "seed and soil" hypothesis. *Mol Cancer,* 16**,** 176.

LIU, Y., LI, H., FENG, J., CUI, X., HUANG, W., LI, Y., SU, F., LIU, Q., ZHU, J., LV, X., CHEN, J., HUANG, D. & YU, F. 2013. Lin28 induces epithelial-to-mesenchymal transition and stemness via downregulation of let-7a in breast cancer cells. *PLoS One,* 8**,** e83083.

LIU, Y. D., ZHUANG, X. P., CAI, D. L., CAO, C., GU, Q. S., LIU, X. N., ZHENG, B. B., GUAN, B. J., YU, L., LI, J. K., DING, H. B. & YAN, D. W. 2021b. Let-7a regulates EV secretion and mitochondrial oxidative phosphorylation by targeting SNAP23 in colorectal cancer. *J Exp Clin Cancer Res,* 40**,** 31.

LOBB, R. J., BECKER, M., WEN, S. W., WONG, C. S., WIEGMANS, A. P., LEIMGRUBER, A. & MOLLER, A. 2015. Optimized exosome isolation protocol for cell culture supernatant and human plasma. *J Extracell Vesicles,* 4**,** 27031.

LODES, M. J., CARABALLO, M., SUCIU, D., MUNRO, S., KUMAR, A. & ANDERSON, B. 2009. Detection of cancer with serum miRNAs on an oligonucleotide microarray. *PLoS One,* 4**,** e6229.

LOPEZ DE SILANES, I., ZHAN, M., LAL, A., YANG, X. & GOROSPE, M. 2004. Identification of a target RNA motif for RNA-binding protein HuR. *Proc Natl Acad Sci U S A,* 101**,** 2987-92.

MA, L., TERUYA-FELDSTEIN, J. & WEINBERG, R. A. 2007. Tumour invasion and metastasis initiated by microRNA-10b in breast cancer. *Nature,* 449**,** 682-8.

MA, L., YOUNG, J., PRABHALA, H., PAN, E., MESTDAGH, P., MUTH, D., TERUYA-FELDSTEIN, J., REINHARDT, F., ONDER, T. T., VALASTYAN, S., WESTERMANN, F., SPELEMAN, F., VANDESOMPELE, J. & WEINBERG, R. A. 2010. miR-9, a MYC/MYCN-activated microRNA, regulates E-cadherin and cancer metastasis. *Nat Cell Biol,* 12**,** 247-56.

MASHOURI, L., YOUSEFI, H., AREF, A. R., AHADI, A. M., MOLAEI, F. & ALAHARI, S. K. 2019. Exosomes: composition, biogenesis, and mechanisms in cancer metastasis and drug resistance. *Mol Cancer,* 18**,** 75.

MASSAGUE, J. & GANESH, K. 2021. Metastasis-Initiating Cells and Ecosystems. *Cancer Discov,* 11**,** 971-994.

MATEI, I., KIM, H. S. & LYDEN, D. 2017. Unshielding Exosomal RNA Unleashes Tumor Growth And Metastasis. *Cell,* 170**,** 223-225.

MATHIEU, M., MARTIN-JAULAR, L., LAVIEU, G. & THERY, C. 2019. Specificities of secretion and uptake of exosomes and other extracellular vesicles for cell-to-cell communication. *Nat Cell Biol,* 21**,** 9-17.

MATHIEU, M., NEVO, N., JOUVE, M., VALENZUELA, J. I., MAURIN, M., VERWEIJ, F. J., PALMULLI, R., LANKAR, D., DINGLI, F., LOEW, D., RUBINSTEIN, E., BONCOMPAIN, G., PEREZ, F. & THERY, C. 2021. Specificities of exosome versus small ectosome secretion revealed by live intracellular tracking of CD63 and CD9. *Nat Commun,* 12**,** 4389.

MATTICK, J. S. & MAKUNIN, I. V. 2006. Non-coding RNA. *Hum Mol Genet,* 15 Spec No 1**,** R17-29.

MAYDANOVYCH, O. & BEAL, P. A. 2006. Breaking the central dogma by RNA editing. *Chem Rev,* 106**,** 3397-411.

MCGARY, E. C., RONDON, I. J. & BECKMAN, B. S. 1997. Post-transcriptional regulation of erythropoietin mRNA stability by erythropoietin mRNA-binding protein. *J Biol Chem,* 272**,** 8628-34.

MEDER, L., KONIG, K., DIETLEIN, F., MACHELEIDT, I., FLORIN, A., ERCANOGLU, M. S., ROMMERSCHEIDT-FUSS, U., KOKER, M., SCHON, G., ODENTHAL, M., KLEIN, F., BUTTNER, R., SCHULTE, J. H., HEUKAMP, L. C. & ULLRICH, R. T. 2018. LIN28B enhanced tumorigenesis in an autochthonous KRAS(G12V)-driven lung carcinoma mouse model. *Oncogene,* 37**,** 2746-2756.

MENDELL, J. T. 2008. miRiad roles for the miR-17-92 cluster in development and disease. *Cell,* 133**,** 217-

22.

MIZUNO, R., KAWADA, K. & SAKAI, Y. 2018. The Molecular Basis and Therapeutic Potential of Let-7 MicroRNAs against Colorectal Cancer. *Can J Gastroenterol Hepatol,* 2018**,** 5769591.

MUKHERJEE, N., CORCORAN, D. L., NUSBAUM, J. D., REID, D. W., GEORGIEV, S., HAFNER, M., ASCANO, M., JR., TUSCHL, T., OHLER, U. & KEENE, J. D. 2011. Integrative regulatory mapping indicates that the RNA-binding protein HuR couples pre-mRNA processing and mRNA stability. *Mol Cell,* 43**,** 327-39.

NGUYEN, D. X., BOS, P. D. & MASSAGUE, J. 2009. Metastasis: from dissemination to organ-specific colonization. *Nat Rev Cancer,* 9**,** 274-84.

NICOLOSO, M. S., SPIZZO, R., SHIMIZU, M., ROSSI, S. & CALIN, G. A. 2009. MicroRNAs--the micro steering wheel of tumour metastases. *Nat Rev Cancer,* 9**,** 293-302.

O'DRISCOLL, L. 2015. Expanding on exosomes and ectosomes in cancer. *N Engl J Med,* 372**,** 2359-62.

OHSHIMA, K., INOUE, K., FUJIWARA, A., HATAKEYAMA, K., KANTO, K., WATANABE, Y., MURAMATSU, K., FUKUDA, Y., OGURA, S., YAMAGUCHI, K. & MOCHIZUKI, T. 2010. Let-7 microRNA family is selectively secreted into the extracellular environment via exosomes in a metastatic gastric cancer cell line. *PLoS One,* 5**,** e13247.

OKTAY, M. H., LEE, Y. F., HARNEY, A., FARRELL, D., KUHN, N. Z., MORRIS, S. A., GREENSPAN, E., MOHLA, S., GRODZINSKI, P. & NORTON, L. 2015. Cell-to-cell communication in cancer: workshop report. *NPJ Breast Cancer,* 1**,** 15022.

OTMANI, K. & LEWALLE, P. 2021. Tumor Suppressor miRNA in Cancer Cells and the Tumor Microenvironment: Mechanism of Deregulation and Clinical Implications. *Front Oncol,* 11**,** 708765.

PACHMANN, K. 2005. Longtime recirculating tumor cells in breast cancer patients. *Clin Cancer Res,* 11**,** 5657; author reply 5657-8.

PASQUINELLI, A. E., REINHART, B. J., SLACK, F., MARTINDALE, M. Q., KURODA, M. I., MALLER, B., HAYWARD, D. C., BALL, E. E., DEGNAN, B., MULLER, P., SPRING, J., SRINIVASAN, A., FISHMAN, M., FINNERTY, J., CORBO, J., LEVINE, M., LEAHY, P., DAVIDSON, E. & RUVKUN, G. 2000. Conservation of the sequence and temporal expression of let-7 heterochronic regulatory RNA. *Nature,* 408**,** 86-9.

PEINADO, H., ZHANG, H., MATEI, I. R., COSTA-SILVA, B., HOSHINO, A., RODRIGUES, G., PSAILA, B., KAPLAN, R. N., BROMBERG, J. F., KANG, Y., BISSELL, M. J., COX, T. R., GIACCIA, A. J., ERLER, J. T., HIRATSUKA, S., GHAJAR, C. M. & LYDEN, D. 2017. Pre-metastatic niches: organ-specific homes for metastases. *Nat Rev Cancer,* 17**,** 302-317.

PENG, S., CHEN, L. L., LEI, X. X., YANG, L., LIN, H., CARMICHAEL, G. G. & HUANG, Y. 2011. Genome-wide studies reveal that Lin28 enhances the translation of genes important for growth and survival of human embryonic stem cells. *Stem Cells,* 29**,** 496-504.

PISKOUNOVA, E., POLYTARCHOU, C., THORNTON, J. E., LAPIERRE, R. J., POTHOULAKIS, C., HAGAN, J. P., ILIOPOULOS, D. & GREGORY, R. I. 2011. Lin28A and Lin28B inhibit let-7 microRNA biogenesis by distinct mechanisms. *Cell,* 147**,** 1066-79.

PLOTNIKOVA, O., BARANOVA, A. & SKOBLOV, M. 2019. Comprehensive Analysis of Human microRNA-mRNA Interactome. *Front Genet,* 10**,** 933.

POWERS, J. T., TSANOV, K. M., PEARSON, D. S., ROELS, F., SPINA, C. S., EBRIGHT, R., SELIGSON, M., DE SOYSA, Y., CAHAN, P., THEISSEN, J., TU, H. C., HAN, A., KUREK, K. C., LAPIER, G. S., OSBORNE, J. K., ROSS, S. J., CESANA, M., COLLINS, J. J., BERTHOLD, F. & DALEY, G. Q. 2016. Multiple

mechanisms disrupt the let-7 microRNA family in neuroblastoma. *Nature,* 535**,** 246-51.

QIAN, P., ZUO, Z., WU, Z., MENG, X., LI, G., WU, Z., ZHANG, W., TAN, S., PANDEY, V., YAO, Y., WANG, P., ZHAO, L., WANG, J., WU, Q., SONG, E., LOBIE, P. E., YIN, Z. & ZHU, T. 2011. Pivotal role of reduced let-7g expression in breast cancer invasion and metastasis. *Cancer Res,* 71**,** 6463-74.

REDDY, T. R., TANG, H., XU, W. & WONG-STAAL, F. 2000. Sam68, RNA helicase A and Tap cooperate in the post-transcriptional regulation of human immunodeficiency virus and type D retroviral mRNA. *Oncogene,* 19**,** 3570-5.

REID, G., KAO, S. C., PAVLAKIS, N., BRAHMBHATT, H., MACDIARMID, J., CLARKE, S., BOYER, M. & VAN ZANDWIJK, N. 2016. Clinical development of TargomiRs, a miRNA mimic-based treatment for patients with recurrent thoracic cancer. *Epigenomics,* 8**,** 1079-85.

REINHART, B. J., SLACK, F. J., BASSON, M., PASQUINELLI, A. E., BETTINGER, J. C., ROUGVIE, A. E., HORVITZ, H. R. & RUVKUN, G. 2000. The 21-nucleotide let-7 RNA regulates developmental timing in Caenorhabditis elegans. *Nature,* 403**,** 901-6.

REN, F., ZHANG, N., ZHANG, L., MILLER, E. & PU, J. J. 2020. Alternative Polyadenylation: a new frontier in post transcriptional regulation. *Biomark Res,* 8**,** 67.

ROOD, J. E. & REGEV, A. 2021. The legacy of the Human Genome Project. *Science,* 373**,** 1442-1443.

ROUSH, S. & SLACK, F. J. 2008. The let-7 family of microRNAs. *Trends Cell Biol,* 18**,** 505-16.

RUPAIMOOLE, R., CALIN, G. A., LOPEZ-BERESTEIN, G. & SOOD, A. K. 2016. miRNA Deregulation in Cancer Cells and the Tumor Microenvironment. *Cancer Discov,* 6**,** 235-46.

SALIMIMOGHADAM, S., TAEFEHSHOKR, S., LOVELESS, R., TENG, Y., BERTOLI, G., TAEFEHSHOKR, N., MUSAVIAROO, F., HAJIASGHARZADEH, K. & BARADARAN, B. 2021. The role of tumor suppressor short non-coding RNAs on breast cancer. *Crit Rev Oncol Hematol,* 158**,** 103210.

SAMADI, P., AFSHAR, S., AMINI, R., NAJAFI, R., MAHDAVINEZHAD, A., SEDIGHI PASHAKI, A., GHOLAMI, M. H. & SAIDIJAM, M. 2019. Let-7e enhances the radiosensitivity of colorectal cancer cells by directly targeting insulin-like growth factor 1 receptor. *J Cell Physiol,* 234**,** 10718-10725.

SAMSONOVA, A., EL HAGE, K., DESFORGES, B., JOSHI, V., CLEMENT, M. J., LAMBERT, G., HENRIE, H., BABAULT, N., CRAVEUR, P., MAROUN, R. C., STEINER, E., BOUHSS, A., MAUCUER, A., LYABIN, D. N., OVCHINNIKOV, L. P., HAMON, L. & PASTRE, D. 2021. Lin28, a major translation reprogramming factor, gains access to YB-1-packaged mRNA through its cold-shock domain. *Commun Biol,* 4**,** 359.

SCHUSTER, E., TAFTAF, R., REDUZZI, C., ALBERT, M. K., ROMERO-CALVO, I. & LIU, H. 2021. Better together: circulating tumor cell clustering in metastatic cancer. *Trends Cancer,* 7**,** 1020-1032.

SCHWARZENBACH, H., NISHIDA, N., CALIN, G. A. & PANTEL, K. 2014. Clinical relevance of circulating cell-free microRNAs in cancer. *Nat Rev Clin Oncol,* 11**,** 145-56.

SHENOUDA, S. K. & ALAHARI, S. K. 2009. MicroRNA function in cancer: oncogene or a tumor suppressor? *Cancer Metastasis Rev,* 28**,** 369-78.

SHI, M., LIU, D., DUAN, H., SHEN, B. & GUO, N. 2010. Metastasis-related miRNAs, active players in breast cancer invasion, and metastasis. *Cancer Metastasis Rev,* 29**,** 785-99.

SHUI, B., LA ROCCA, G., VENTURA, A. & HAIGIS, K. M. 2022. Interplay between K-RAS and miRNAs. *Trends Cancer*.

SHUMAN, S. 2002. What messenger RNA capping tells us about eukaryotic evolution. *Nat Rev Mol Cell Biol,* 3**,** 619-25.

SHYH-CHANG, N. & DALEY, G. Q. 2013. Lin28: primal regulator of growth and metabolism in stem cells. *Cell Stem Cell,* 12**,** 395-406.

SI, M. L., ZHU, S., WU, H., LU, Z., WU, F. & MO, Y. Y. 2007. miR-21-mediated tumor growth. *Oncogene,* 26**,** 2799-803.

SIEGEL, R. L., MILLER, K. D., FUCHS, H. E. & JEMAL, A. 2021. Cancer Statistics, 2021. *CA Cancer J Clin,* 71**,** 7-33.

SLOMOVIC, S. & SCHUSTER, G. 2011. Exonucleases and endonucleases involved in polyadenylation-assisted RNA decay. *Wiley Interdiscip Rev RNA,* 2**,** 106-23.

SOLE, C. & LAWRIE, C. H. 2021. MicroRNAs in Metastasis and the Tumour Microenvironment. *Int J Mol Sci,* 22.

SPANO, D., HECK, C., DE ANTONELLIS, P., CHRISTOFORI, G. & ZOLLO, M. 2012. Molecular networks that regulate cancer metastasis. *Semin Cancer Biol,* 22**,** 234-49.

ST JOHNSTON, D., BROWN, N. H., GALL, J. G. & JANTSCH, M. 1992. A conserved double-stranded RNA-binding domain. *Proc Natl Acad Sci U S A,* 89**,** 10979-83.

STEEG, P. S. 2016. Targeting metastasis. *Nat Rev Cancer,* 16**,** 201-18.

STEWART, M. 2010. Nuclear export of mRNA. *Trends Biochem Sci,* 35**,** 609-17.

STRATTON, M. R., CAMPBELL, P. J. & FUTREAL, P. A. 2009. The cancer genome. *Nature,* 458**,** 719-24.

TAFTAF, R., LIU, X., SINGH, S., JIA, Y., DASHZEVEG, N. K., HOFFMANN, A. D., EL-SHENNAWY, L., RAMOS, E. K., ADORNO-CRUZ, V., SCHUSTER, E. J., SCHOLTEN, D., PATEL, D., ZHANG, Y., DAVIS, A. A., REDUZZI, C., CAO, Y., D'AMICO, P., SHEN, Y., CRISTOFANILLI, M., MULLER, W. A., VARADAN, V. & LIU, H. 2021. ICAM1 initiates CTC cluster formation and trans-endothelial migration in lung metastasis of breast cancer. *Nat Commun,* 12**,** 4867.

TAGUCHI, A., YANAGISAWA, K., TANAKA, M., CAO, K., MATSUYAMA, Y., GOTO, H. & TAKAHASHI, T. 2008. Identification of hypoxia-inducible factor-1 alpha as a novel target for miR-17-92 microRNA cluster. *Cancer Res,* 68**,** 5540-5.

TANNOCK, I. F. & HICKMAN, J. A. 2016. Limits to Personalized Cancer Medicine. *N Engl J Med,* 375**,** 1289-94.

TIE, Y., CHEN, C., YANG, Y., QIAN, Z., YUAN, H., WANG, H., TANG, H., PENG, Y., DU, X. & LIU, B. 2018. Upregulation of let-7f-5p promotes chemotherapeutic resistance in colorectal cancer by directly repressing several pro-apoptotic proteins. *Oncol Lett,* 15**,** 8695-8702.

TRAN, N. 2016. Cancer Exosomes as miRNA Factories. *Trends Cancer,* 2**,** 329-331.

TRANG, P., WIGGINS, J. F., DAIGE, C. L., CHO, C., OMOTOLA, M., BROWN, D., WEIDHAAS, J. B., BADER, A. G. & SLACK, F. J. 2011. Systemic delivery of tumor suppressor microRNA mimics using a neutral lipid emulsion inhibits lung tumors in mice. *Mol Ther,* 19**,** 1116-22.

TSAI, W. C., HSU, P. W., LAI, T. C., CHAU, G. Y., LIN, C. W., CHEN, C. M., LIN, C. D., LIAO, Y. L., WANG, J. L., CHAU, Y. P., HSU, M. T., HSIAO, M., HUANG, H. D. & TSOU, A. P. 2009. MicroRNA-122, a tumor suppressor microRNA that regulates intrahepatic metastasis of hepatocellular carcinoma. *Hepatology,* 49**,** 1571-82.

USTIANENKO, D., CHIU, H. S., TREIBER, T., WEYN-VANHENTENRYCK, S. M., TREIBER, N., MEISTER, G., SUMAZIN, P. & ZHANG, C. 2018. LIN28 Selectively Modulates a Subclass of Let-7 MicroRNAs. *Mol Cell,* 71**,** 271-283 e5.

VALASTYAN, S. & WEINBERG, R. A. 2011. Tumor metastasis: molecular insights and evolving paradigms. *Cell,* 147**,** 275-92.

VALENTINO, A., RECLUSA, P., SIRERA, R., GIALLOMBARDO, M., CAMPS, C., PAUWELS, P., CRISPI, S. & ROLFO, C. 2017. Exosomal microRNAs in liquid biopsies: future biomarkers for prostate cancer. *Clin Transl Oncol,* 19**,** 651-657.

VAN KOUWENHOVE, M., KEDDE, M. & AGAMI, R. 2011. MicroRNA regulation by RNA-binding proteins and its implications for cancer. *Nat Rev Cancer,* 11**,** 644-56.

VAN ZANDWIJK, N., PAVLAKIS, N., KAO, S. C., LINTON, A., BOYER, M. J., CLARKE, S., HUYNH, Y., CHRZANOWSKA, A., FULHAM, M. J., BAILEY, D. L., COOPER, W. A., KRITHARIDES, L., RIDLEY, L., PATTISON, S. T., MACDIARMID, J., BRAHMBHATT, H. & REID, G. 2017. Safety and activity of microRNA-loaded minicells in patients with recurrent malignant pleural mesothelioma: a first-in-man, phase 1, open-label, dose-escalation study. *The Lancet Oncology,* 18**,** 1386-1396.

VENTER, J. C., ADAMS, M. D., MYERS, E. W., LI, P. W., MURAL, R. J., SUTTON, G. G., SMITH, H. O., YANDELL, M., EVANS, C. A., HOLT, R. A., GOCAYNE, J. D., AMANATIDES, P., BALLEW, R. M., HUSON, D. H., WORTMAN, J. R., ZHANG, Q., KODIRA, C. D., ZHENG, X. H., CHEN, L., SKUPSKI, M., SUBRAMANIAN, G., THOMAS, P. D., ZHANG, J., GABOR MIKLOS, G. L., NELSON, C., BRODER, S., CLARK, A. G., NADEAU, J., MCKUSICK, V. A., ZINDER, N., LEVINE, A. J., ROBERTS, R. J., SIMON, M., SLAYMAN, C., HUNKAPILLER, M., BOLANOS, R., DELCHER, A., DEW, I., FASULO, D., FLANIGAN, M., FLOREA, L., HALPERN, A., HANNENHALLI, S., KRAVITZ, S., LEVY, S., MOBARRY, C., REINERT, K., REMINGTON, K., ABU-THREIDEH, J., BEASLEY, E., BIDDICK, K., BONAZZI, V., BRANDON, R., CARGILL, M., CHANDRAMOULISWARAN, I., CHARLAB, R., CHATURVEDI, K., DENG, Z., DI FRANCESCO, V., DUNN, P., EILBECK, K., EVANGELISTA, C., GABRIELIAN, A. E., GAN, W., GE, W., GONG, F., GU, Z., GUAN, P., HEIMAN, T. J., HIGGINS, M. E., JI, R. R., KE, Z., KETCHUM, K. A., LAI, Z., LEI, Y., LI, Z., LI, J., LIANG, Y., LIN, X., LU, F., MERKULOV, G. V., MILSHINA, N., MOORE, H. M., NAIK, A. K., NARAYAN, V. A., NEELAM, B., NUSSKERN, D., RUSCH, D. B., SALZBERG, S., SHAO, W., SHUE, B., SUN, J., WANG, Z., WANG, A., WANG, X., WANG, J., WEI, M., WIDES, R., XIAO, C., YAN, C., et al. 2001. The sequence of the human genome. *Science,* 291**,** 1304-51.

VOS, P. D., LEEDMAN, P. J., FILIPOVSKA, A. & RACKHAM, O. 2019. Modulation of miRNA function by natural and synthetic RNA-binding proteins in cancer. *Cell Mol Life Sci,* 76**,** 3745-3752.

WANG, L., NAM, Y., LEE, A. K., YU, C., ROTH, K., CHEN, C., RANSEY, E. M. & SLIZ, P. 2017. LIN28 Zinc Knuckle Domain Is Required and Sufficient to Induce let-7 Oligouridylation. *Cell Rep,* 18**,** 2664-2675.

WANG, L., YUAN, C., LV, K., XIE, S., FU, P., LIU, X., CHEN, Y., QIN, C., DENG, W. & HU, W. 2013. Lin28 mediates radiation resistance of breast cancer cells via regulation of caspase, H2A.X and Let-7 signaling. *PLoS One,* 8**,** e67373.

WANG, T., GILKES, D. M., TAKANO, N., XIANG, L., LUO, W., BISHOP, C. J., CHATURVEDI, P., GREEN, J. J. & SEMENZA, G. L. 2014. Hypoxia-inducible factors and RAB22A mediate formation of microvesicles that stimulate breast cancer invasion and metastasis. *Proc Natl Acad Sci U S A,* 111**,** E3234-42.

WANG, T., WANG, G., HAO, D., LIU, X., WANG, D., NING, N. & LI, X. 2015. Aberrant regulation of the LIN28A/LIN28B and let-7 loop in human malignant tumors and its effects on the hallmarks of cancer. *Mol Cancer,* 14**,** 125.

WILKINSON, M. E., CHARENTON, C. & NAGAI, K. 2020. RNA Splicing by the Spliceosome. *Annu Rev Biochem,* 89**,** 359-388.

WITTEN, J. T. & ULE, J. 2011. Understanding splicing regulation through RNA splicing maps. *Trends Genet,* 27**,** 89-97.

WITWER, K. W., BUZAS, E. I., BEMIS, L. T., BORA, A., LASSER, C., LOTVALL, J., NOLTE-'T HOEN, E. N., PIPER, M. G., SIVARAMAN, S., SKOG, J., THERY, C., WAUBEN, M. H. & HOCHBERG, F. 2013. Standardization of sample collection, isolation and analysis methods in extracellular vesicle

research. *J Extracell Vesicles,* 2.

XU, B., ZHANG, K. & HUANG, Y. 2009. Lin28 modulates cell growth and associates with a subset of cell cycle regulator mRNAs in mouse embryonic stem cells. *RNA,* 15**,** 357-61.

XU, R., RAI, A., CHEN, M., SUWAKULSIRI, W., GREENING, D. W. & SIMPSON, R. J. 2018. Extracellular vesicles in cancer - implications for future improvements in cancer care. *Nat Rev Clin Oncol,* 15**,** 617-638.

XU, W., BISWAS, J., SINGER, R. H. & ROSBASH, M. 2022. Targeted RNA editing: novel tools to study post-transcriptional regulation. *Mol Cell,* 82**,** 389-403.

XU, Y., HUANGYANG, P., WANG, Y., XUE, L., DEVERICKS, E., NGUYEN, H. G., YU, X., OSES-PRIETO, J. A., BURLINGAME, A. L., MIGLANI, S., GOODARZI, H. & RUGGERO, D. 2021. ERalpha is an RNA-binding protein sustaining tumor cell survival and drug resistance. *Cell,* 184**,** 5215-5229 e17.

YANG, C., DOU, R., WEI, C., LIU, K., SHI, D., ZHANG, C., LIU, Q., WANG, S. & XIONG, B. 2021. Tumor-derived exosomal microRNA-106b-5p activates EMT-cancer cell and M2-subtype TAM interaction to facilitate CRC metastasis. *Mol Ther,* 29**,** 2088-2107.

YU, F., YAO, H., ZHU, P., ZHANG, X., PAN, Q., GONG, C., HUANG, Y., HU, X., SU, F., LIEBERMAN, J. & SONG, E. 2007. let-7 regulates self renewal and tumorigenicity of breast cancer cells. *Cell,* 131**,** 1109-23.

ZENG, Z., LI, Y., PAN, Y., LAN, X., SONG, F., SUN, J., ZHOU, K., LIU, X., REN, X., WANG, F., HU, J., ZHU, X., YANG, W., LIAO, W., LI, G., DING, Y. & LIANG, L. 2018. Cancer-derived exosomal miR-25-3p promotes pre-metastatic niche formation by inducing vascular permeability and angiogenesis. *Nat Commun,* 9**,** 5395.

ZHANG, B., TIAN, L., XIE, J., CHEN, G. & WANG, F. 2020. Targeting miRNAs by natural products: A new way for cancer therapy. *Biomed Pharmacother,* 130**,** 110546.

ZHANG, H., LI, Y. & LAI, M. 2010. The microRNA network and tumor metastasis. *Oncogene,* 29**,** 937-48.

ZHANG, J., RATANASIRINTRAWOOT, S., CHANDRASEKARAN, S., WU, Z., FICARRO, S. B., YU, C., ROSS, C. A., CACCHIARELLI, D., XIA, Q., SELIGSON, M., SHINODA, G., XIE, W., CAHAN, P., WANG, L., NG, S. C., TINTARA, S., TRAPNELL, C., ONDER, T., LOH, Y. H., MIKKELSEN, T., SLIZ, P., TEITELL, M. A., ASARA, J. M., MARTO, J. A., LI, H., COLLINS, J. J. & DALEY, G. Q. 2016. LIN28 Regulates Stem Cell Metabolism and Conversion to Primed Pluripotency. *Cell Stem Cell,* 19**,** 66-80.

ZHANG, N., WANG, X., HUO, Q., SUN, M., CAI, C., LIU, Z., HU, G. & YANG, Q. 2014. MicroRNA-30a suppresses breast tumor growth and metastasis by targeting metadherin. *Oncogene,* 33**,** 3119-28.

ZHANG, X. H., WANG, Q., GERALD, W., HUDIS, C. A., NORTON, L., SMID, M., FOEKENS, J. A. & MASSAGUE, J. 2009. Latent bone metastasis in breast cancer tied to Src-dependent survival signals. *Cancer Cell,* 16**,** 67-78.

ZHANG, Y. & LI, Z. 2021. RNA binding proteins: Linking mechanotransduction and tumor metastasis. *Cancer Lett,* 496**,** 30-40.

ZHANG, Y. F., ZHOU, Y. Z., ZHANG, B., HUANG, S. F., LI, P. P., HE, X. M., CAO, G. D., KANG, M. X., DONG, X. & WU, Y. L. 2019. Pancreatic cancer-derived exosomes promoted pancreatic stellate cells recruitment by pancreatic cancer. *J Cancer,* 10**,** 4397-4407.

ZHAO, B. S., ROUNDTREE, I. A. & HE, C. 2017. Post-transcriptional gene regulation by mRNA modifications. *Nat Rev Mol Cell Biol,* 18**,** 31-42.

ZHAO, Y., DENG, C., WANG, J., XIAO, J., GATALICA, Z., RECKER, R. R. & XIAO, G. G. 2011. Let-7 family miRNAs regulate estrogen receptor alpha signaling in estrogen receptor positive breast cancer.

Breast Cancer Res Treat, 127**,** 69-80.

ZHOU, J., NG, S. B. & CHNG, W. J. 2013. LIN28/LIN28B: an emerging oncogenic driver in cancer stem cells. *Int J Biochem Cell Biol,* 45**,** 973-8.

ZHU, S., WU, H., WU, F., NIE, D., SHENG, S. & MO, Y. Y. 2008. MicroRNA-21 targets tumor suppressor genes in invasion and metastasis. *Cell Res,* 18**,** 350-9.

8. Declaration of Contribution

The research was entirely conducted in Internal Medince I, University Hospital Tübingen, Eberhard Karls Universität Tübingen, Tübingen.

Prof. Dr. Nisar Peter Malek and Dr. rer. med. Pavlos Missios conceptualized the study. Dr. rer. med. Pavlos Missios and I conceived and designed all experiments. Dr. rer. med. Pavlos Missios provided plasmids that were used in this study, including CRISPR/Cas9 LIN28B knockout plasmid and wildtype LIN28B overexpressing plasmid. I independently carried out all experiments and analyzed data.

I declare that all relevant data are our original work, except for the quoted references and figures. In addition, the reprintable licenses have been permitted and reveived from publishing groups for the reusing of cited texts and figures in this dissertation.

I hereby declare that I wrote the dissertation entitled: “Examining the role of *let-7* microRNA transfer in the metastatic niche”. Dr. rer. med. Pavlos Missios proofread this dissertation. This work was not submitted for any other degree application. Partial results in this dissertation will be used for publication in the furture.

_____

Place/date/signature of doctoral candidate

9. Acknowledgement

I would like to express my sincere gratitude to my supervisor Prof. Dr. med. Nisar Peter Malek for the fully support of my doctoral program with great patience and immense knowledge.

My heartfelt gratitude goes to my academic tutor Dr. rer. med. Pavlos Missios for the huge assistance of my research project. He has greatly encouraged me and helped me to overcome every research challenge I encountered. He was very patient in helping me to proofread my dissertation. He is always enthusiastic and optimistic. I feel very fortunate and really cherish the time working in his group.

A very special gratitude goes to Dr. Przemyslaw Bozko for their tremendous help during my work. Meanwhile, I thank my colleagues Dr. Mathias Riebold, Sebastian Reuter, Sebastian Klein, Anna Kamer, Khac Cuong Bui, Dr. Verena Wagner and Dr. Julius Joos for their precious supports.

Last but not the least, I would like to appriciate my family and my friends for their endless love and supports that are always with me in my life.